UNIVERSITY OF CALGARY

Dynamics of Pipelines with a Finite Element Method

by

Jawad Nadeem Durrani

A THESIS

SUBMITTED TO THE FACULTY OF GRADUATE STUDIES

IN PARTIAL FULFILLMENT OF THE REQUIREMENTS FOR THE

DEGREE OF MASTER OF SCIENCE IN MECHANICAL ENGINEERING

DEPARTMENT OF MECHANICAL AND MANUFACTURING ENGINEERING

CALGARY, ALBERTA

August, 2001

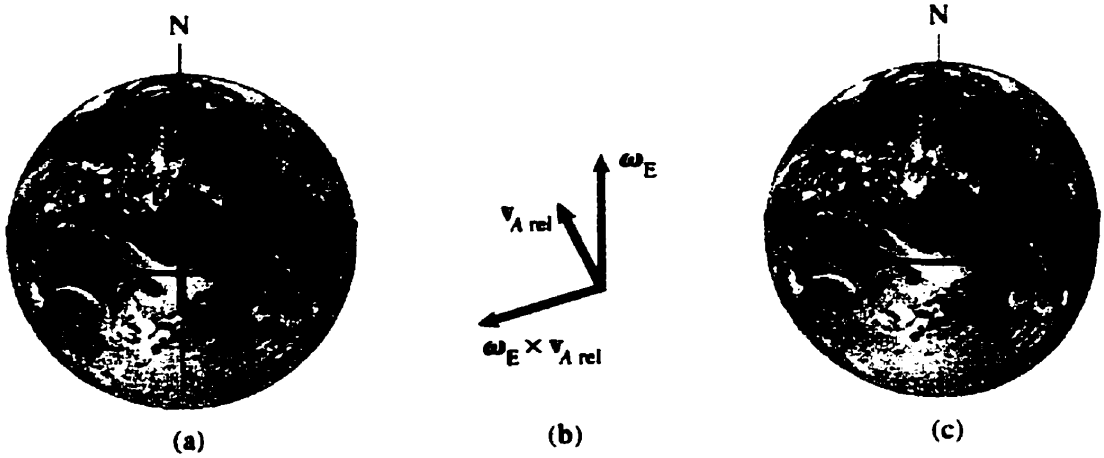

CORIOLIS FORCE

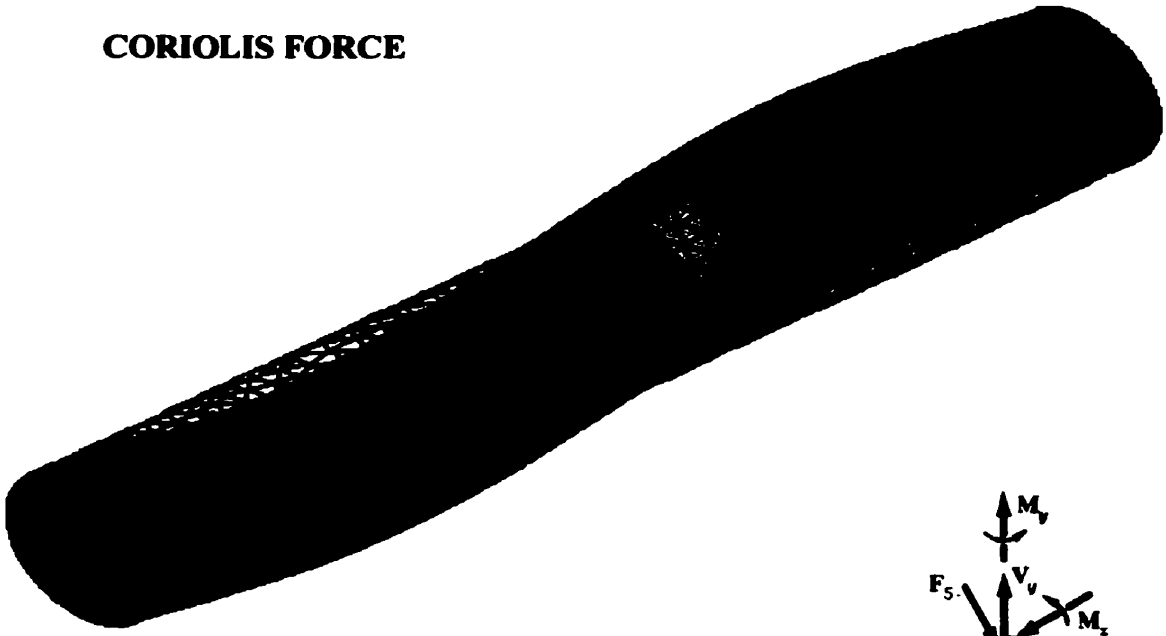

PIPELINE VIBRATIONS

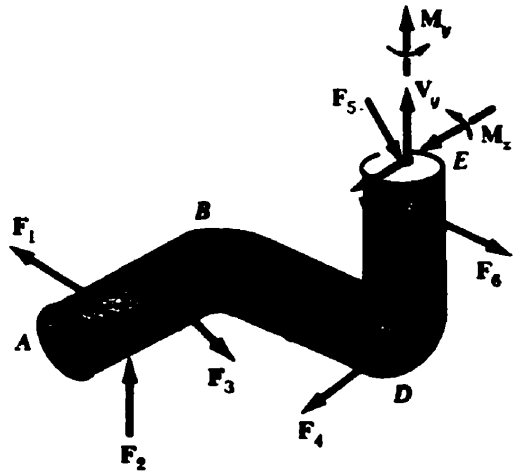

ABSTRACT

Current methods in design and analysis of the Pipelines using Engineering formulae given in textbooks form the basis of industrial computational techniques for stress and vibration analysis. However, these methods do not take into consideration the dynamic effects of Coriolis Force on a fluid filled Pipeline.

Problems of Pipeline vibration due to Coriolis Force are known to the industry, though not much work has been done to correlate the two.

In this thesis a Finite Element Method (FEM) has been developed for the application of Coriolis Force on a fluid filled Pipeline.

Nine cases were studied using this FEM and actual industrial project data. The resultant data shows noticeable effects of Coriolis Force at relatively higher flow velocities. Versatility of the format of this FEM equation is shown by its correlation to research work by other scholars and future prospects in this field are indicated.

ACKNOWLEDGEMENTS

The author wishes to express thanks to his Supervisor – Dr. M. C. Singh, for his guidance and appreciation throughout the different stages towards the completion of this thesis.

The author wishes to thank Dr. M. Epstein helping develop the FEM, Dr. D. Westbrook for guidance deriving mathematical functions, Dr. W. Shaw for guidance with density calculations and Dr. R. Babaei clarifying portions of FEM techniques. Mr. H. Benmekki, a Ph.D student, for technical discussions and help with mathematical derivations. Dr. J. Ronsky for encouragement and help, Dr. K. Chowdhury in encouragement and initial thesis organization, staff of Mechanical Engineering Department for assistance.

The author expresses his appreciation to Dr. T. Chiba [4] [5] from Japan, for guidance and provision of research data to which the author made reference.

Last, but not the least, the author acknowledges his sister, S. Durrani in helping to locate J. P. Vayda [3] in Switzerland and communicating in German language. Also, thanks to his brother K. Durrani in editing certain sections of the thesis.

DEDICATIONS

This thesis is dedicated to my darling daughter Romella Jawad Durrani and beloved wife Tabassum Jawad Durrani who inspired me to take up this M. Sc. Mechanical Engineering programme, constantly boosting my moral and have been patiently waiting for this happy day.

This thesis is also dedicated to my mother Azra Sultana Durrani and father (late) Nisar Hussain Durrani for their strong support in my quest for higher education and many a blessings without, which I would not have progressed so far in life.

A special reference is made by the author with great gratitude to his sisters: Shahnaz, Naila, Mahnaz and Gulrukh Durrani; brother Khurram Durrani and brother-in-law Saif Ahmad for immense encouragement and extending wishes throughout the thesis stages.

TABLE OF CONTENTS

LIST OF TABLES

LIST OF FIGURES

ABBREVIATIONS

- AES Saudi ARAMCO Engineering Standards
- ANSI American National Standards Institute
- ANSYS Analysis System, a commercial FEM computer program
- API American Petroleum Institute
- ASME American Society of Mechanical Engineers
- ASTM America Society for Testing and Materials
- b.p.d barrels per day
- EPC Engineer Procure and Construct
- FEM Finite Element Method
- ISAP a commercial computer program
- M.B.O.D million barrels per day = 10^3 barrels per day

NOMENCLATURE

In addition to the nomenclature defined hereunder, in some places symbols have been defined in the text where deemed necessary. The present work is written mainly in FPI system of units using pounds, inches, and degree Fahrenheit; however at some places especially in the ANSYS computer runs, due to the ANSYS educational version system constraints inches were converted to feet. Also in some particular instances SI units have been mentioned like the industrial project taken. That was done due to the fact in this project some units were taken as in FPI and others in SI system of units.

$\ddot{x}$	acceleration
y'	derivative of y with respect to distance x
$\dot{y}$	derivative of y with respect to time giving velocity
N_i'	derivative of the shape function
$\dot{y}'$	derivative with respect to time and distance
y''	double derivative of y with respect to distance x
$\ddot{y}$	double derivative of y with respect to time giving acceleration
N_i''	double derivative of the shape function
υ	Poisson's ratio
$\bar{k}$	reduced stiffness
$\dot{x}$	velocity

$\lvert\ \rvert$	a determinant
$\sigma_{allow.}$	Maximum allowable operating stress
$\sigma_{allow\text{-}tens.}$	basic allowable stress in tension
ω_E	angular velocity of the earth
σ_{hot}	stress hot or allowable stress at design temperature
ω_i	mode shapes frequency of the order $i = 1 \rightarrow n$
$\sigma_{max.flow}$	stress with maximum flow
$\sigma_{min.flow}$	stress with minimum flow
ω_n	natural frequency or circular frequency or angular frequency
ω	external loading frequency, circular frequency or angular frequency
σ_{shear}	shear stress
σ_{SMTS}	specified minimum tensile strength or specified minimum tensile stress
σ_{SMYS}	specified minimum yield strength or specified minimum yield stress
δ_{sn}	snubber deflection
[ ]	a matrix
$[c]$	damping matrix or coriolis force matrix
$[D]$	centrifugal force matrix
$[I]$	identity matrix
$[k]$	material stiffness matrix

$[m]$	mass matrix of pipe+fluid system
a	acceleration of a body denoted by the suffix of a as a_A or a_B
A	constant
A_{flow}	cross-sectional area of the flow
A_{metal}	cross-sectional area of the metal
a_n	constant, $n = 1, 2, 3\ldots$
θ	angular nodal displacement in degrees or radians
B	constant
C	constant
c	damping
c_{cr}	critical damping
cps	cycles per second
D_0	amplitude of support motion or amplitude of applied force
Δ	deflection
$D_{I.D}$	inside diameter
D_{nom}	nominal diameter
$D_{O.D}$	outside diameter
E	modulus of elasticity
E_j	joint quality factor or weld joint quality factor

E_q	quality factor
F	force
f_n	natural frequency
F_{sn}	snubber force
F_{shear}	shear force
g	acceleration due to earth's gravitational pull or acceleration due to gravity
G	modulus of rigidity or shear modulus
Hz	hertz
I	area moment of inertia, also called moment of inertia
i	i^{th} coordinate or row number in a matrix or vector
j	jth coordinate or column number in a matrix or vector
J	polar moment of inertia of the circular cross section
k	stiffness or spring constant
k_g	combined spring constant of pipe+snubber system
km	kilometer
k_n	stiffness or spring constant of spring or body numbered $n = 1, 2, 3$ .....
L	length
$\mathbb{R}$	loading function
α	loading function frequency or externally applied frequency

m	mass of pipeline+fluid system per unit length, mass of the body or support
M	moment
ρ	mass of fluid per unit length
M_b	bending moment
MP_a	mega Pascal or million rascals or 10^6 Pascal
N_i	finite element shape function, $i = 1, 2, 3\ldots$
P_{design}	design pressure
ϕ	phase angle
$P_{hydro.}$	hydraulic test pressure
P_{MAOP}	maximum allowable operating pressure
$P_{oper.}$	operating pressure
$psig$	pounds per square inch gauge pressure
$P_{steam\text{-}out}$	steam out pressure
q	flow volume
q_n	non-dimensional loading amplitude, $n = 1, 2, 3$ .....
r	radius
r_A	radius of body A from the defined origin
$r_{A/B}$	radius of body A from body B
r_B	radius of body B from the defined origin

$R_{gyr.}$	radius of gyration
S_a	basic allowable stress
T	temperature or kinetic energy of the system
t	time
T_{design}	design temperature
$t_{min.}$	minimum thickness
$T_{oper.}$	operating temperature
$t_{THK.}$	thickness
U	strain energy of flexure
UDL	uniformly distributed load
v	velocity of fluid flow
$v_{A\ rel}$	relative velocity of body A
v_{rel}	relative velocity
v_y	deflection of pipe in y-direction
v_2	deflection at node point 2
W_{pipe}	total weight of pipe
W_{fluid}	total weight of contained fluid
w_{pipe}	weight per unit length of pipe
w_{fluid}	weight per unit length of contained fluid

$W_{conc.}$ concentrated load

$W_{eff.}$ effective weight

W_{UDL} uniformly distributed load

x distance from a fixed axis or displacement

x_g pipe to snubber gap

Y coefficient of material property and design temperature

y deflection

Z section modulus

CHAPTER 1 – INTRODUCTION AND FUNDAMENTALS

1.1 Introduction

Effect of vibrations and stresses on different structures will be briefly discussed here.

What is Vibration? It is to and fro motion or oscillation of a structure or part of it. The key word here is oscillation.

Vibration is a universal fact and the law of nature. Table 1.1 below gives a few examples of the effects of vibrations.

Helpful	Damaging	Destructive	Noisy	Pleasing
Ear Drum lets us hear and Lungs help breathe	Missed Heart Beat: damages heart mussels and valves.	Resonant frequency vibrations: Tacoma Narrows Bridge; Pine Ridge Tanker.	Loud Music.	Muscles message vibrator.
Concrete and Chemical Vibrators.	Rotating Machinery: damages seals; foundations; bearings; impellers.	Excessive atoms vibration in a tumbler.	Road Roller. Exhaust Pipe of Motor.	Dancing. Vocal Chord/ Larynges helps make pleasant sounds.

Table 1.1: Friendly and Foe Vibrations [55]

If Table 1.1 was not interesting perhaps, look at figures here. Tacoma Narrows Bridge collapsed due to violent swaying in the steady wind, Figure 1.1, or Pine Ridge Tanker Figure 1.2, which broke in two due to stresses developed in its hull by the wave vibrations.

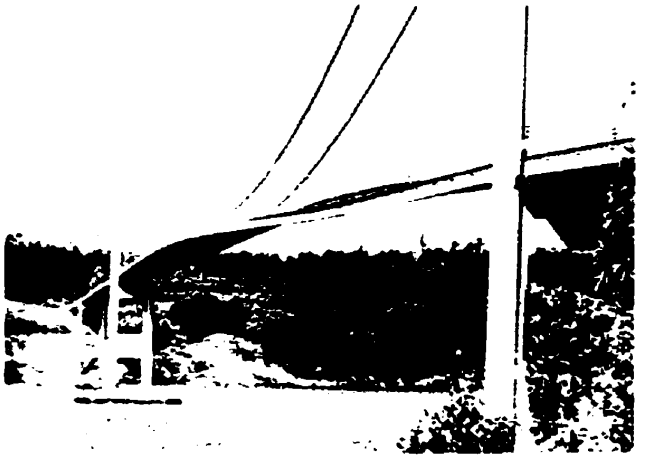

Figure 1.1: Tacoma Narrows Bridge, Washington, U.S.A [55]
Swaying Violently in Wind before Self Destruction

Figure 1.2: Pine Ridge Tanker, Cape Hatteras, Western Atlantic [55]
Tanker Broke in two due to Vibration Stresses

Neglecting that useful range in which vibratory influences are helpful, vibrations are deleterious to both human and equipment.

1.1.1 Natural Phenomenon - Vibration

May be before understanding the engineering aspects of this natural phenomenon of vibration, we should observe the reactions of our own bodies to vibration.

Take a ship in the ocean pitching in high seas. The first class passengers located near the middle of ship oscillate up and down the same way as the tourist class passengers in the bows. The first class passengers are relatively comfortable oscillating at same frequency as tourist class but the amplitude for first class is smaller. Refer to Figure 1.3; even for small amplitudes different frequencies will have different effects on the human body. Here amplitude is not the factor so much so as is the frequency.

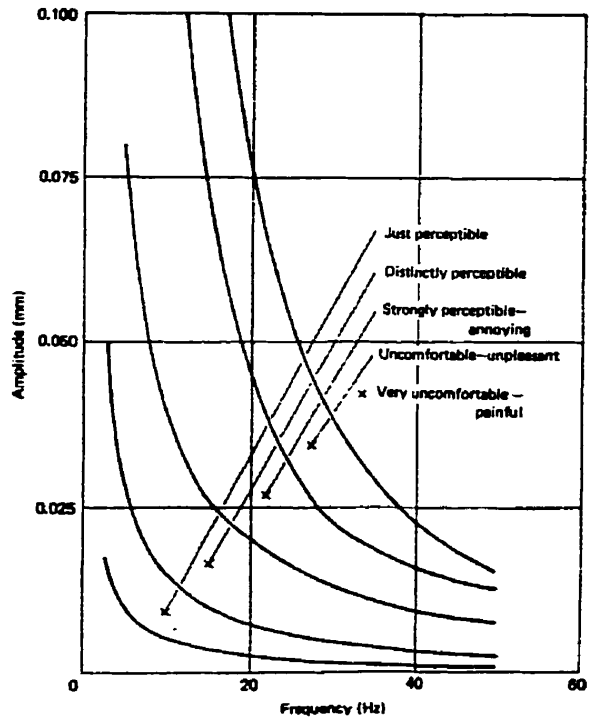

Figure 1.3: Response of Human Body to Small Amplitudes [55]
Small Amplitudes and Different Frequencies

The flow of fluid causes self-excitation. Stacks sway not necessarily due to wind puffs, even in steady breeze. It is due to periodic shedding of vortices, first from one side and then the other side of the chimney. These eddies cause pressure fluctuations and hence swaying, which are generally self-maintaining. This simple explanation does not show how complex chimney swaying is. One method to stop swaying is by guying them, or with helical spoils on

chimney sides to break vortex pattern. So that no clearly defined excitation is applied to the chimney sides.

1.1.2 Physiological Effects of Vibration

Vibration effects on human body vary from acute sickness like dizziness in ships and aircraft to very severe causing bone fractures.

Human body when in contact with moving machinery is induced with vibrations. Low-frequency large-amplitude vibrations irritate the labyrinth, which conducts nervous stimuli to both the brain and the spinal chord. From these centres abnormal impulses may be directed to the eyes, stomach, sweat glands, or viscometer system, and may therefore produce different conditions, which are characteristics of sickness. In general, these symptoms are only experienced by the induction of vibration of frequencies 1 to 10 Hz. With amplitudes 10 to 50 ft., the acceleration produced by a vibration may cause: Induced fractures or loss of consciousness.

Tests show rapid deceleration of aircraft and cars of 4.5g (144 ft/sec^2.) can break skull bones, while accelerations of 5.75g can fracture shinbones.

In mechanical vibrations, the acceleration varying from zero to maximum during one cycle lasts for only an infinitesimal period. Industrial medicine experiments suggest vibrations can cause fatigue, nervous irritability, unconsciousness or abnormal mental reactions.

1.1.2.1 Experiments on persons resting on mattress subjected to continuous vibrations show deleterious effects. Below 3 Hertz (cycles/sec) it effects the stomach, above 8 Hz it effects the head, 8 to 20 Hertz produces dizziness, 20 to 1000+ Hz produces loss of sight focus. Large amplitudes relax muscles, irrespective of attempts by human to resist.

1.1.3 Vibration Stresses

When a bar, beam or a pipe supported in some manner, is subjected to lateral loading, the form of deformation is termed as bending. This results in normal and shear stresses, neither of which is uniform over the cross-section.

A simply supported beam or pipe is free to take up any desired slope in deflection without any restraint at the supports. At fixed ends, also called built-in or encastre', a beam or a pipe is fully restrained and no rotation can occur at the support.

Every component in real life is subjected to forces causing stresses and deflection. Every component has a fundamental frequency and other corresponding higher modes of vibration depending on system properties like mass and stiffness, and end conditions.

Whenever a part of a structure is deflected due to vibration, it is subjected to stress. The stress may vary over the cross section of the structure. Under vibration conditions the stresses at any point of the structure are generally a combination of tension or compression, bending and twist; they increase or decrease depending on vibration amplitude.

1.1.4 Vibration and Fatigue

Each to-and-fro motion, is one vibration cycle, the stresses in the structure will be reversed twice e.g., tensile-compressive- tensile-compressive. Such reversals of stress produce fatigue. If the vibration amplitude is so great that it produces a stress greater than the ultimate strength of the material, then the structure may fail even in one cycle or a part there of. However, even if the vibration stress is less than the ultimate strength, the material may still fail due to fatigue.

The graph in Figure 1.4 relating to the number of reversals of stress, to the frequency, shows that permissible number of vibrations decrease as the vibration stress increases. It will be seen that if the amplitude of vibration is sufficiently large, a structure will fail after a certain number of vibrations, i.e., it will have a limited working life. If, however, the vibrations do not impose high stresses, but a stress just equal to the constant stress to which the curve in Figure 1.4 tends reached, then the number of vibrations for the material to fail will be infinite. Further still, if the amplitude is so small that the stresses produced are less than the constant, there will be an even greater factor of safety and the possibility of failure will be far less.

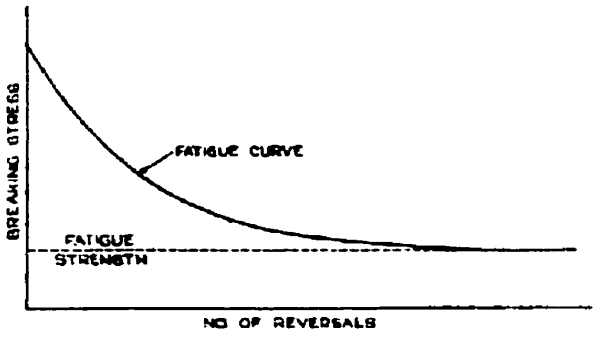

Figure 1.4: Fatigue Curve for Strength of a Vibrated Beam. [56]
Number of Reversals verses Breaking Stress

In practice, uncontrolled vibrations generally produce such high stresses that a limitation of life is most frequently involved, or, to put it more explicitly, the structure will ultimately break. For that reason, all vibrations must be regulated so that they do not fatigue the metal beyond its endurance limit.

1.1.5 Superimposed Vibration Stresses

When, as is common with torsional oscillations, the alternating stresses caused by the vibration are superimposed upon a constant stress, it is possible that on occasions the peak stress will exceed the maximum endurance stress, which can be carried by the material. For example, a 1.2 % C-Steel shaft carrying a load producing a stress of 16 tonf/in^2 and additionally carrying an alternating stress of ± 9 tons/in^2, the peak stress in one cycle will then be 16 + 9 = 25 tonf/in^2. This is in excess of the maximum ultimate stress that the shaft is capable of carrying, which may cause failure.

The imposition of vibration stresses on a structure, which is already stressed, also decreases its fatigue life. Although unloaded a material may be capable of taking an alternating stress of ± 10 tonf/in^2. Then from considerations of fatigue alone, the endurance limit may be reduced to ± 8 tonf/in^2. Any vibrations of such a material are most likely to create stresses from which failure may result, unless the amplitude of vibration is kept very small.

1.1.6 Vibration Amplitude Limits

The permissible fatigue stress of a metal, and therefore the permissible amplitude of vibration, depends upon a number of factors of which the following are most important:

Nature of the material, fatigue and impact stresses, stress concentration, corrosion, temperature and resonance.

Resonant vibration is one of the causes of blade failure in turbo-machinery. As, in steady motion, any given blade passes any given point at accurately fixed intervals. If, for instance, a water turbine blade receives a splash, then it will do so at regular intervals and may break as a consequence of resonance. If on a pelton wheel a water jet acts tangentially, usually at a

very high speed, it will drive the buckets to go around. Any one-bucket thus receives a periodic blow. If the frequency of jet impingement or the frequency of the components of this far-from-sinusoidal force were to coincide with the natural frequency of a bucket, then the bucket could break due to sufficiently high excitation.

1.2 Coriolis Force

The Earth's pull downwards along with its angular velocity ω_E results in a term $2\omega_E \mid V_{A\ rel.} \mid$. This term is called the Coriolis acceleration, and the term $-2m\omega_E \mid V_{A\ rel.} \mid$ is called Coriolis Force. [57] [72]

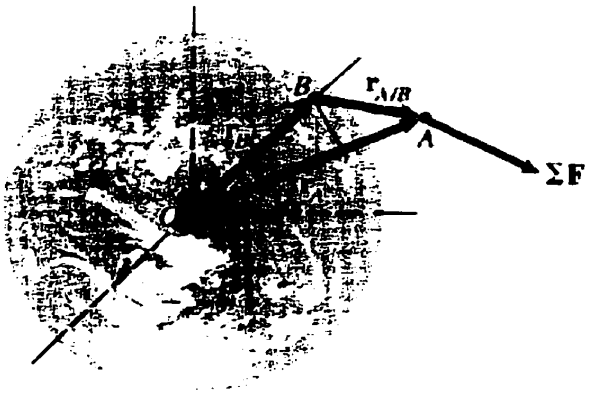

Figure 1.5: Earth Centred, Non-Rotating Reference Frame [72]

For down to earth application, the most convenient reference frame is a local earth fixed coordinate system. Figure 1.5 shows a non-rotating coordinate system with its origin at the centre of the earth O and an earth-fixed coordinate system with its origin at a point B. Since we can assume that the earth-centred, non-rotating coordinate system is inertial, we can write Newton's second law for an object A of mass m as:

$$\sum F = ma_A \tag{1.1}$$

Where a_A is A's acceleration relative to O. The earth-fixed reference frame rotates with the angular velocity of the earth ω_E. We can write the equation of motion as:

$$\sum F = ma_{Arel} + m[a_B + 2\omega_E \times V_{Arel} + \omega_E \times (\omega_E \times r_{A/B})] \tag{1.2}$$

Term ω_E x $(\omega_E$ x $r_{A/B})$: $\omega_E \cong$ one revolution/day = 7.27 x 10^{-5} rad/sec. Thus $\omega^2_E \, |r_{A/B}| = 5.29\text{x}10^{-9} |r_{A/B}|$.

Term a_B: is the acceleration of the origin B of the earth-fixed coordinate system relative to O. B moves in a circular path due to the earth's rotation. If B lies on the surface of the earth $\omega^2_E R_E = 0.0337$ m/sec^2, where R_E is the radius of earth = 6370 km. This value is too large to neglect for many purposes. However, under normal circumstances this term is accounted for as a part of the local value of the acceleration due to gravity.

Term $2\omega_E$ x $V_{A\ rel.}$: is called the Coriolis acceleration. Its magnitude is bounded by $2\omega_E \, | \, V_{A\ rel.} | = 1.45 \text{ x } 10^{-4} | \, V_{A\ rel.} |$.

We see that in most applications one can neglect terms in brackets of equation (1.2), thus the earth-fixed coordinate system is seen to be inertial. However, in some cases this is not possible. The Coriolis acceleration becomes significant if an object's velocity relative to the earth is large, and even very small accelerations become significant if an object's motion must be predicted over a large period of time. In such cases, one can still use equation (1.2) to determine the motion, but one must retain the significant terms.

Accordingly, rearranging equation (1.2), we obtain:

$$\sum F - ma_B - 2m\omega_E \times V_{A\ rel.} - m\omega_E \times (\omega_E \times r_{A/B}) = ma_{A\ rel.} \tag{1.3}$$

The term $-2m\omega_E \times V_{A\,rel.}$ in equation (1.3) is called the Coriolis Force. It explains a number of physical phenomena that exhibit different behaviours in the northern and southern hemispheres: the direction a liquid rotates when it goes down a drain, the direction vine grows around a shaft and the direction of rotation of a storm. The earth's angular velocity vector ω_E points north. When an object in the northern hemisphere moving tangent to the earth's surface travels north, Figure 1.6 (a), the Coriolis Force points towards east. This causes the object to turn to the right, Figure 1.6 (c). If the object is moving south, the direction is reversed, Coriolis force points west, causing the object to turn to the left, Figure 1.6 (c).

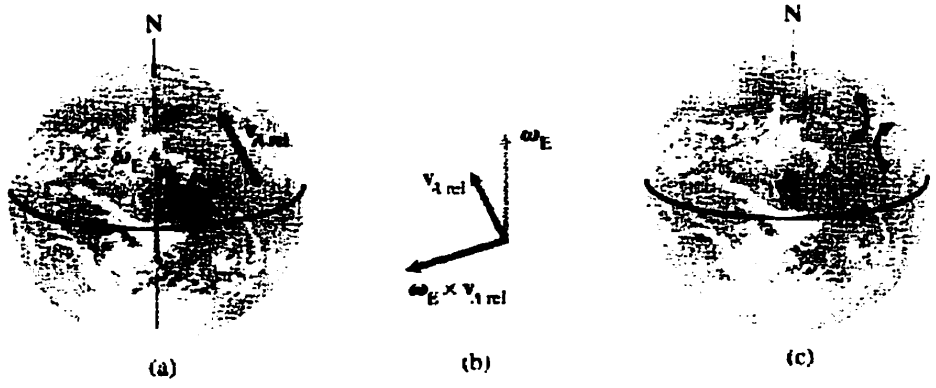

Figure 1.6: Effects of Coriolis Force on Object in Earth's North Hemisphere [72]
(a) Object in north hemisphere moving north (b) Cross product of Earth's angular velocity and object's velocity (c) Effects of Coriolis Force in north hemisphere

The reverse of what is explained respecting Figure 1.6 is true for Southern Hemisphere

Generally the flow velocity in pipelines and vessels is low and thus the effects of Coriolis Force would either be not there or negligibly small. But there are times during operations when the velocity of flow is high like in flare up gas flow, steam out condition, purging

conditions etc. Also some process plant operations are such that the flow must continually if not continuously be at high velocities. At these high flow velocities the pipeline and even pressure vessels have been noticed to experience vibrations. In some cases the unexplained vibrations were analyzed and found to be due to Coriolis Force. As not enough work has been done on this subject, generally in industry such problems are solved by working around them, if the vibration cannot be ignored.

This Thesis takes into consideration the effects of Coriolis Force and the resultant vibrations on a pipeline with fluid flow. Chapter 3 and Appendix A, provide an in-depth analysis using a Finite Element Method with Coriolis Force developed in this Thesis.

1.3 Pipeline Vibrations

Indeed, vibrations of a pipeline are very important, as it dampens the wave, which would otherwise pass on to the equipment. On the other hand vibrations could damage pipelines or the tie-in equipment.

When encouraged to vibrate at normal frequency, pipelines tend to absorb the cyclic stresses. If, then, a pulsating excitation (a forcing function) is applied with, or almost with, the natural frequency, then a violent motion may be expected. This magnified motion is Resonance.

A forced vibration usually becomes significant only if resonance occurs. This may some times be damaging and sometimes useful. As experienced personally by the author once, resonance breaks pump impellers and bearings when the pump is pushed hard enough by overstressed pipe thus forcing the pump natural frequency to coincide with the forcing frequency. In certain cases the scenario of resonance is unavoidable, forcing pump operations

at a much lower rotational speed than designed for. Lower speeds of pumps in some Oil and Gas operations could be drastic on production, refer to Appendix B.

For most Refinery or in-plant piping a natural frequency of about 4 cps is sufficient to avoid resonance in non-pulsating pipelines. However, natural frequency ω_n is related to maximum deflection Δ. Therefore ω_n for a simple beam corresponding to 1-inch sag is 3.12 cps, refer to section 2.5.4.2 and [28]. One of the reasons for limiting deflection, is to make pipe stiff enough with high enough natural frequency to avoid large amplitude under any small disturbing force. Cold or hot springing of pipes, also called pipe cut short or cut long is to compensate for the thrust forces on anchors and equipment. Like cut short for hot conditions and cut long for cryogenic conditions. This also contributes towards lowering and increasing of natural frequency of equipment attached or the pipe itself. It is not to compensate for the pipe or equipment nozzle over stress condition as is sometimes mistakenly understood.

1.4 Review of Literature on Pipeline Vibrations and Stress Analysis

Pipelines fluid filled and without, have been under microscopic and macroscopic analysis for about a century.

Different techniques from as crude as rules of thumb, experimental methods, energy methods, industrial techniques, transfer matrix to Finite Element Methods have been employed to study the different aspects of interest.

The earliest recorded study dates back to 1876 by reference [68]. Chiba [4]; [5]; [6]; [16] in 1988-90, has extensively researched the study of piping response using multiple support systems generally under the action of seismic conditions for both linear and non-linear behaviours. Vayda [3] has in 1981 presented his research on the dynamic behaviour of piping

systems under the influence of support to pipe gap with the seismic conditions and the non-linearity of the system. Chens [70] looked at the chaotic vibration in fluid-stiffness-controlled pipe tube rows in fluid cross flow. Lockau, Haas and Steinwender [9] in 1984 presented their work on piping and support design due to high frequency excitation as the criterion.

In 1982 Journal of Pressure Vessel technology reported that the Pressure Vessel and Piping Codes in 1981 edition of ASME Nuclear Power Plant Components Code for Controlling Primary Loads in Piping Systems, have been changed to accommodate, recognize and utilize some of the results from the research conducted.

Kaladi [27] has studied pipes behaviour with and without the presence of Coriolis force, and has indicated the effects of fluid flow velocity on the pipe vibrations. Though also indicated the limitations in the use of his transfer matrix methodology. Similarly, Ashley and Havilland [8], Housner [10], Naguleswaran and Williams [13], Thurman and Mote [15], Chen [38], Paz and Michelow [58] and Holmes [69] have studied the transverse vibration of pipes with fluid flow using Coriolis Force concept. They have studied different end conditions and found the effects on pipe deflections and frequencies due to increases in flow velocities. All researchers have used different analytical techniques arriving at varied results but one thing being common among all, there is clear evidence of effects of fluid flow velocity in the form of Coriolis Force on the pipe deflections and frequencies.

This Thesis has taken a similar approach as all other scholars cited above, excepting that a Finite Element Method with Coriolis Force has been developed and flow velocities to a very high value have been considered. Thus using the power and flexibility of Finite Element Method and the computers, additionally clearly brining out the effects of Coriolis Force, which are expected to be pronounced at relatively higher, flow velocities.

1.5 Review of Literature on Finite Element Methods

Finite Element Methods have been developed to study various aspects of pipelines, in fluid filled conditions, without fluid and even in fluid flow conditions. There are various commercially available computer programs like the ANSYS, which use the Finite Element Method to analyze various aspects of pipelines in various conditions. However, ANSYS software does not have the capability to analyze a piping system with Coriolis Force as presented in this Thesis.

The author of this thesis has not come across any research conducted so far on the dynamics of pipelines, developing and/or utilizing the Finite Element Method in the presence of Coriolis force. This important and unique feature is being presented in this thesis, which also opens the doors for new research in this area.

1.6 Equations and derivations

Deflections can be calculated using total weight or effective weight of the pipe between supports. Effective weight is the equivalent concentrated weight substituted for the uniformly distributed weight. The ratio of effective weight to total weight is called weight factor. Effective weight is found from dynamic deflection curves equation for a particular mode of vibration in a system, which would differ with end conditions. It is reasonable to use fundamental mode of vibration to find dynamic deflection curve.

The dynamic deflection curve equation for fixed ends condition is taken as: [22]

$$f(x) = Sin^4 \frac{x\pi}{L} \tag{1.4}$$

Effective weight is found by multiplying the infinitesimal weight of pipe $dw = \frac{W}{L} dx$ with equation (1.4) and integrating, giving:

$$W_{eff} = \frac{W}{L} \int_0^L Sin^4 \frac{\pi x}{L} dx \tag{1.5}$$

$$W_{eff} = \frac{3}{8} W \qquad \text{(fixed ends case)} \tag{1.6}$$

In industrial methods of calculations, to eliminate the need to check the sum of the longitudinal pressure stress + dead load stresses; the limit for dead load stress is set at $\sigma_{hot}/2$.

Beam formulas are also used for pipes. Following beam formulas can be used for different end conditions, as utilized in Chapter 2:

Simply supported, concentrated and UDL load, for maximum bending stress: [22]

$$(0.75WL^2 + 1.5W_{conc.}L)\frac{D_o}{I} = S_b \tag{1.7}$$

$$(0.5WL^2 + 0.75W_{conc.}L)\frac{D_o}{I} = S_b \qquad \text{(continuous system)} \tag{1.8}$$

Simply supported, concentrated and UDL load, for max. deflection: [22]

$$(22.5WL^4 + 36W_{conc.}L^3)\frac{1}{EI} = y \tag{1.9}$$

$$(4.5WL^4 + 9W_{conc.}L^3)\frac{1}{EI} = y \qquad \text{(continuous system)} \tag{1.10}$$

Other beam formulas of interest to us are: [22] [28] [31]

$$M_b = \frac{W_{con.}L}{8} \qquad \text{(fixed ends)} \tag{1.11}$$

$$M_b = \frac{W_{con.} L}{4} \quad \text{(simple supports)} \tag{1.12}$$

$$y = \frac{-W_{conc.} L^3}{192EI} \quad \text{(fixed ends)} \tag{1.13}$$

$$y = \frac{-W_{conc.} L^3}{48EI} \quad \text{(simply supported)} \tag{1.14}$$

$$U = \int \frac{M_b^2}{2EI} dx \quad \text{(strain energy of flexure)} \tag{1.15}$$

$$R = \frac{EI}{M_b} \quad \text{(radius of curvature)} \tag{1.16}$$

$$y = \frac{\partial U_f}{\partial W_{conc.}} \quad \text{(Castigliano's first theorem)} \tag{1.17}$$

$$y = \frac{PL^3}{CEI} \quad \text{(C=constant depends on end conditions)} \tag{1.18}$$

$$\frac{y_1}{y} = \frac{\frac{PL_1^3}{CEI}}{\frac{PL_1^3}{CEI} + \frac{PL_2^3}{CEI} + \frac{PL_3^3}{CEI} + ...} \quad \text{(continuous system: } y = y_1 + y_2 + \ldots\text{)} \tag{1.19}$$

Deflection formulae for different end conditions:

$$y = \frac{5wL^4}{384EI} \quad \text{(simple supports)} \tag{1.20}$$

$$y = \frac{wL^4}{384EI} \quad \text{(fixed ends)} \tag{1.21}$$

$$y = \frac{wL^4}{128EI} \quad \text{(from equations (1.20), (1.21) as } y = \frac{y_1 + y_2}{2}\text{)} \tag{1.22}$$

For homogenous units we convert equation (1.22), feet to inches:

$$y = \frac{13.5wL^4}{EI} \qquad \text{(fixed+simply supported case, like a pipe run)} \qquad (1.23)$$

$$y = \frac{9W_{eff}L^3}{EI} \qquad \text{(fixed ends)} \qquad (1.24)$$

$$y = \frac{3.375wL^4}{EI} \qquad \text{(putting } W_{eff} = \frac{3}{8}W \text{ in equation (1.24)) (fixed ends)} \qquad (1.25)$$

$$y = \frac{36W_{eff}L^3}{EI} \qquad \text{(simple supports)} \qquad (1.26)$$

$$y = \frac{18wL^4}{EI} \qquad \text{(putting } W_{eff} = \frac{1}{2}W \text{ in equation (1.26)) (simple supports)} \qquad (1.27)$$

$$y = \frac{16.1W_{eff}L^3}{EI} \qquad \text{(fixed and simple support ends)} \qquad (1.28)$$

$$y = \frac{7WL^3}{EI} \qquad \text{(putting } W_{eff} = \frac{7}{16}W \text{ in equation (1.28)) (fixed and simple support ends)} \qquad (1.29)$$

1.7 Static Condensation Method

Static Condensation Method is a practical method of accomplishing the reduction of the matrix, like the stiffness matrix. It is accomplished through the process of identifying those degrees of freedom to be condensed. The relation between dependent degrees a and independent degrees of freedom b, is found by establishing static relation between them, to reduce the matrix. Detailed procedures are given in [19] and [21] for both static and dynamic systems. This method is also used to eliminate unwanted internal degrees of freedom of an element in the Finite Element Method.

The stiffness equation of a structure can thus be written in partitioned matrix form as:

$$\left[\begin{array}{c|c} [k_a] & [k_{ab}] \\ \hline [k_{ba}] & [k_b] \end{array}\right]\left\{\begin{array}{c} \{y_a\} \\ \hline \{y_b\} \end{array}\right\} = \left\{\begin{array}{c} \{0\} \\ \hline \{F_b\} \end{array}\right\}$$

Through static condensation method, we reduce the above partitioned matrix to:

$$\left[\begin{array}{c|c} [I] & [\bar{T}] \\ \hline [0] & [\bar{K}] \end{array}\right]\left[\begin{array}{c} \{y_A\} \\ \hline \{y_B\} \end{array}\right] = \left[\begin{array}{c} \{0\} \\ \hline \{F_B\} \end{array}\right] \tag{1.30}$$

Where $[\bar{T}] = -[k_a]^{-1}[k_{ab}]$

And $[\bar{k}] = [k_b] - [k_{ba}][k_a]^{-1}[k_{ab}]$

Equation (1.30) is the reduced stiffness equation. In which the relation between force and deflection at the independent coordinates or degrees of freedom, is given. Here $[\bar{k}]$ is the reduced stiffness matrix. Dynamic matrix can also be similarly reduced.

1.8 Various Methods

Various methods can be used to find the displacement and frequency of the system. Some methods used by other authors as reported in Chapter 4, are referenced for study and understanding here.

We take the following equation of motion for consideration:

$$m_i \Delta\ddot{x}_i + c_i \Delta\dot{x}_i + k_i \Delta x_i = \Delta F_i \tag{1.31}$$

On examination of the above equation we see that k_i and c_i values are calculated for values of displacement and velocity respectively, corresponding to time t_i, and are obviously assumed to stay constant during the incremental time Δt. As in general k_i and c_i do change during Δt, thus equation (1.31) will give approximate results. [19]

Using Linear Acceleration Step-by-Step Method shown in Figure 1.7, equation (1.31) transforms into equation (1.32), which is used to calculate displacement x_{i+1}, velocity $\dot{x}_{i+1}$ and acceleration $\ddot{x}_{i+1}$ for time step t_{i+1}.

$$\ddot{x}_{i+1} = \frac{1}{m}\{F(t_{i+1}) - F_{D,i+1} - F_{S,i+1}\} \tag{1.32}$$

Where $F_{D,\,i+1}$ = Damping force at t_{i+1}

$F_{S,\,i+1}$ = Spring force at t_{i+1}

F_t = External force

There are two approximations in this method: [19]

1- Acceleration varies linearly in the time increment Δt.

2- Damping and stiffness are evaluated at the initiation of each time increment Δt and remains constant in this time step.

These assumptions produce error, which is reducible.

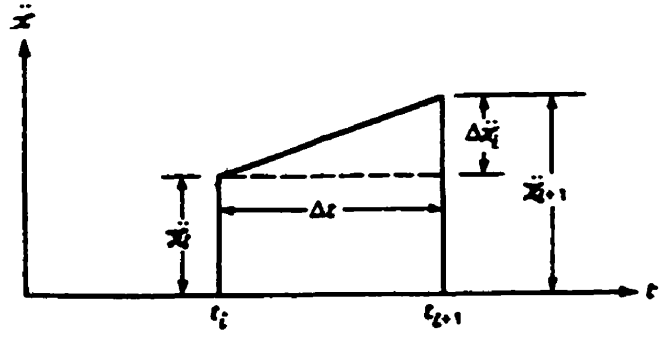

Figure 1.7: Linear Acceleration Step-by-Step Method [19]
Assumed Linear Variation of Acceleration During Time Interval

Average Acceleration Method also called Constant Average Acceleration Method or also called Newmark-β Method or Newmark-β = ¼ Method, in this method the displacement and velocity at a time station t_i are approximated using trapezoidal rule. The velocity and acceleration respectively in the time step are taken to be average of *i* and i+*1*. This method gives not as accurate results as would be obtained by the Linear Acceleration Step-by-Step Method. On the other hand Average Acceleration Method is unconditionally stable and Linear Acceleration Step-by-Step Method is conditionally stable.

The modification of Linear Acceleration Step-by-Step Method is called Wilson-θ Method. This modification assumes numerical stability of the solution process regardless of the magnitude selected for the time step. Thus this method is called unconditionally stable. [19][71]

The assumptions taken in this method are:

1- Acceleration varies linearly over the time interval.

2- $\theta \geq 1.0$, θ is a factor determined to obtain optimum stability and accuracy. Wilson has shown $\theta \geq 1.38$ gives unconditional stability.

Details on the above methods are given in [4][5][6][19][71][73].

1.9 Linear, Forced Multi-Degree Freedom System

The following derivation and principles are very important as they form the basis of the derivations and numerical results we achieve in the Chapter 3.

The system presented is a two-degree of freedom forced vibration spring-mass system. Also called multi-degree freedom forced system. Refer to Figure 1.8.

This is a two-degree freedom (2 mass) system with 3 springs, bouncing off the two rigid end supports of infinite stiffness. [19] [30][63]

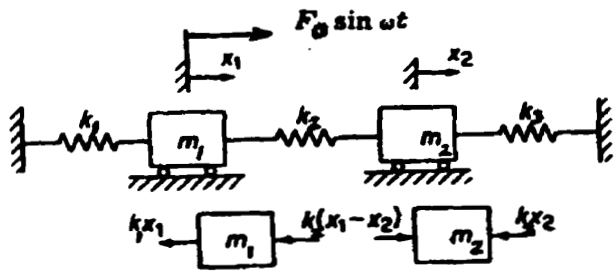

Figure 1.8: Two-Degree Freedom Forced System

Applying Newton's second law of motion to the system shown in Figure 1.8:

$$\sum F_x = ma_x \tag{1.33}$$

Equation of motion for m_1:

$$- k\,x = m_1\,a_1 + F_0\,Sin\,\omega t \tag{1.34}$$

$$-k\,x = - k_1\,x_1 - k_2\,(x_1 - x_2) \tag{1.35}$$

Putting equation (1.35) in (1.34):

$$m_1\,\ddot{x}_1 + (k_1 + k_2)\,x_1 - k_2\,x_2 = F_0\,Sin\,\omega t \tag{1.36}$$

Similarly equation of motion for m_2:

$$m_2\,a_2 = - k\,x \tag{1.37}$$

$$- k\,x = - k_3\,x_2 - k_2\,(x_2 - x_1) \tag{1.38}$$

$$m_2\,\ddot{x}_2 + (k_2 + k_3)\,x_2 - k_2\,x_1 = 0 \tag{1.39}$$

Assuming motion to be periodic and composed of harmonic motions of various amplitudes and frequencies. Let one of these harmonic components, fundamental mode, be:

$$x_1 = A\ Sin\ (\omega t + \varphi) \tag{1.40}$$

$$x_2 = B\ Sin\ (\omega t + \varphi) \tag{1.41}$$

Where A, B and φ are constants and ω is the forcing frequency.

Differentiating equations (1.40) and (1.41) twice gives:

$$\ddot{x}_1 = -A\ \omega^2\ Sin\ (\omega t + \varphi) \tag{1.42}$$

$$\ddot{x}_2 = -B\ \omega^2\ Sin\ (\omega t + \varphi) \tag{1.43}$$

Putting equations (1.40), (1.41), (1.42) and (1.43) in (1.36), (1.39) gives:

$$A\ \{k_1 + k_2 - m_1\ \omega^2\} - k_2\ B = F_0 \tag{1.44}$$

$$-\ k_2\ A + (k_2 + k_3 - m_2\ \omega^2)\ B = 0 \tag{1.45}$$

By Cramer's rule A and B constants can be found from equations (1.44), (1.45):

$$A = \frac{\begin{vmatrix} F_0 & -k_2 \\ 0 & (k_2 + k_3 - m_2\omega^2) \end{vmatrix}}{(k_1 + k_2 - m_1\omega^2)(k_2 + k_3 - m_2\omega^2) - k_2^2}$$

Solving the above determinant gives:

$$A = \frac{F_0(k_2 + k_3 - m_2\omega^2)}{(k_1 + k_2 - m_1\omega^2)(k_2 + k_3 - m_2\omega^2) - k_2^2} \tag{1.46}$$

$$B = \frac{\begin{vmatrix} (k_1 + k_2 - m_1\omega^2) & F_0 \\ -k_2 & 0 \end{vmatrix}}{(k_1 + k_2 - m_1\omega^2)(k_2 + k_3 - m_2\omega^2) - k_2^2}$$

Solving the above determinant gives:

$$B = \frac{F_0 k_2}{(k_1 + k_2 - m_1\omega^2)(k_2 + k_3 - m_2\omega^2) - k_2^2} \tag{1.47}$$

Assuming after some time the free vibrations die out, a steady state motion remains with a frequency equal to the forcing frequency. Using equations (1.40) and (1.41), as the motion of the mass is either in phase or out of phase with the excitation, the phase angle $\varphi = 0^0$ or 180^0, thus:

Putting equation (1.46) and (1.47) in (1.40) and (1.41) respectively, gives the steady state vibration as:

$$x_1 = \frac{F_0(k_2 + k_3 - m_2\omega^2)}{(k_1 + k_2 - m_1\omega^2)(k_2 + k_3 - m_2\omega^2) - k_2^2} Sin\omega t \tag{1.48}$$

$$x_2 = \frac{F_0 k_2}{(k_1 + k_2 - m_1\omega^2)(k_2 + k_3 - m_2\omega^2) - k_2^2} Sin\omega t \tag{1.49}$$

To find natural frequencies of the system, we solve for the homogeneous part of equations (1.36) and (1.39) by taking the right hand side equal to zero. Thus with the same assumption that the motion is periodic and harmonic we use equations (1.40) through (1.43) with the exception that ω is replaced by ω_n, being one of the system natural frequencies.

By equating to zero the determinant of the coefficients of A and B, $\Delta\omega_n$ the natural frequency equation called characteristic of the system is obtained:

$$\Delta\omega_n = \frac{\begin{vmatrix} (k_1 + k_2 - m_1\omega_n^2) & k_2 \\ -k_2 & (k_2 + k_3 - m_2\omega_n^2) \end{vmatrix}}{(k_1 + k_2 - m_1\omega_n^2)(k_2 + k_3 - m_2\omega_n^2) - k_2^2} = 0$$

Expanding the above equation and dividing out $m_1 m_2$, we get the frequency equation of the system:

$$\omega_n^4 - \left\{\frac{k_1 + k_2}{m_1} + \frac{k_2 + k_3}{m_2}\right\}\omega_n^2 + \frac{k_1k_2 + k_1k_3 + k_2k_3}{m_1m_2} = 0 \tag{1.50}$$

From equation (1.50) we take the positive values of ω_n^2, as ω_{n1}^2 and ω_{n2}^2.

The general solution of equation (1.36) and (1.39) can be written as:

$$x_1 = A_{11}\, Sin\,(\omega_1 t + \varphi_1) + A_{12}\, Sin\,(\omega_2 t + \varphi_2) \tag{1.51}$$

$$x_2 = \mu_1 A_{11}\, Sin\,(\omega_1 t + \varphi_1) + \mu_2 A_{12}\, Sin\,(\omega_2 t + \varphi_2) \tag{1.52}$$

Where A's and φ's are constants and μ's are amplitude ratios corresponding to ω_1 and ω_2.

With ω_1 and ω_2 being two harmonic components of frequencies, i.e., fundamental and 2nd harmonic. When the initial conditions are appropriate, it is possible that the entire system oscillate at one of the natural frequencies. These particular patterns of motion are called the principal modes of vibration. The lower frequency is called first mode and higher frequency as second mode.

Initial conditions if being such that A_{12} in equation (1.51) is equal to zero, the motions in first mode are:

$$x_1 = A_{11}\, Sin\,(\omega_1 t + \varphi_1) \tag{1.53}$$

$$x_2 = \mu_1 A_{11}\, Sin\,(\omega_1 t + \varphi_1) \tag{1.54}$$

Similarly if by initial conditions $A_{11} = 0$, the motions in 2nd mode are:

$$x_1 = A_{12}\, Sin\,(\omega_2 t + \varphi_2) \tag{1.55}$$

$x_2 = \mu_2 A_{12} \ Sin\ (\omega_2 t + \varphi_2)$ (1.56)

1.10 Lagrange's Equations

Lagrange's equation in fundamental form for generalized coordinates q_i: [30]

$$\frac{d}{dt}\left(\frac{\partial L}{\partial \dot{q}_i}\right) - \frac{\partial L}{\partial q_i} = Q_i \tag{1.57}$$

Where L = K.E - P.E = T –U (1.58)

With K.E = T = Kinetic energy of system = $\frac{1}{2} m_i \dot{x}_i^2$

And P.E = U = Potential energy or strain energy of a system = $\frac{1}{2} k_i x_i^2$

$q_i = q_1$ and $q_2 \cong x_1$ and x_2

Q_i = Generalized external force on system = $F_0 \ Sin\ \omega t$

From equation (1.57) we get:

$$\frac{d}{dt}\left\{\frac{\partial (T-U)}{\partial \dot{q}_i}\right\} - \frac{\partial (T-U)}{\partial q_i} + \frac{\partial (T-U)}{\partial q_i} = Q_i \tag{1.59}$$

With $T = \frac{1}{2} m_1 \dot{x}_1^2 + \frac{1}{2} m_2 \dot{x}_2^2$ (1.60)

And $U = \frac{1}{2} k_1 x_1^2 + \frac{1}{2} k_2 (x_1 - x_2)^2 + \frac{1}{2} k_3 x_2^2$ (1.61)

$$L = T - U = \frac{1}{2} m_1 \dot{x}_1^2 + \frac{1}{2} m_2 \dot{x}_2^2 - \left\{\frac{1}{2} k_1 x_1^2 + \frac{1}{2} k_2 (x_1 - x_2)^2 + \frac{1}{2} k_3 x_2^2\right\} \tag{1.62}$$

From equation (1.62) for m_1:

$$\frac{\partial L}{\partial \dot{x}_1} = m_1 \dot{x}_1 \Rightarrow \frac{d}{dt}\left(\frac{\partial L}{\partial \dot{x}_1}\right) = m_1 \ddot{x}_1 \tag{1.63}$$

And $$\frac{\partial L}{\partial x_1} = -k_1 x_1 - k_2 x_1 + k_2 x_2 = -k_1 x_1 - k_2 (x_1 - x_2) \tag{1.64}$$

Similarly for m_2 :

$$\frac{\partial L}{\partial \dot{x}_2} = m_2 \dot{x}_2 \Rightarrow \frac{d}{dt}\left(\frac{\partial L}{\partial \dot{x}_2}\right) = m_2 \ddot{x}_2 \tag{1.65}$$

And $$\frac{\partial L}{\partial x_2} = -k_2 x_2 + k_2 x_1 - k_3 x_2 = -k_2 (x_2 - x_1) - k_3 x_2 \tag{1.66}$$

Putting equation (1.75), (1.76) in (1.69) for m_1:

$$m_1 \ddot{x}_1 + (k_1 + k_2) x_1 - k_2 x_2 = F_1 Sin\omega t \tag{1.67}$$

Similarly for m_2, putting equation (1.63), (1.64) in (1.57):

$$m_2 \ddot{x}_2 + (k_2 + k_3) x_2 - k_2 x_1 = 0 \tag{1.68}$$

Equations (1.67) and (1.68) are the same as (1.36) and (1.39), though a different approach. Equation (1.67) and (1.68) onwards we can use the same method as from (1.36), (1.39) till (1.56). Lagrange method makes use of the generalized coordinates and gives directly the equations of motion.

1.11 Impedance Method

Newton's Law of motion gives the equations of motion of masses, as derived in (1.67) and (1.68).

The steady state solution is obtained quite easily by the use of mechanical impedance method. [19][43][63]

If we substitute:

$$F_0 e^{j\omega t} = F_0 Sin\omega t$$
$$\overline{X}_1 e^{j\omega t} = x(t) \rightarrow (\overline{X}_1 \text{ is complex amplitude of } x_1(t))$$
$$\overline{X}_2 e^{j\omega t} = x(t) \rightarrow (\overline{X}_2 \text{ is complex amplitude of } x_2(t))$$

And its derivatives:

$$\ddot{x}_1(t) = j^2\omega^2 \overline{X}_1 e^{j\omega t}$$

$$\ddot{x}_2(t) = j^2\omega^2 \overline{X}_2 e^{j\omega t}$$

In equations (1.67) and (1.68):

$$m_1 j^2\omega^2 \overline{X}_1 e^{j\omega t} + (k_1 + k_2)\overline{X}_1 e^{j\omega t} - k_2 \overline{X}_2 e^{j\omega t} = F_0 e^{j\omega t} \tag{1.69}$$

$$m_2 j^2\omega^2 \overline{X}_2 e^{j\omega t} + (k_2 + k_3)\overline{X}_2 e^{j\omega t} - k_2 \overline{X}_1 e^{j\omega t} = 0 \tag{1.70}$$

Where $j = \sqrt{-1}$

Resolving equations (1.69) and (1.70) and using value of j:

$$\overline{X}_1(k_1 + k_2 - m_1\omega^2) - k_2 \overline{X}_2 = F_0 \tag{1.71}$$

$$-\overline{X}_1 k_2 + \overline{X}_2(k_2 + k_3 - m_2\omega^2) = 0 \tag{1.72}$$

Using Cramer's rule:

$$\overline{X}_1 = \frac{\begin{vmatrix} F_0 & -k_2 \\ 0 & (k_2 + k_3 - m_2\omega^2) \end{vmatrix}}{(k_1 + k_2 - m_1\omega^2)(k_2 + k_3 - m_2\omega^2) - k_2^2}$$

Solving the above determinant gives:

$$\bar{X}_1 = \frac{F_0(k_2 + k_3 - m_2\omega^2)}{(k_1 + k_2 - m_1\omega^2)(k_2 + k_3 - m_2\omega^2) - k_2^2} \tag{1.73}$$

$$\bar{X}_2 = \frac{\begin{vmatrix} (k_1 + k_2 - m_1\omega^2) & F_0 \\ -k_2 & 0 \end{vmatrix}}{(k_1 + k_2 - m_1\omega^2)(k_2 + k_3 - m_2\omega^2) - k_2^2}$$

Solving the above determinant gives:

$$\bar{X}_2 = \frac{F_0 k_2}{(k_1 + k_2 - m_1\omega^2)(k_2 + k_3 - m_2\omega^2) - k_2^2} \tag{1.74}$$

In equations (1.73), (1.74) and their preceding determinant forms, by equating to zero the determinant of the coefficients $\bar{X}_1$ *and* $\bar{X}_2$ in equations (1.71) and (1.72); $\Delta\omega_n$ the system natural frequency equation called characteristic, of the system is:

$$\Delta\omega = \frac{\begin{vmatrix} (k_1 + k_2 - m_1\omega^2) & k_2 \\ -k_2 & (k_2 + k_3 - m_2\omega^2) \end{vmatrix}}{(k_1 + k_2 - m_1\omega^2)(k_2 + k_3 - m_2\omega^2) - k_2^2} = 0$$

The displacement vector is written as:

$$\bar{X} = Xe^{j(\omega t - \phi)}$$

As $F_0 Sin\omega t = \mathrm{Im}[F_0 e^{j\omega t}]$

Then, $x_1 = \mathrm{Im}[\bar{X}_1 e^{j\omega t}] = \mathrm{Im}[X_1 e^{-j\phi_1} e^{j\omega t}] = \mathrm{Im}[X_1 e^{j(\omega t - \phi_1)}] = X_1 Sin(\omega t - \phi_1)$

Similarly, $x_2 = \mathrm{Im}[\bar{X}_2 e^{j\omega t}] = \mathrm{Im}[X_2 e^{-j\phi_2} e^{j\omega t}] = \mathrm{Im}[X_2 e^{j(\omega t - \phi_2)}] = X_2 Sin(\omega t - \phi_2)$

Here the displacements $x_1(t)$ and $x_2(t)$ will be either in phase (0 degrees) or out of phase by 180 degrees, with excitation. The steady state response as above is same as in equations (1.48) and (1.49).

Certain vibration problems are conveniently solved by the Mechanical Impedance Method, which makes use of the fact that those impedances of the spring, dashpot and mass are K, $ic\omega$, and $-m\omega^2$ respectively. This method yields steady state response for forced vibration and leads to frequency equation of the system. If differential equations of motion of a multi-degree of freedom system are linear, steady state response of the system to a harmonic excitation is also harmonic at the excitation frequency. This method simplifies work to solve steady state response. In Chapter 3 we see its utility.

1.12 Objectives of this Thesis

To study the dynamic aspects of pipelines. Consider conditions such as deflections, natural frequency and normal modes pertaining to empty pipe, fluid filled pipe and pipe with fluid flow velocity.

As a case study, an industrial Multibillion-dollar in-plant pipeline project is considered to utilize its pertinent data and to compare its results with the other methods used in this Thesis. The author was part of the well-reputed team contracted to design. This project is currently in successful operation for many years. The project drawings are huge and respecting the limitations of tools available at this research stage, we will analyze only some portions and segments of the project in this thesis.

Textbook methods, Industrial methods and ANSYS computer program will be used to study and compare the different techniques and their results. Derive equation of motion using

energy methods with Coriolis Force as the component there in. Develop a Finite Element Method, which employs the use of Coriolis Force along with other aspects of analysis.

Analyse the introduction of this FEM with Coriolis Force into the research work carried out by other scholars [3], [5] and [6].

Draw conclusions based on comparison of techniques and results obtained using data from the actual industrial project considered in this Thesis. Enumerate future research work in this area to improve this Finite Element Method with Coriolis Force.

Take into account the following assumptions in the derivations of equations in this Thesis:

1.12.1 Pipe vibrations are of small amplitudes keeping the terms linear.

1.12.2 Take uniform mass density, keeping terms linear.

1.12.3 Effects of rotary inertia, transverse shear and damping are negligible.

1.12.4 Fluid velocity and pressure taken to be constant.

CHAPTER 2 - METHODS OF CALCULATION

2.1 Introduction

This chapter presents an actual multi-billion dollar industrial project. The project is too large to be dealt with in this thesis as a whole, refer to Figure 2.1. The project is divided into segments and a small part of a segment is analyzed piece-wise, Figures 2.2 and 2.3.

This project was designed by a professional design engineering consulting company as an EPC project. It has been constructed and is ever since in successful operations for one of the largest oil and gas producing companies in the world.

2.2 Calculation and Analysis of the Project

We are going to calculate the deflections and mode shape frequencies with the selected project data, first using standard textbook methods, second using the industrial methods and third using one of the commercial software ANSYS student version. Then we conclude with our analysis.

2.3 Data from Actual Project and Reference Material

The following data is taken from an actual completed project, which is in successful operation at this time.

A set of typical Plant drawings, reference Figures 2.1, 2.2 and 2.3, for such projects are included here for the readers benefit to appreciate the complexity of such design work and the constraints of working with available formulae and software limitations.

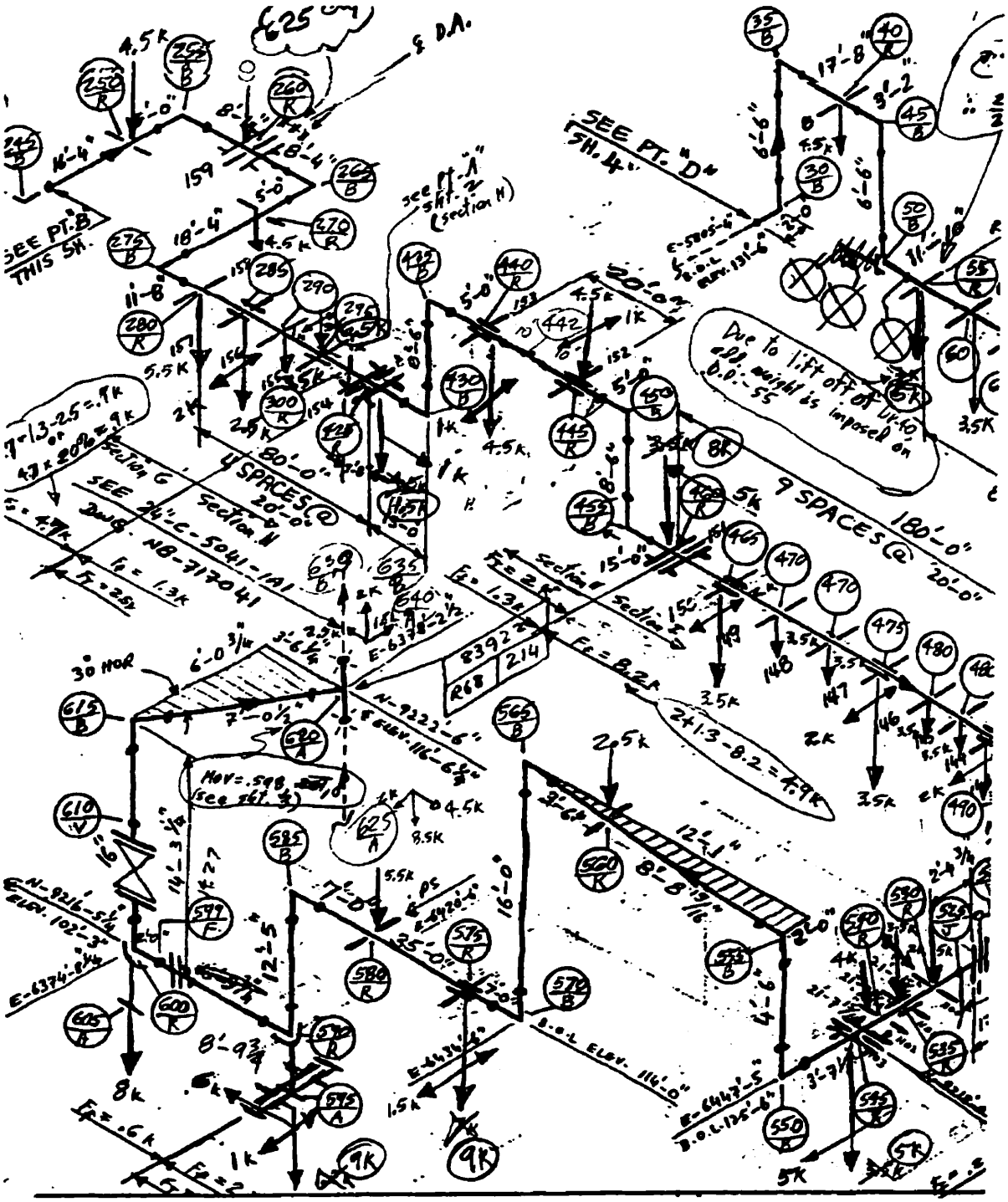

Figure 2.1: Typical Plant Piping Layout

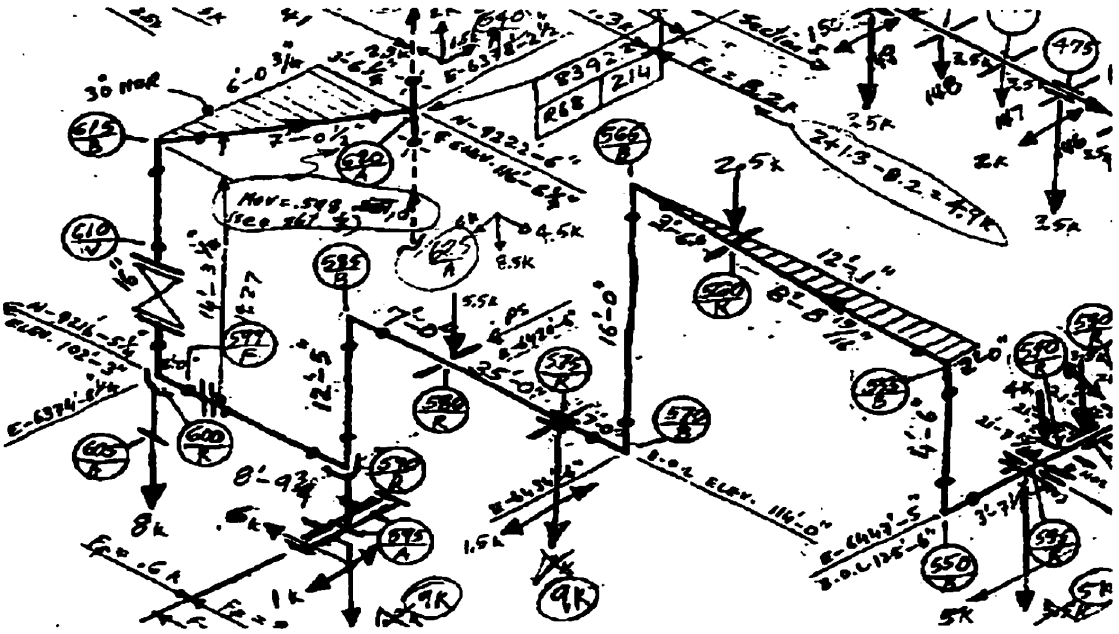

Figure 2.2: View of a Section used for Fixed Ends and Simple Support Cases

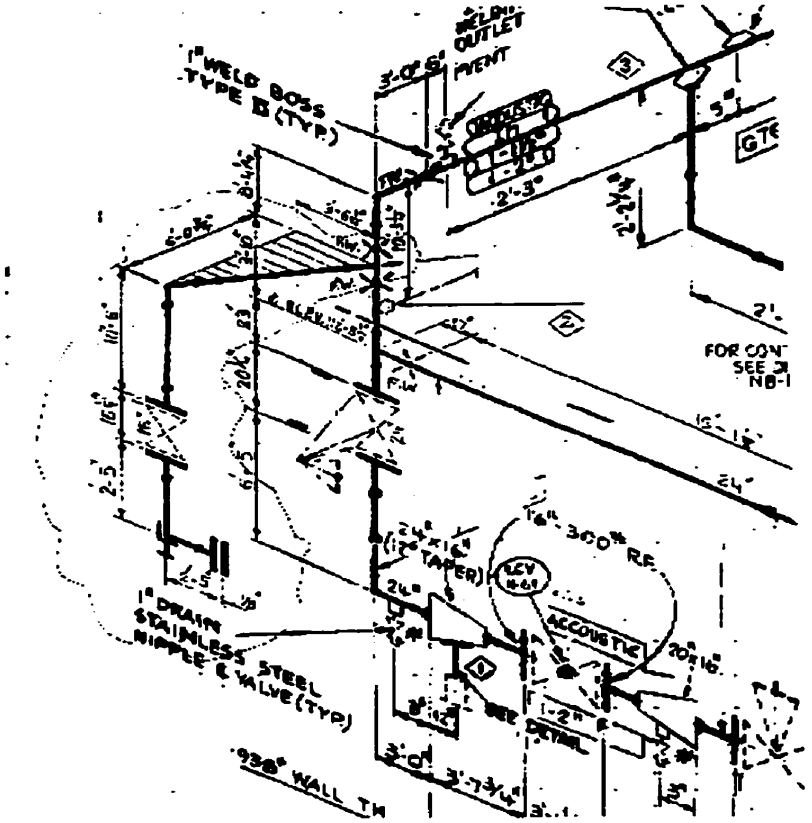

Figure 2.3: Another Section used for Cantilever Case

Analytical and numerical analysis of a portion of the said project is presented here.

The method given hereunder is exactly as was followed by the Design Consulting Company during its design stages of this EPC project. Most professional design consultants use similar methods.

Standards referenced:

ANSI-B 31.3; ASTM A-106; AES-L; ANSI-B 16.5; API-5L; API-6A

Data: (Mostly from the Project, some from the reference material)

Commodity Carried = Liquid Steam

Temperature of Steam-out $T_{steam\text{-}out} = 307^0$ F or 152.78^0 C

Steam-out Pressure $P_{steam\text{-}out} = 60$ psig

Operating Pressure $P_{oper.} = 200$ psig or 13.79 bars

Operating Temperature $T_{oper.} = 170^0$ F or 76.67^0 C

Mass density = 0.97489 lb/ft^3 @ 200 psig/170^0 F

Flow volume $q = 1.02576$ ft^3 @ 200 psig/170^0 F

Design Pressure $P_{design} = 230$ psig or 15.86 bar

Design Temperature $T_{design} = 244^0$ F or 117.78^0 C

Mass density = 0.9434 lb/ft^3 @ 230 psig/244^0 F

Flow volume $q = 1.0601$ ft^3 @ 230 psig/244^0 F

Nominal Pipe Diameter / Outside Diameter ($O.D_{nom.} / O.D$) = 16 inch

Wall Thickness $t_{wall} = 0.375$ inch

Inside Diameter $I.D$ = 15.25 inch

Cross Sectional Metal Area A_{metal} = 18.4 in^2.

Moment of Inertia I = 562 in^4.

Pipe material = Carbon Steel; ASTM-A 53 Gr. B (seamless)

16 in. Nominal Dia. – Standard Weight Designation Pipe; Sch. 30

Section Modulus Z = 70.3 in^3.

Modulus of Elasticity E = $\begin{cases} 27.9 \times 10^6 \text{ psig } @70^0 \text{ F} \\ 27.4 \times 10^6 \text{ psig } @300^0 \text{ F} \end{cases}$

Specified Minimum Yield Strength $\sigma_{yield\text{-}SMYS}$ = 35 X 10^3 psig

Specified Minimum Tensile Strength $\sigma_{tensile\text{-}SMTS}$ = 60 X 10^3 psig

Basic Allowable Stress in Tension $\sigma_{allow\text{-}tension}$ = $\begin{cases} -20 \text{ X } 10^3 \text{ psig } @26^0 \text{ F} \\ 20 \text{ X } 10^3 \text{ psig } @26^0\text{F} \rightarrow 300^0\text{F} \end{cases}$

Radius of Gyration $R_{gyration}$ = 5.53 in.

Gravitational Acceleration g = 386 in/sec^2 or 32.12 ft/sec^2

Weight of Pipe w_{pipe} = 62.6 lb/ft. [23]

Weight of Water w_{water} = 79.1 lb/ft. [23]

Quality Factor E_q = Joint quality factor E_j = 1.0 (seamless) (0.6 – 1.0)

$E_q = E_j$; E_c ; Es

Thickness allowance for corrosion, erosion, manufacturing mill tolerance, material removal in threading; if any of these apply, A = 12.5% = 0.125

Coefficient of material properties and design temperature [22] [28]

$$\begin{cases} Y = 0.4 \ @ \ T < 900^0\text{F} \\ Y = \dfrac{D_{I.D}}{D_{O.D} + D_{I.D}} @ t_{THK.} \geq \dfrac{D_{I.D}}{6} \end{cases}$$

Maximum Allowable Operating Stress $\sigma_{allow.}$ = 0.72 x SMYS = 25,200 psig

Stress with maximum flow $\sigma_{max.-flow} = \sigma_{SMYS}$ + 10,000psig (or 70 MPa) + Q

$$= 35 \times 10^3 + 10{,}000 + 15{,}000 = 60 \times 10^3 \text{ psig}$$

Stress with minimum flow $\sigma_{min.-flow} = \sigma_{SMYS}$ + 10,000psig (or 70 MPa)

$$= 35 \times 10^3 + 10{,}000 = 45 \times 10^3 \text{ psig}$$

Allowable stress at design temperature $\sigma_{hot} = 20 \times 10^3$ psig

2.4 Calculations

Based on the data in section 2.3 and the Figures 2.1, 2.2, 2.3, in the following sections 2.5, 2.6 and 2.7 the calculations as mentioned in section 2.2, shall be carried out.

2.5 Using Standard Text Books

2.5.1 Wall Thickness Calculations [28]

$$t_{\min.} = \frac{P_{design} \times O.D}{2(\sigma_{hot} E_q + P_{design} \times Y)} + A \qquad (2.1)$$

P_{design} = 230 psig.

$O.D$ = 16 inch

$t_{min.} \cong 0.22$ inch

Minimum thickness can also be calculated by the following equations: [28]

$$t_{\min} = \frac{P_{design} \times O.D}{2 \times \sigma_{hot} \times E_q} \tag{2.2}$$

$t_{min.} \cong 0.09$ inch

$$\text{Also; } t_{\min.} = \frac{O.D}{2}\left(1 - \sqrt{\frac{\sigma_{hot} \times E_q - P_{design}}{\sigma_{hot} \times E_q + P_{design}}}\right) \tag{2.3}$$

$t_{min.} \cong 0.18$ inch

One can see that different textbook literature gives different results, as above.

Selected thickness per Proponent and Project design:

$t = 0.375$ inch

2.5.2 Allowable Pressure Calculations [28][35]

To find the maximum allowable operating pressure based on the selected wall thickness:

$$P_{MAOP} = \frac{2\sigma_{hot} \times E_q t}{O.D - 2Yt} \tag{2.4}$$

$P_{MAOP} \cong 955$ psig

2.5.3 Hydrostatic Test Pressure Calculations [28][35]

$$P_{hydrotest} = 1.5\ P_{design} \tag{2.5}$$

$P_{hydrotest} = 345$ psig

Textbook literature does not limit the test pressures. So we take 345 psig as the test pressure.

2.5.4 Fixed Ends Case

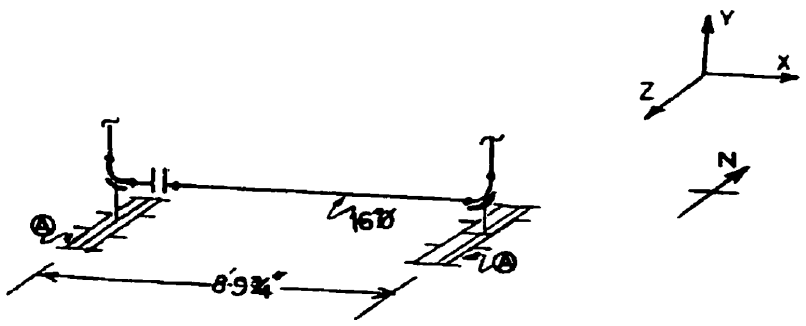

Figure 2.4: Segment of the Project
Fixed End Conditions

2.5.4.1 Pipe Span Calculations [28]

Limited by Bending Stress

$$L = \sqrt{\frac{0.4Z\sigma_{hot}}{w_{pipe} + w_{water}}} \tag{2.6}$$

$L \cong 63$ ft.

Limited by Deflection

$$L = \sqrt[4]{\frac{\Delta EI}{13.5(w_{pipe} + w_{water})}} \qquad \text{(taking maximum } \Delta = 1 \text{ inch)} \tag{2.7}$$

$L \cong 53.3$ ft

Thus, we can take the pipe span to be 53.3 ft. being the lesser of the two spans calculated. But the Piping Engineer/Designer has selected a span of 8'-9.75" or 8.8125ft, due to other project constraints and requirements.

Thus, we will check both, our calculated span and the project designer proposed span.

2.5.4.2 Natural Frequency [28][30][42]

$$f_n = \frac{1}{2\pi}\sqrt{\frac{g}{\Delta}} \tag{2.8}$$

$$f_n = \frac{3.12}{\sqrt{\Delta}} \tag{2.9}$$

f_n = 3.12 cps or 19.6 rad/sec (For pipe span of 53.3 ft.)

f_n = 3.6cps or 22.62 rad/sec. (For pipe span of 8.8125 ft.)

We shall use the actual project designer selected pipe span as it gives a higher natural frequency and lower deflections.

2.5.4.3 Mode Shapes Frequencies [42]

$$\omega_n = a_n\sqrt{\frac{EI}{mL^4}} \tag{2.10}$$

m = mass per unit length

$$\omega_n = a_n\sqrt{\frac{EIgL}{WL^4}} \tag{2.11}$$

Where a_n depends on end conditions. For n = 1, 2, 3, 4, 5 mode shapes, the numeric constant values and corresponding mode shapes/harmonic frequencies of empty pipe are:

For a_1 = 22 ⟶ ω_1 = 2099.92 rad/sec or 334.21 cps

For a_2 = 61.7 ⟶ ω_2 = 5889.32 rad/sec or 937.31 cps

For a_3 = 121 ⟶ ω_3 = 11549.55 rad/sec or 1838.17 cps

For a_4 = 200 ⟶ ω_4 = 19090.17 rad/sec or 3038.30 cps

For $a_5 = 298.2$ ⟶ ω_5 = 28463.44 rad/sec or 4530.10 cps

The numerical constant values of a_n for n = 1, 2, 3, 4, 5 mode shapes, and the corresponding mode shapes/harmonic frequencies of fluid filled pipe are:

For $a_1 = 22$ ⟶ ω_1 = 1395.74 rad/sec or 222.14 cps

For $a_2 = 61.7$ ⟶ ω_2 = 3914.42 rad/sec or 623.00 cps

For $a_3 = 121$ ⟶ ω_3 = 7676.57 rad/sec or 1221.76 cps

For $a_4 = 200$ ⟶ ω_4 = 12688.55 rad/sec or 2019.45 cps

For $a_5 = 298.2$ ⟶ ω_5 = 18918.63 rad/sec or 3010.99 cps

2.5.4.4 Bending Moment and Shear Force [31]

Here we will find out the shear stress, bending moments and end supports reaction forces, for the fixed end conditions:

At the fixed ends deflection Δ and slope φ are zero.

Shear Force:

$$F_{shear} = \frac{(w_{pipe} + w_{water})L}{2} \tag{2.12}$$

F_{shear} = 624.37 lbs.

Bending Moment:

Moment at mid span: $M_1 = \frac{(w_{pipe} + w_{water})L^4}{24}$ (2.13)

M_1 = 458.52 ft-lb.

Moment at each end: $M_{\max.} = \dfrac{(w_{pipe} + w_{water})L^2}{12}$ (2.14)

$M_{max.}$ = 917.04 ft-lb.

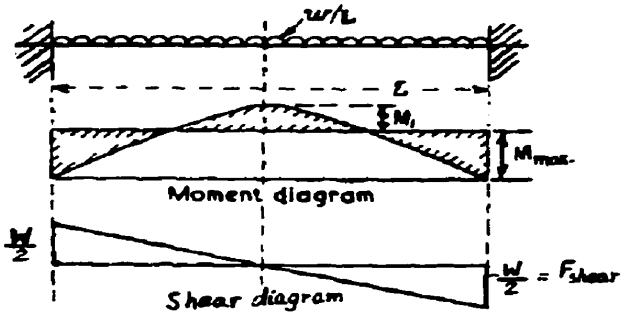

Figure 2.5: Bending Moment / Shear Force Diagrams
Fixed End Conditions

2.5.5 Simple Supported Ends Case

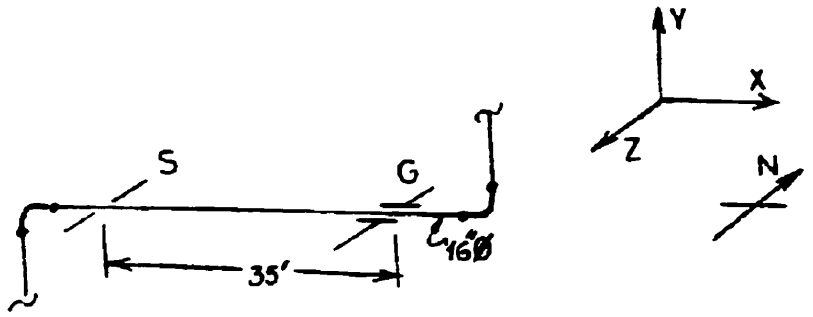

Figure 2.6: Segment of the Project
Simply Supported End Conditions

The basic project, material and other data is the same as in the previous case, where we considered the pipe as with fixed ends condition.

We need not make some of the calculations we did for the previous case; like wall thickness calculations; allowable pressure calculations; and hydrostatic test Pressure Calculations. As conditions for these calculations have not changed for this segment of the pipeline of this project.

Thus we carry out the other required calculations as here:

2.5.5.1 Pipe Span Calculations [28] [31]

Limited by bending stress

$$L = \sqrt{\frac{0.33 Z \sigma_{hot}}{(\omega_{pipe} + \omega_{fluid})}} \tag{2.15}$$

$L \cong 57$ ft

Limited by Deflection

$$L = \sqrt[4]{\frac{384 \Delta E I}{5(\omega_{pipe} + \omega_{fluid})}} \quad \text{(taking maximum } \Delta = 1 \text{ inch, using consistent units)} \tag{2.16}$$

$L \cong$ 46.88 ft

Thus we could take the pipe span to be 46.88 ft. being the lesser of the two calculated spans. But the piping engineer/designer has selected a span of 35 ft., due to other project considerations.

Thus we will have to check both, our calculated span and the project designer proposed span.

2.5.5.2 Natural Frequency

Making use of equations (2.8) or (2.9):

$f_n = 3.12$ cps or 19.6 rad/sec. (for pipe span of 46.88 ft.)

f_n = 5.6 cps or 35.2 rad/sec. (for pipe span of 35 ft.)

We shall use pipe span of 35ft., giving higher natural frequency and lower deflections.

2.5.5.3 Mode Shapes Frequencies [42]

$$\omega_n = a_n \sqrt{\frac{EI}{mL^4}} \tag{2.17}$$

$$\omega_n = a_n \sqrt{\frac{EIg}{WL^3}} \tag{2.18}$$

Where a_n depends on end conditions. For n = 1, 2, 3, 4, 5 mode shapes, the numerical constant values and the corresponding mode shapes/ frequencies are:

For $a_1 = 9.87 \rightarrow \omega_1 = 39.7$ rad/sec. or 6.32 cps

For $a_2 = 39.5 \rightarrow \omega_2 = 158.7$ rad/sec. or 25.29 cps

For $a_3 = 88.9 \rightarrow \omega_3 = 357.6$ rad/sec. or 56.91 cps

For $a_4 = 158 \rightarrow \omega_4 = 635.5$ rad/sec. or 101.14 cps

For $a_5 = 247 \rightarrow \omega_5 = 993.4$ rad/sec. or 158.11 cps

2.5.5.4 Bending Moment and Shear Force [31]

Shear stress and bending moments, for the case of simply supported end conditions, are calculated here:

Deflection Δ is zero and slope Φ is not zero, at the ends.

Shear force:

$$F_{shear} = \frac{(\omega_{pipe} + \omega_{fluid})}{2} \tag{2.19}$$

F_{shear} = 70.85 lb.

Bending moment:

Moment at mid span: $M_{\max} = \dfrac{(\omega_{pipe} + \omega_{fluid})L^2}{8}$ (2.20)

M_{max} = 21,697.81 ft-lb.

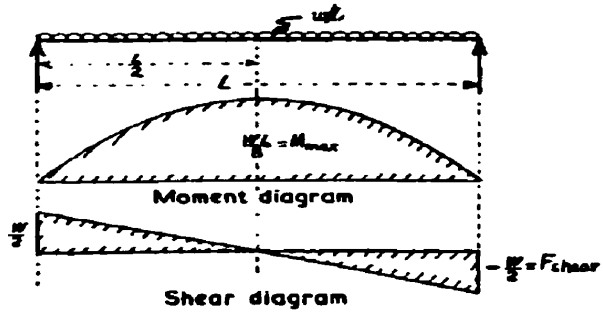

Figure 2.7: Bending Moment /Shear Force Diagrams
Simply Supported End Conditions

2.5.6 Cantilever End Case

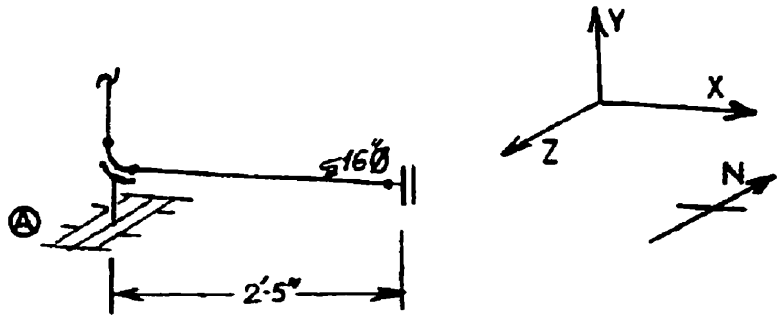

Figure 2.8: Segment of the Project
Cantilever End Conditions

With rest of the project, and other data being the same as for calculated cases, we study the cantilevered section of the project as:

2.5.6.1 Pipe Span Calculations

Limited by bending stress

$$L = \sqrt{\frac{0.083\sigma_{hot} Z}{(\omega_{pipe} + \omega_{fluid})}} \tag{2.21}$$

$L \cong 28.7$ ft.

Limited by deflection: [31]

$$L = \sqrt[4]{\frac{8EI\Delta}{(\omega_{pipe} + \omega_{fluid})}} \quad \text{(taking maximum } \Delta = 1 \text{ inch, using consistent units)} \tag{2.22}$$

$L = 26.63$ ft.

2.5.6.2 Natural Frequency

$$f_n = \sqrt{\frac{3.12}{1.63 \times 10^{-8}}} \tag{2.23}$$

$f_n = 24{,}666$ cps or 1,54,981.1 rad/sec.

2.5.6.3 Mode Shapes Frequencies [42]

$$\omega_n = a_n \sqrt{\frac{EIg}{WL^3}} \tag{2.24}$$

Where a_n depends on end conditions. For n = 1, 2, 3, 4, 5 mode shapes, the numerical constant values and the corresponding mode shapes/harmonic frequencies are:

For $a_1 = 3.52$ $\rightarrow$ $\omega_1 = 2{,}961.37$ rad/sec. or 471.32 cps

For $a_2 = 22.0$ → $\omega_2 = 18{,}508.54$ rad/sec. or 2,945.73 cps

For $a_3 = 61.7$ → $\omega_3 = 51908.05$ rad/sec. or 8,261.42 cps

For $a_4 = 121.0$ → $\omega_4 = 1{,}01{,}796.99$ rad/sec. or 1,6201.49 cps

For $a_5 = 200.0$ → $\omega_5 = 1{,}68{,}259.49$ rad/sec. or 26,779.33 cps

2.5.6.4 Bending Moment and Shear Force

Shear force and bending moments, for this cantilevered end conditions, are:

Slope ϕ and deflection $\Delta \neq 0$ at free end.

Shear force:

$$F_{shear} = -(\omega_{pipe} + \omega_{fluid})L \tag{2.25}$$

F_{shear} = -342.9 lbs

$$M_{\max} = -\frac{(\omega_{pipe} + \omega_{fluid})L^2}{2} \qquad \text{(Bending moment at fixed ends)} \tag{2.26}$$

M_{max} = - 414.93 ft-lb

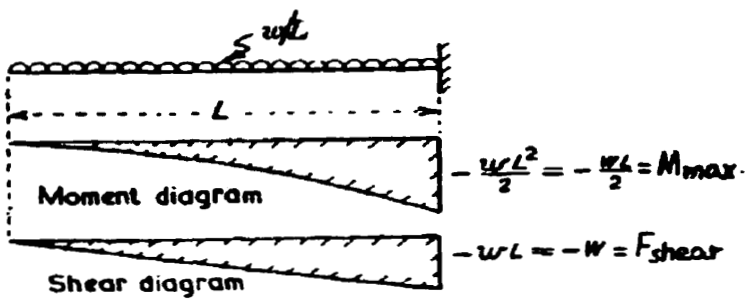

Figure 2.9: Bending Moment/Shear Force Diagrams
Cantilever End Conditions

2.6 Using Industrial Methods

The following calculations are based on standard methods used in the industry.

Saudi ARAMCO design practice, Fluor Daniel design and stress analyst design guides, Chiyoda Chemical Engineering and Construction, and Kellogg design handbook are referred to. [22] [23] [39]

2.6.1 Wall thickness Calculations

$$t_{\min} = \frac{P_{design} O.D}{2(\sigma_{hot} E_q + P_{design} Y)(1.0 - A)} \tag{2.27}$$

$t_{min.} \cong 0.11$ inch

We check here if the special considerations of theory of failure, fatigue and thermal stress are needed: [22]

$O.D/6 = 2.67$ (as $t_{min} \leq D_o/6$, no special conditions as described above are required)

Also, $\frac{P_{design}}{\sigma_{hot} E_q} = 0.0115$ (for $\frac{P_{design}}{\sigma_{hot} E_q} < 0.385$, no special considerations are needed)

Due to the above two results; theory of failure, fatigue and thermal stress need not have special consideration. As it is taken to be a thin wall pipe.

For construction reasons a 16" dia. Pipe will have a minimum wall thickness of 0.25 inch.

Proponent and project design selected:

$t_{THK.} = 0.375$ inch.

Which still satisfies the above criteria for a thin wall pipe.

2.6.2 Allowable Pressure Calculations

Maximum allowable operating pressure based on selected t_{THK}, per ANSI-B31.3: [35]

$$P_{MAOP} = \frac{2t(1.0 - A)\sigma_{hot}E_q}{O.D - 2t(1.0 - A)Y} \tag{2.28}$$

$P_{MAOP} \cong 8.5$ psig

2.6.3 Hydrostatic Test Pressure Calculations

$$P_{hydrotest} = \frac{2 \times 0.9\sigma_{hot}t(1.0 - A)}{O.D} \tag{2.39}$$

$P_{hydrotest} \cong 740$ psig

2.6.4 Fixed Ends Case

Reference Figure 2.4.

2.6.4.1 Pipe Span Calculations [22]

Limited by Bending Stress:

$$L \leq \sqrt{\frac{0.5Z\sigma_{hot}}{(w_{pipe} + w_{fluid})}} \tag{2.30}$$

$L \leq 70.4$ ft.

Limited by Deflection:

$$L \leq \sqrt[4]{\frac{\Delta EI}{3.375(w_{pipe} + w_{fluid})}} \qquad \text{(taking maximum } \Delta = 1 \text{ inch)} \tag{2.31}$$

L $\cong 75$ ft.

Obviously, using shorter of the two lengths, we take L = 70.4 ft., to keep the natural frequency as high possible.

Project designer and Proponent have selected 8.8125 ft. span for this segment of pipeline.

Thus we are obliged to check for L = 70.4 ft. and L = 8.8125 ft. both.

2.6.4.2 Natural Frequency

$$f_n = \frac{1.7}{L^2}\sqrt{\frac{EI}{(w_{pipe} + w_{fluid})}} \tag{2.32}$$

$f_n \cong$ 228.2 c.p.s or 1433.8 rad/sec. (for span of 8.8125 ft.)

$f_n \cong$ 3.6 c.p.s or 22.6 rad/sec. (for span of 70.4 ft.)

Thus we take pipe span of 8.8125ft. giving lower deflection and higher natural frequency.

2.6.4.3 Mode Shapes and Frequencies [42]

$$\omega_n = a_n\sqrt{\frac{gEI}{(w_{pipe} + w_{fluid})L^4}} \tag{2.33}$$

Where a_n depends on end conditions. For n = 1, 2, 3, 4, 5 mode shapes, the numeric constant values and corresponding mode shapes/harmonic frequencies of empty pipe are:

For a_1 = 3.56 $\rightarrow$ ω_1 = 339.81 c.p.s or 2135.06 rad/sec.

For a_2 = 9.82 $\rightarrow$ ω_2 = 937.33 c.p.s or 5889.4 rad/sec.

For a_3 = 19.24 $\rightarrow$ ω_3 = 1836.47 c.p.s or 11538.91 rad/sec.

For a_4 = 31.81 $\rightarrow$ ω_4 = 3036.29 c.p.s or 19077.58 rad/sec.

For a_5 = 47.52 $\rightarrow$ ω_5 = 4535.82 c.p.s or 28499.43 rad/sec.

The numerical constant values of a_n for n = 1, 2, 3, 4, 5 mode shapes, and the corresponding mode shapes/harmonic frequencies of fluid filled pipe are:

For $a_1 = 3.56 \rightarrow \omega_1 = 225.85$ c.p.s or 1419.06 rad/sec.

For $a_2 = 9.82 \rightarrow \omega_2 = 623.0$ c.p.s or 3914.47 rad/sec.

For $a_3 = 19.24 \rightarrow \omega_3 = 1223.64$ c.p.s or 7669.50 rad/sec.

For $a_4 = 31.81 \rightarrow \omega_4 = 2018.11$ c.p.s or 12680.19 rad/sec.

For $a_5 = 47.52 \rightarrow \omega_5 = 3014.80$ c.p.s or 18942.55 rad/sec.

2.6.5 Simply Supported Ends Case

Reference Figure 2.6

2.6.5.1 Pipe Span Calculations [22]

There are quite often contiguously supported pipelines. Also, a segment of pipeline on either side of a support may be connected to the other segments of the same pipeline. The effects of simple support are overshadowed by the continuity of the pipe passed the supports. Continuity of a pipe over a support gives somewhat of a fixed end condition. It is not truly fixed end either. Thus some designers just take the average of the effects of fixed end and that of simply supported end condition. Others take a little more caution towards actual picture. Here we will present different possible approaches and compare:

2.6.5.1.1 Simply Supported-Simple Support Effects

Pipe span limited by bending stress:

$$L \leq \sqrt{\frac{0.33 Z \sigma_{hot}}{(\omega_{pipe} + \omega_{fluid})}} \tag{2.34}$$

$L \leq 57.2\text{ft}$

Limited by deflection

$$L \leq \sqrt[4]{\frac{\Delta EI}{18(\omega_{pipe} + \omega_{fluid})}} \qquad \text{(taking maximum } \Delta = 1 \text{ inch)} \qquad (2.35)$$

$L \leq 49.57\text{ft}$

One can take $L = 49.57$ ft., as shorter of two lengths. But project designer selected 35ft.

Thus we calculate frequencies for both L = 49.57ft. and 35ft.

2.6.5.1.2 Natural Frequency

$$f_n = \frac{0.737}{L^2}\sqrt{\frac{EI}{(\omega_{pipe} + \omega_{fluid})}} \qquad (2.36)$$

$f_n = 3.13$ cps or 19.7 rad/sec. (for $L = 49.57$ft.)

$$\Delta = \frac{18(\omega_{pipe} + \omega_{fluid})L^4}{EI} \qquad \text{(for } L = 35\text{ft.)} \qquad (2.37)$$

$\Delta = 0.249$ inch

$f_n = 6.27$ cps or 39.4 rad/sec. (using equation (2.37))

Thus we take $L = 35$ft. as the frequency is higher with this length.

2.6.5.1.3 Mode Shapes and Frequencies

Using equation (2.34). Where a_n depends on end conditions. For n = 1, 2, 3, 4, 5 the numerical constant values and the corresponding mode shapes/harmonic frequencies are:

For $a_1 = 1.57 \quad \rightarrow \quad \omega_1 = 6.31$ rad/sec. or 39.7cps

For $a_2 = 6.28 \rightarrow \omega_2 = 25.25$ rad/sec. or 158.7 cps

For $a_3 = 14.14 \rightarrow \omega_3 = 56.84$ rad/sec. or 357.2 cps

For $a_4 = 25.13 \rightarrow \omega_4 = 101.02$ rad/sec. or 634.7 cps

For $a_5 = 39.27 \rightarrow \omega_5 = 157.87$ rad/sec. or 991.9cps

2.6.5.2 Simply Supported-Combined Conditions Effects [22] [28]

Pipes are segments of generally 20 ft. (6 meter) lengths combined to form a pipeline. Elbows, tees, continuous supports etc are all these factors that add-up to diminish the effects of pipes being simply supported. Their welding and other above given factors, give rigidity but not enough to be called totally fixed end condition. Thus experience has shown to the industry to take the combined effect of simply supported or pinned joint and that of fixed end as a more close to true representation of pipes on continuous supports.

Limited by stress:

$$L \leq \sqrt{\frac{0.4Z\sigma_{hot}}{(\omega_{pipe} + \omega_{fluid})}} \tag{2.38}$$

L = 63 ft.

Limited by deflection:

$$L \leq \sqrt[4]{\frac{\Delta EI}{13.5(\omega_{pipe} + \omega_{fluid})}} \qquad \text{(taking maximum } \Delta = 1 \text{ inch)} \tag{2.39}$$

L = 53.26 ft.

Taking L = 53.26 ft. being shorter of the two lengths.

As seen from article (2.6.5.1.1) and (2.6.5.2), L = 35 ft. being shortest length thus the frequencies will be higher. Hence we need not calculate for any other pipe lengths and conclude to take L = 35ft. for this piece of project.

2.6.6 Cantilever End Case

Reference Figure 2.8

2.6.6.1 Pipe Span Calculations

Such a case is not found too often but not rare either. Having long horizontal cantilevered pipes is extremely rare. Only short sections, usually less than 5 ft. in length are found in practice. But one can find quite often, vertical cantilever pipes such as exhaust chimney of a plant, gas flare line, distillation columns, and storage vessels.

This nature of support is thus very beneficial but poses enormous challenges to the designers. Like the effect of wind load on cantilever sections. Wind load is a dynamic load, at times as catastrophic as seismic can be. We discuss this later in the thesis.

Limited by deflection:[22]

$$L \leq \sqrt[4]{\frac{\Delta EI}{144(\omega_{pipe} + \omega_{fluid})}} \qquad \text{(taking maximum } \Delta = 1 \text{ inch)} \qquad (2.40)$$

$L \leq$ 29.47 ft.

Limited by bending stress:

$$L \leq \sqrt{\frac{0.083Z\sigma_{hot}}{(\omega_{pipe} + \omega_{fluid})}} \qquad (2.41)$$

$L \leq$ 28.7 ft.

We can thus opt for $L \leq 28.7$ ft. being shorter of the two lengths. But project designer selected, based on other project requirements, length of $L = 2.42$ ft.

Thus we will evaluate both lengths.

2.6.6.2 Natural Frequency

$$f_n = \frac{0.2606}{L^2}\sqrt{\frac{EI}{(\omega_{pipe} + \omega_{fluid})}} \tag{2.42}$$

$f_n = 3.3$cps or 20.7 rad/sec. (for $L \leq 28.7$ft.)

$f_n = 463.88$cps or 2914.6 rad/sec. (for $L = 2.42$ft.)

We shall then take $L = 2.42$ft.

2.6.6.3 Mode Shapes and Frequencies

Using equation (2.34). Where a_n depends on end conditions. For n = 1, 2, 3, 4, 5 the numerical constant values and the corresponding mode shapes/harmonic frequencies are:

For $a_1 = 0.56$ → $\omega_1 = 471.13$ rad/sec. or 2960.2 cps

For $a_2 = 3.51$ → $\omega_2 = 2952.96$ rad/sec. or 18554.0 cps

For $a_3 = 9.82$ → $\omega_3 = 8261.57$ rad/sec. or 51909.0 cps

For $a_4 = 19.24$ → $\omega_4 = 16186.61$ rad/sec. or 101703.5 cps

For $a_5 = 31.81$ → $\omega_5 = 26761.75$ rad/sec. or 168149.0 cps

2.6.7 Both Ends Anchored, 90^0 Elbow in Horizontal xz-Plane [22] [39]

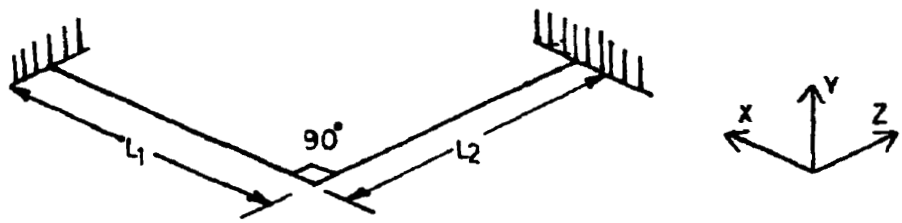

Figure 2.10: Horizontal Pipe Bend in xz Plane
Pipe Anchored at Both Ends, 90^0 Elbow

Assuming all mass for the two legs is at the elbow.

Assuming here:

$L_1 = L_2$ and $L_1/L_2 = 1.0$

Then, $EI/GJ = 1.0$

As EI/GJ = Bending Rigidity/Torsional Rigidity = $1.3 \cong 1.0$ [22] [39]

The above is assumed for pipes as an industrial practice

$W_{eff} = 5/16\ W = 5/16\ L$

$L_{eff} = 1/2\ L$

$L = L_1 + L_2$

Thus each pipe segment L_1 and L_2 is cantilevered.

2.6.7.1 Deflection

$$\Delta = \frac{\frac{576W_{eff}}{EI}}{\frac{\frac{1}{L^3_1}}{1-\frac{0.75}{1+\frac{EIL_2}{GJL_1}}} + \frac{\frac{1}{L^3_2}}{1-\frac{0.75}{1+\frac{EIL_1}{GJL_2}}}} \qquad [22] \qquad (2.43)$$

$$\Delta = \frac{180W_{eff}L^3_{eff}}{EI} \qquad (2.44)$$

$$\Delta = \frac{7.03WL^3}{EI}$$
$$\Delta = \frac{7.03wL^4}{EI} \qquad (2.45)$$

$L_1 = L_2$, and $L = L_1 + L_2 = 8 + 8 = 16$ ft.

$\Delta = 4.24 \times 10^{-3}$ inch.

2.6.7.2 Frequency

$$f_n = \frac{1}{2\pi}\frac{\sqrt{g}}{\sqrt{\Delta}} = \frac{3.127}{\sqrt{\Delta}}$$

$f_n = 48.03$ cps

Similarly we can derive and calculate for various unequal lengths, angles in horizontal plane and also in the vertical plane.

2.7 Using ANSYS Computer Program [2] [67]

In this section, numerical results by Finite Element Program ANSYS have been calculated for the case of fixed ends pipe using data from section 2.3.

The idea is to present the results as could be obtained using a commercial computer program. ANSYS, educational version being available at the Department of Mechanical and Manufacturing Engineering – University of Calgary, was the obvious choice. To see if similar output as produced using the Finite Element Method developed in Chapter 3, could be generated through the commercially available program. To analyze the difference in quality, ability, versatility, ease and accuracy of the use of the commercial package to that offered by the Finite Element Method developed in Chapter 3.

The following data has been used as input to the ANSYS computer program.

2.7.1 Data

$E = 27.4 \times 10^6$ lb/in^2 $= 3.9456 \times 10^9$ lb/ft^2

$I = 562$ in^4 $= 0.0271$ ft^4

$D_{O.D} = 16$ in. $= 1.33$ ft $\qquad R_{O.D} = 8$ in. $= 0.667$ ft

$D_{I.D} = 15.25$ in. 1.271 ft $\qquad R_{I.D} = 7.625$ in. $= 0.635$ ft

$L = 105.75$ in. $= 8.8125$ ft

$t_{wall} = 0.375$ in. $= 0.03125$ ft.

$g = 386$ in/sec^2 $= 32.2$ ft/sec^2

$\upsilon = 0.3$ (Poisson's ratio)

Density of pipe = 489.71 lb/ft^3

Density of pipe + fluid = 685.09 lb/ft^3

Element = Solid Brick 8 node 45

2.7.2 Cases Considered

Cases considered, all with fixed end boundary conditions:

Case1a: Empty pipe with pipe self-load acting. No external and internal loads taken. Static analysis, for deflections and stresses.

Case1b: Empty pipe with pipe self-load acting. No external and internal loads taken. Modal analysis, for frequency mode shapes.

Case2a: Fluid filled pipe with pipe and fluid self-load acting. No external and internal loads taken. Static analysis, for deflections and stresses.

Case2b: Fluid filled pipe with pipe and fluid self-load acting. No external and internal loads taken. Modal analysis, for frequency mode shapes.

2.7.3 Computer Outputs and Results

In this section are given the outputs as directly taken from the computer program ANSYS. The different cases considered, as described in section 2.7.2 above, are given below. Attached are the pertinent graphic form of the results giving the deflections, stresses and the mode shape frequencies. Some of the graphics included are to give the isometric view of the cases considered. Tables of system mode shape frequencies have been included for each case too.

An element called, Solid-Brick-8 node 45 with 6 degrees of freedom at each node was used for the fixed ends section of the pipe chosen.

As this version of ANSYS does not give the option of using uniformly distributed load, self-load of pipe and the fluid were applied as concentrated loads calculated through effective weight method, given in Chapter 1. System density was also used in the model.

Figures 2.11 through 2.36 are self-explanatory. The range of values of forces, deflections and stresses for the particular deflection cases and vibration cases, are shown in the deflected figures. The same is also given numerically and as a colour band to the right of the figures.

Summary of System Frequencies

SET	TIME/FREQ	LOAD STEP	SUBSTEP	CUMULATIVE
1	265.53	1	1	1
2	266.07	1	2	2
3	580.15	1	3	3
4	598.16	1	4	4
5	599.20	1	5	5

Table 2.1: Summary of System Frequencies – Empty Pipe
Case1b PipeEmptyVibrations

SET	TIME/FREQ	LOAD STEP	SUBSTEP	CUMULATIVE
1	224.50	1	1	1
2	224.96	1	2	2
3	490.50	1	3	3
4	505.72	1	4	4
5	506.60	1	5	5

Table 2.2: Summary of System Frequencies – Fluid Filled Pipe
Case2b PipeFluidFilledVibrations

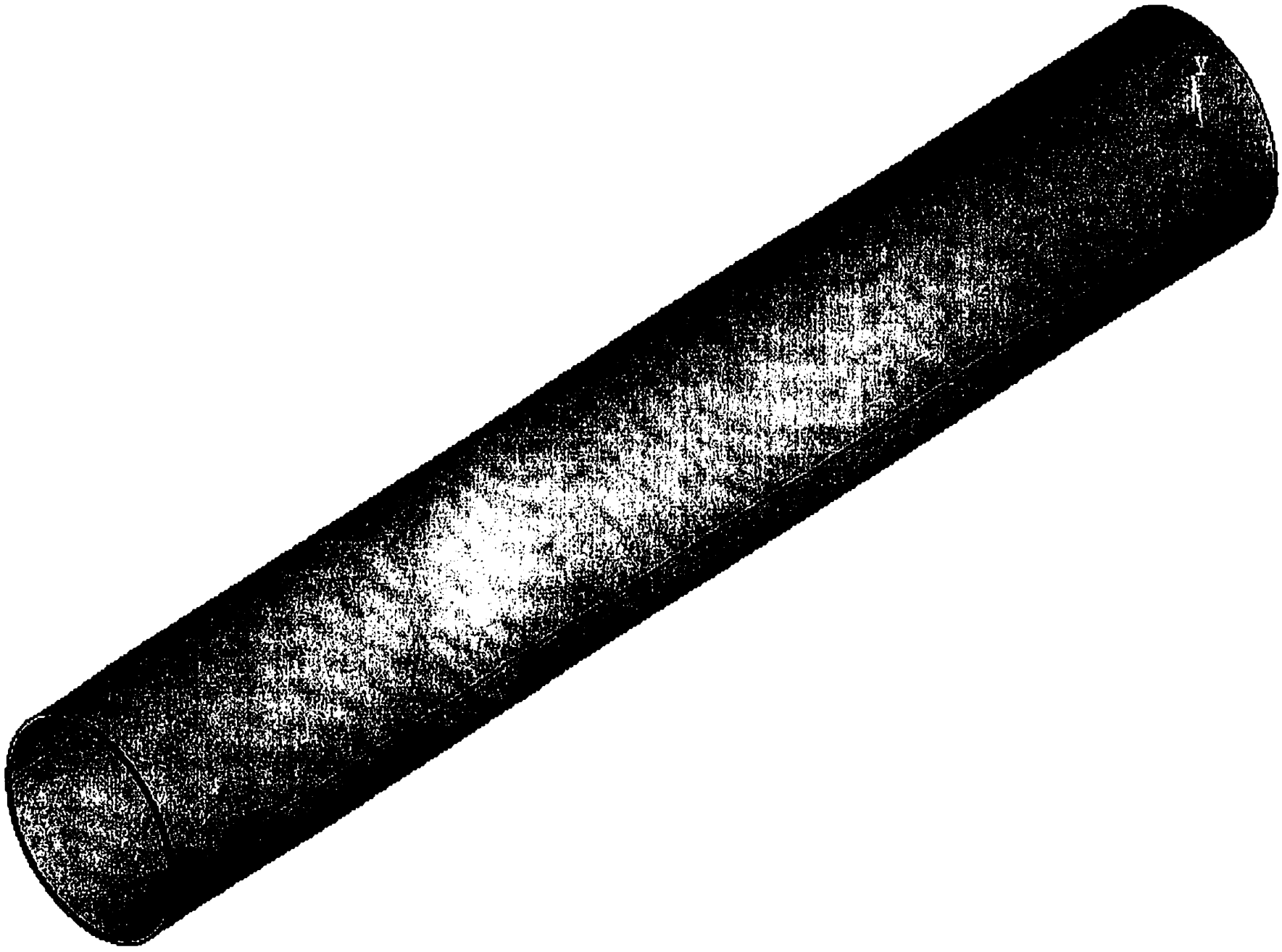

Figure 2.11 Isometric View of Pipe

Case1aPipeEmptyDeflStress **Case1a Pipe Empty - Deflection and Stress**

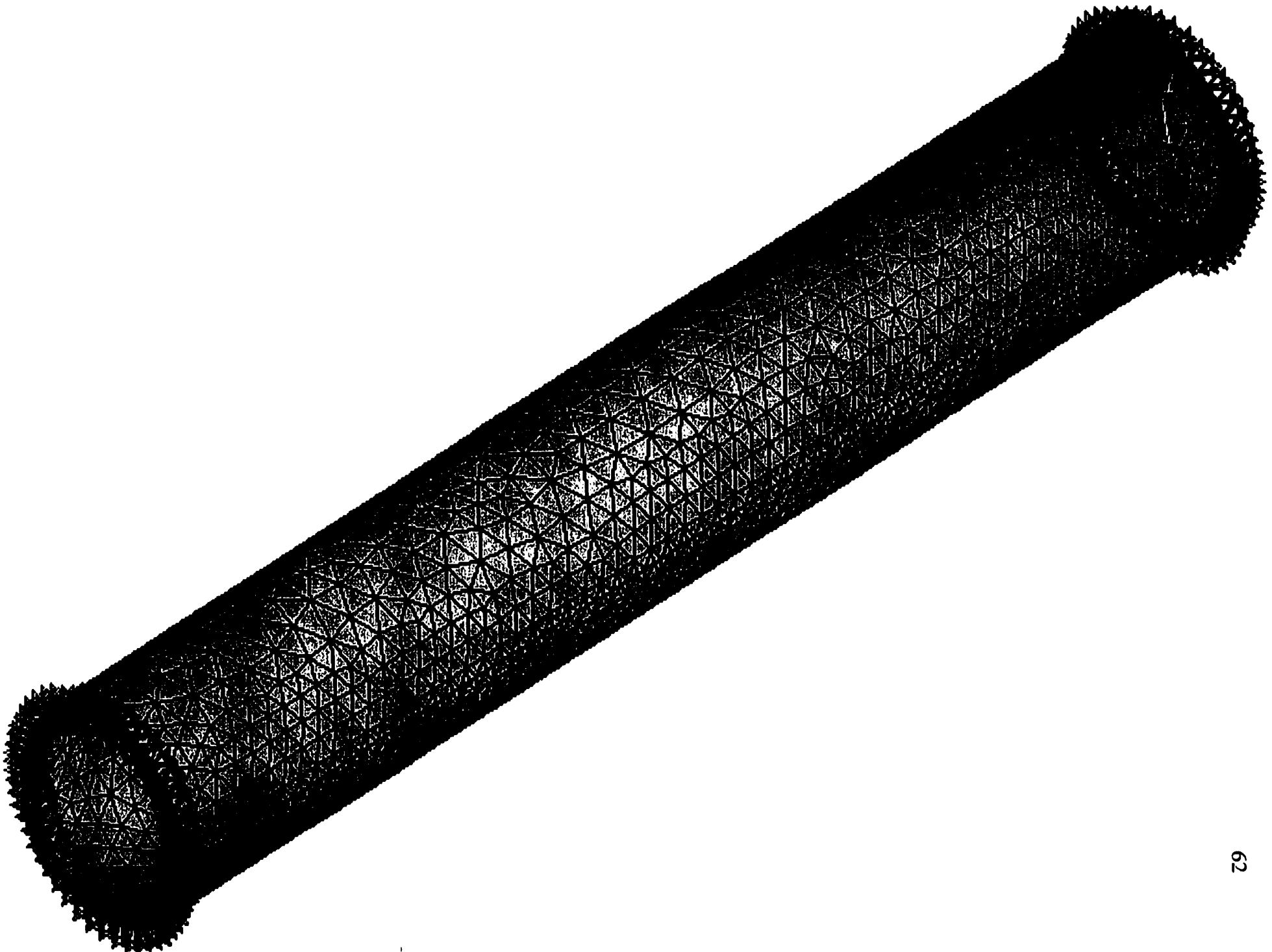

Figure 2.12 Isometric View of Pipe Meshed and Anchored

Case1a Pipe Empty - Deflection and Stress

Case1aPipeEmptyDeflStress

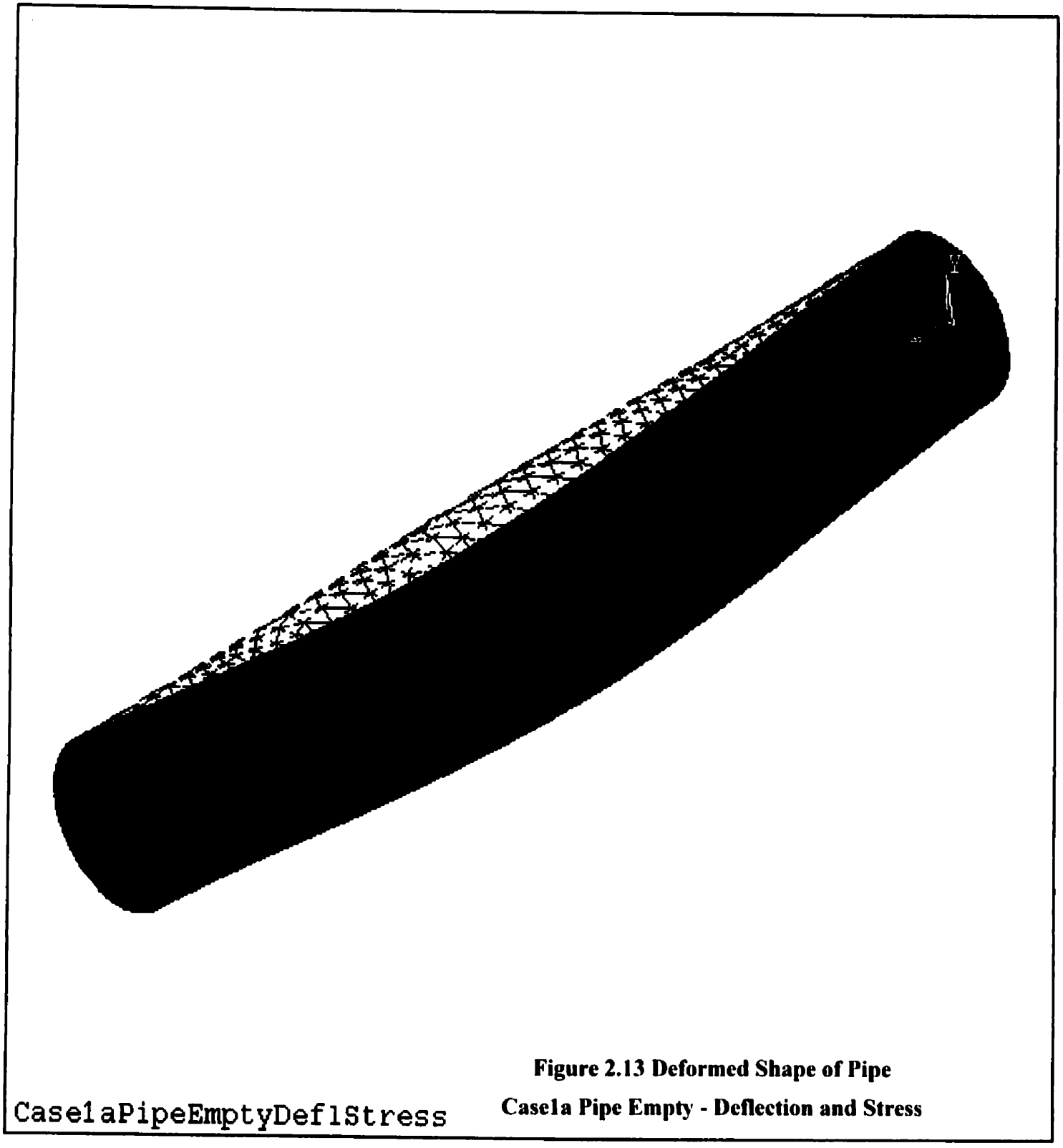

Figure 2.13 Deformed Shape of Pipe

Case1a Pipe Empty - Deflection and Stress

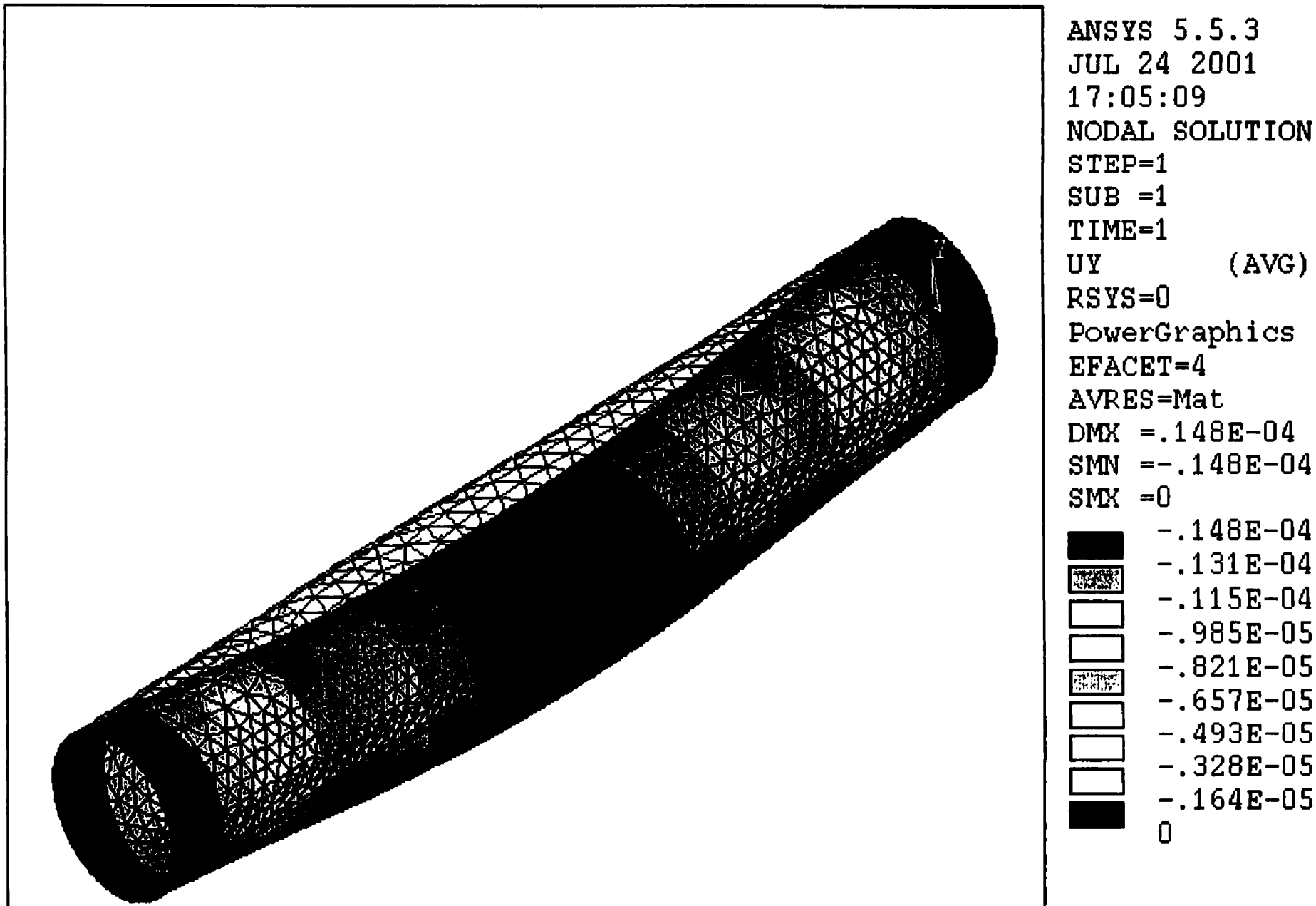

Figure 2.14 Deflections of Pipe

Case1aPipeEmptyDefl Stress **Case1a Pipe Empty - Deflection and Stress**

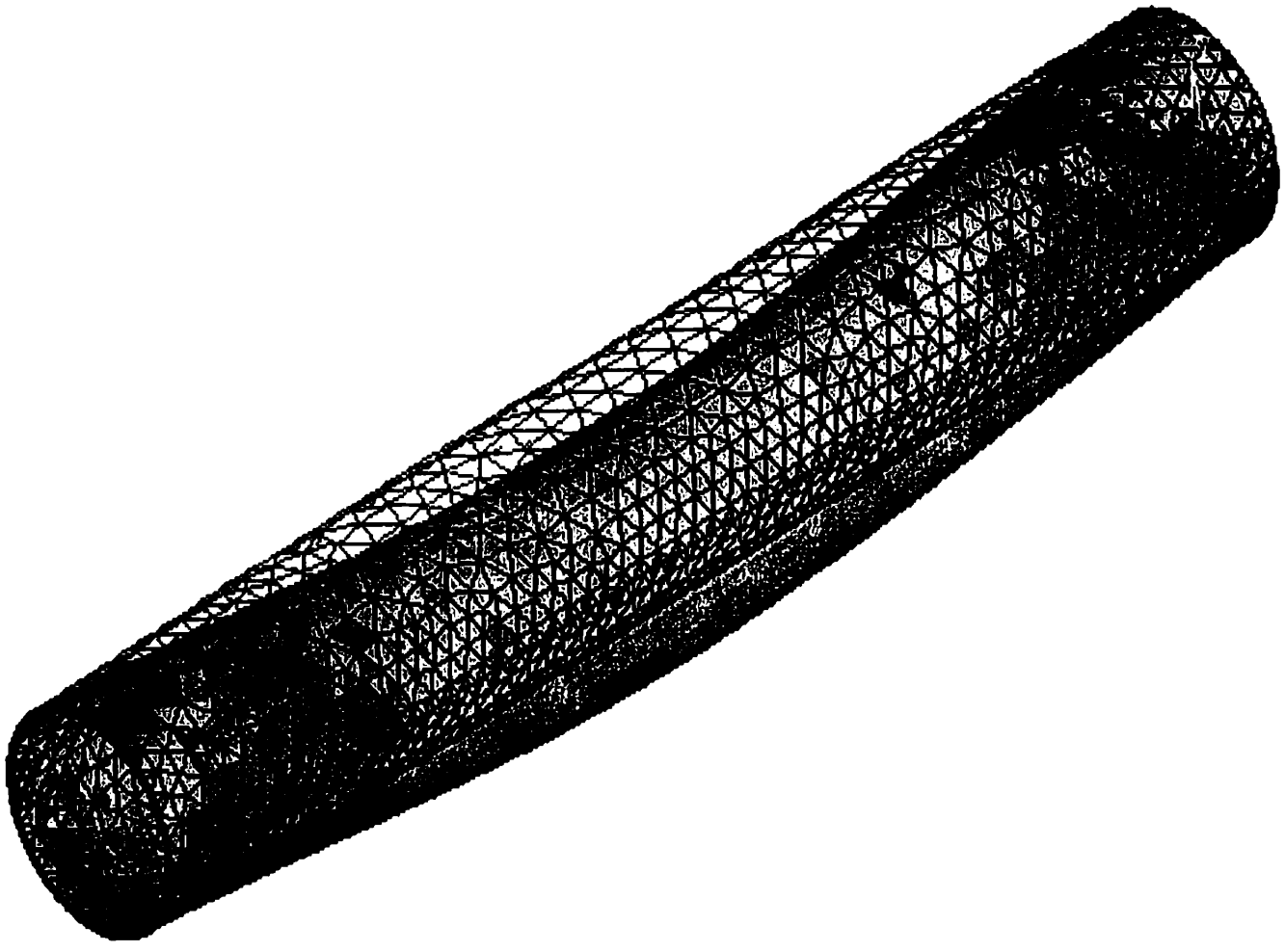

ANSYS 5.5.3
JUL 24 2001
17:28:33
NODAL SOLUTION
STEP=1
SUB =1
TIME=1
SY (AVG)
RSYS=0
PowerGraphics
EFACET=4
AVRES=Mat
DMX =.148E-04
SMN =-7038
SMX =5591

-7038
-5634
-4231
-2828
-1425
-21.912
1381
2784
4187
5591

Figure 2.15 Normal Stresses in Pipe - Nodal Solution

Case1aPipeEmptyDeflStress

Case1a Pipe Empty - Deflection and Stress

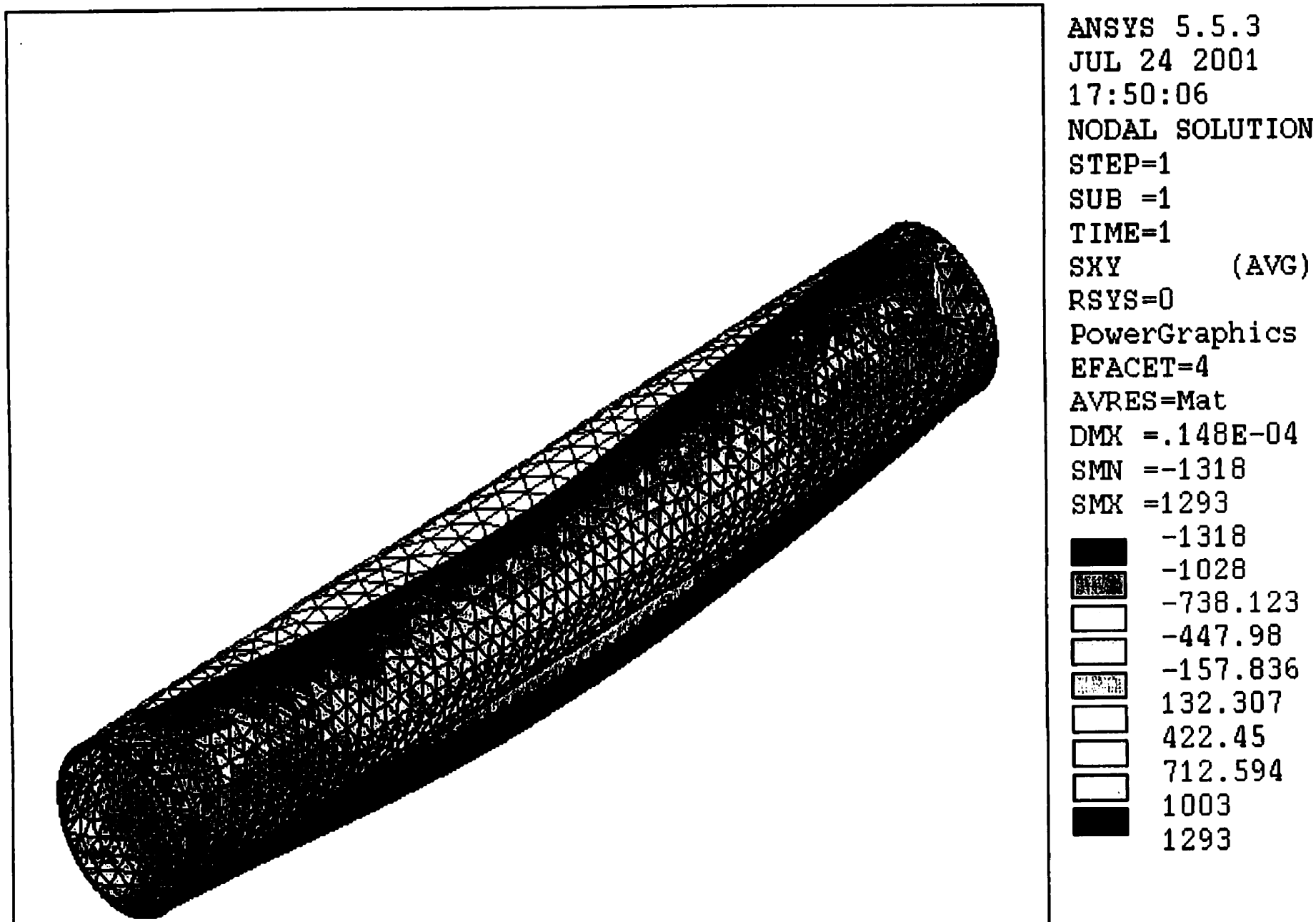

Figure 2.16 Shear Stresses in Pipe - Nodal Solution

Case1aPipeEmptyDefl Stress **Case1a Pipe Empty - Deflection and Stress**

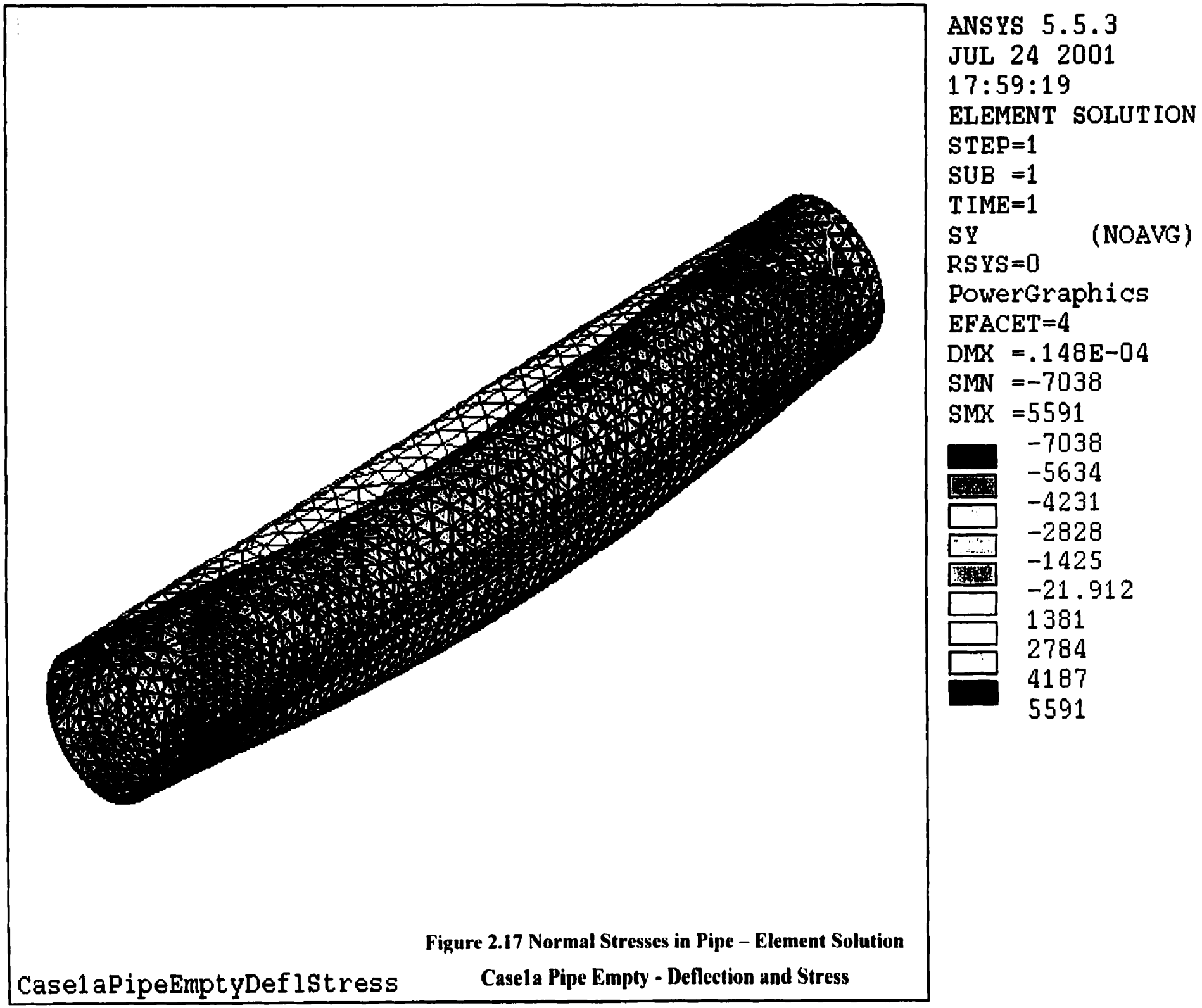

Figure 2.17 Normal Stresses in Pipe – Element Solution

Case1a Pipe Empty - Deflection and Stress

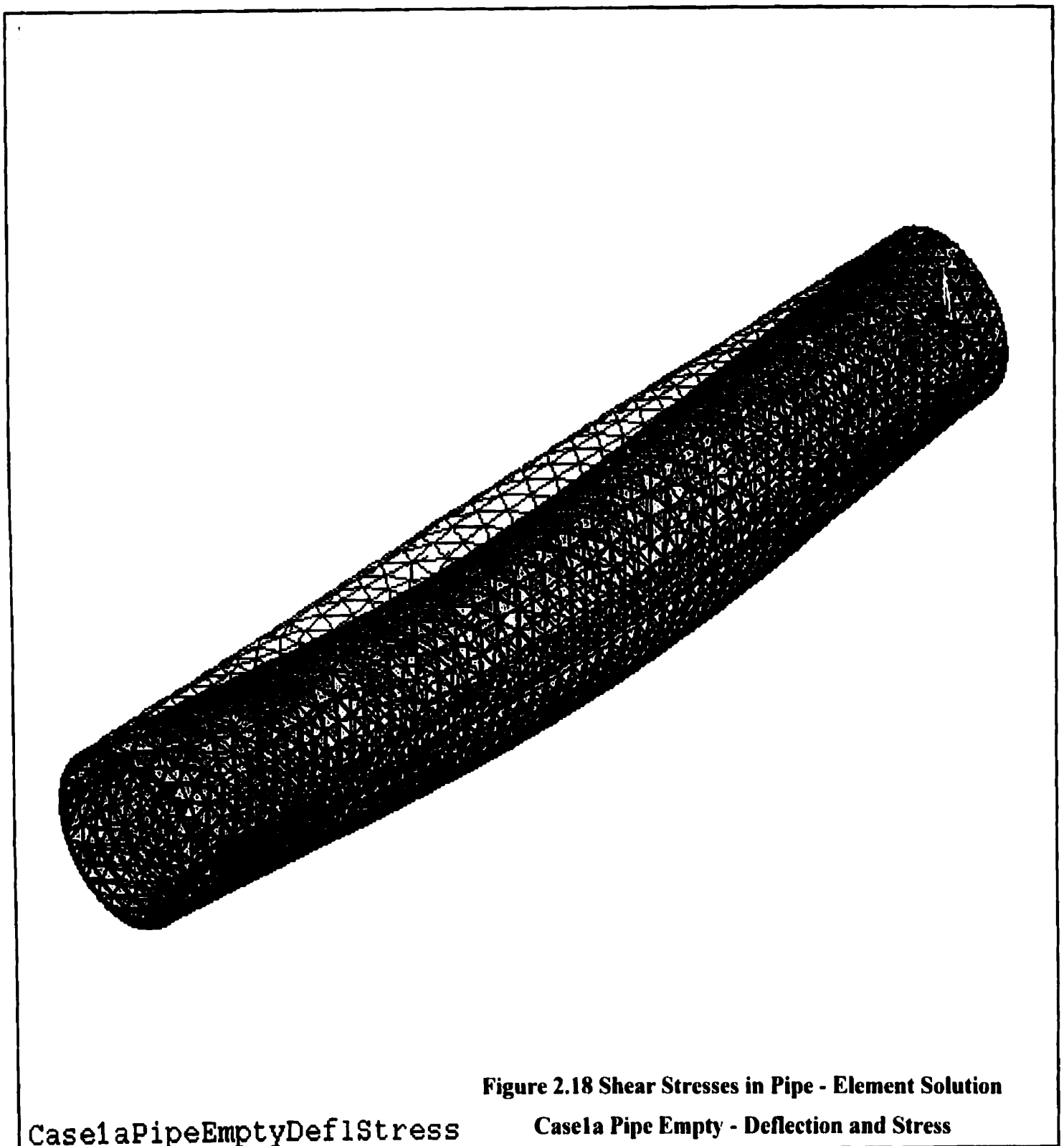

Figure 2.18 Shear Stresses in Pipe - Element Solution

Case1a Pipe Empty - Deflection and Stress

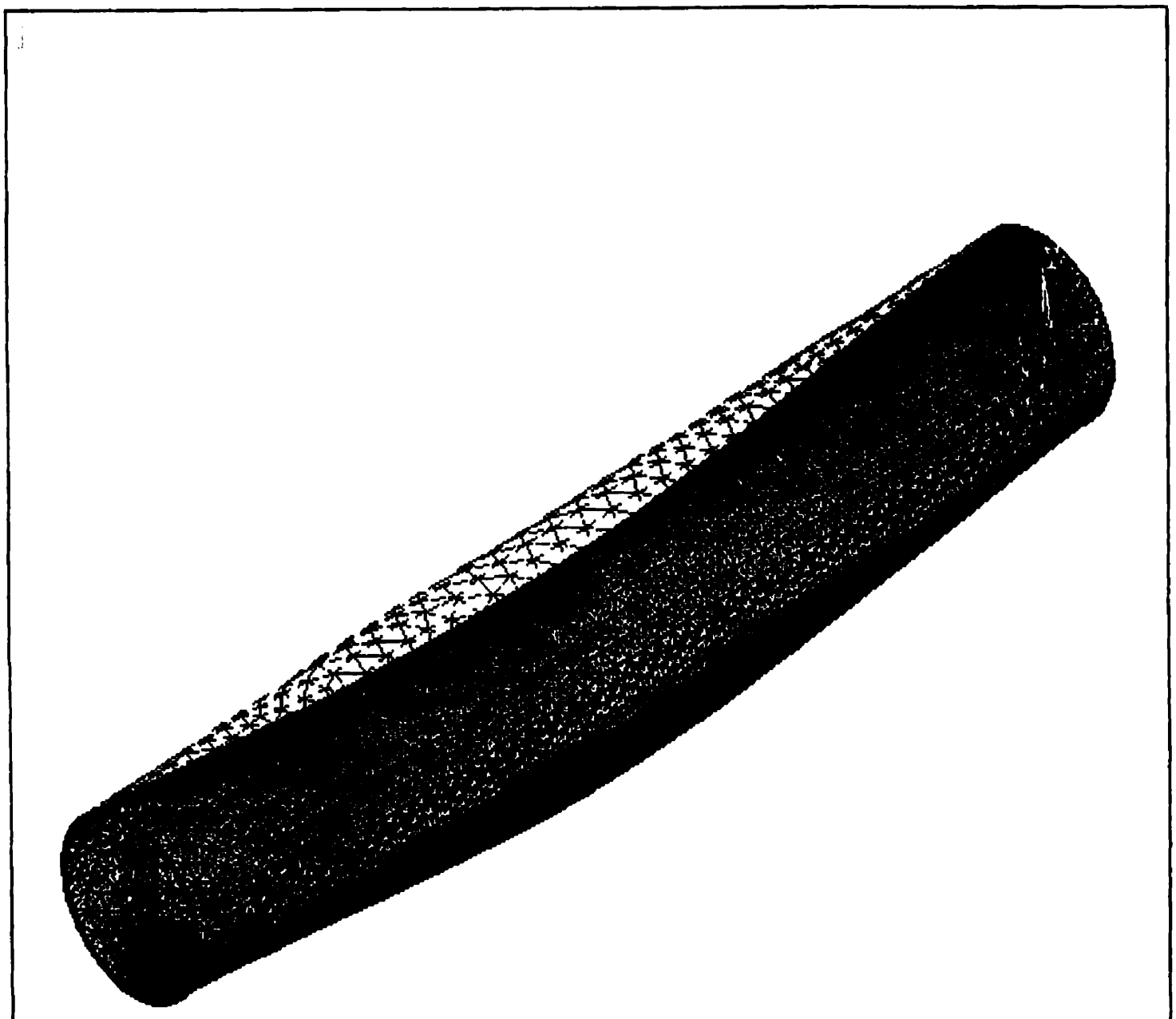

Figure 2.19 Element Forces on Pipe – Element Solution

Case1aPipeEmptyDefl Stress

Case1a Pipe Empty - Deflection and Stress

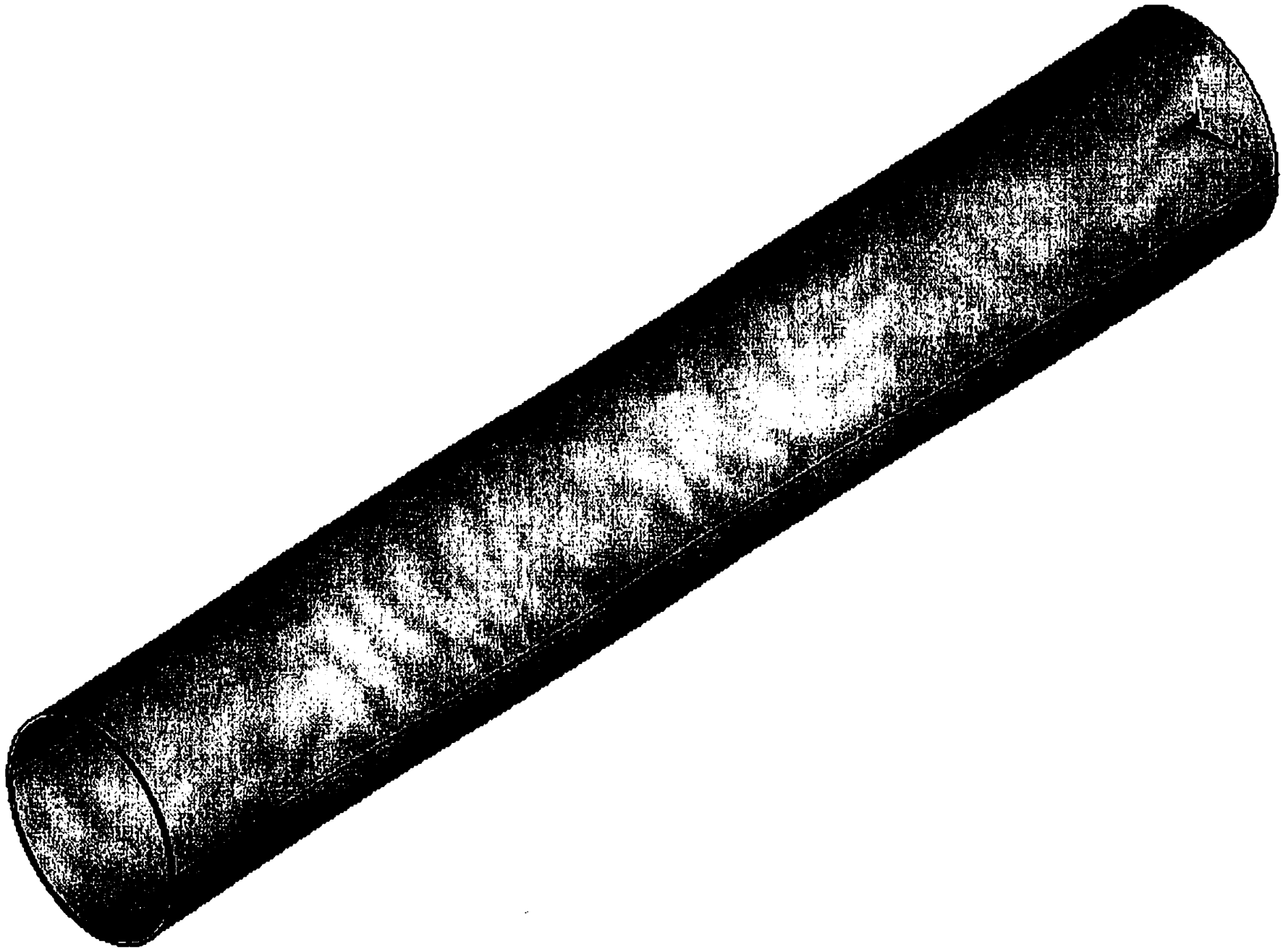

Figure 2.20 Isometric View of Pipe

Case1bPipeEmptyVibrations

Case1b Pipe Empty – Mode Shapes

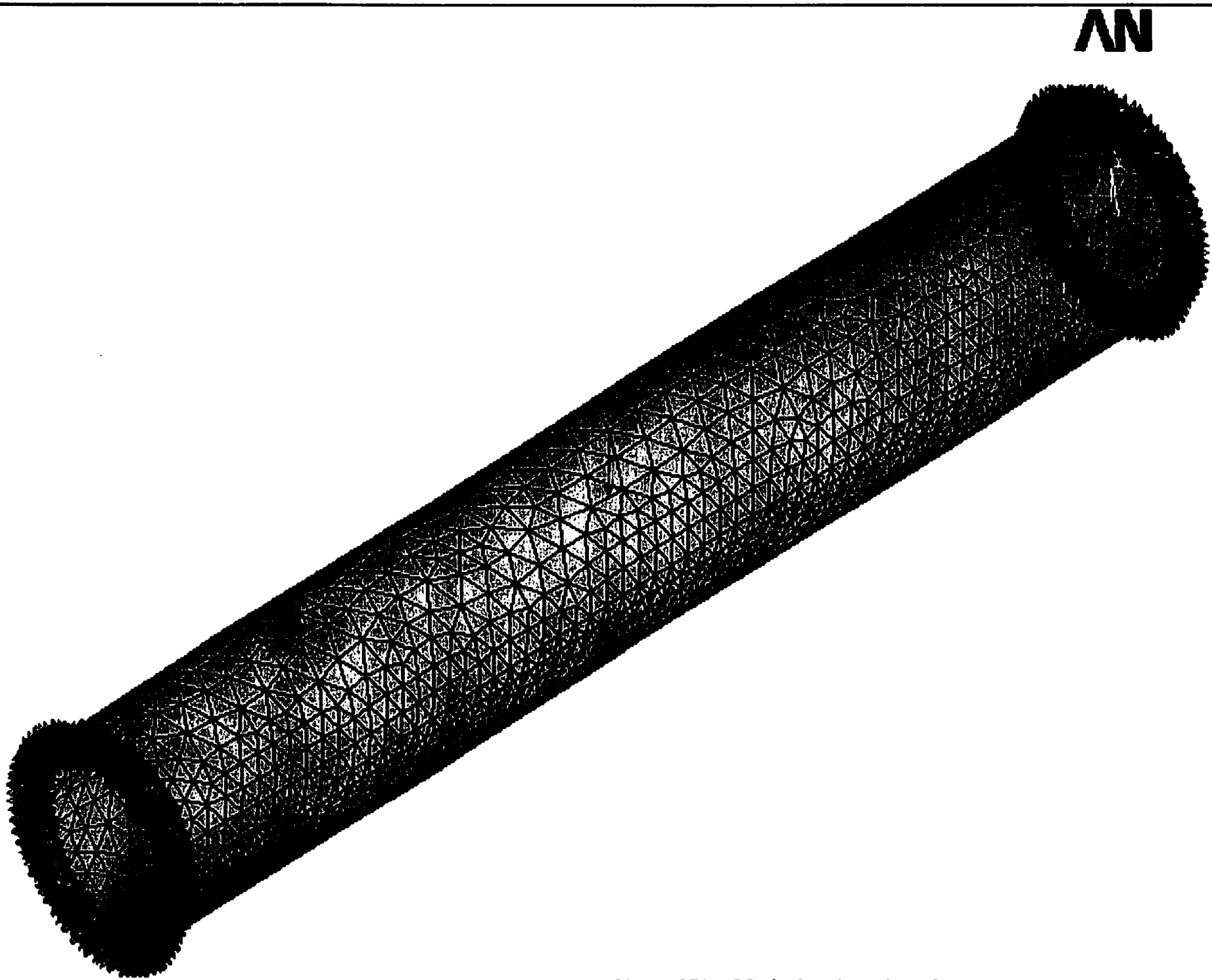

Figure 2.21 Isometric View of Pipe Meshed and Anchored

Case1bPipeEmptyVibrations

Case1b Pipe Empty – Mode Shapes

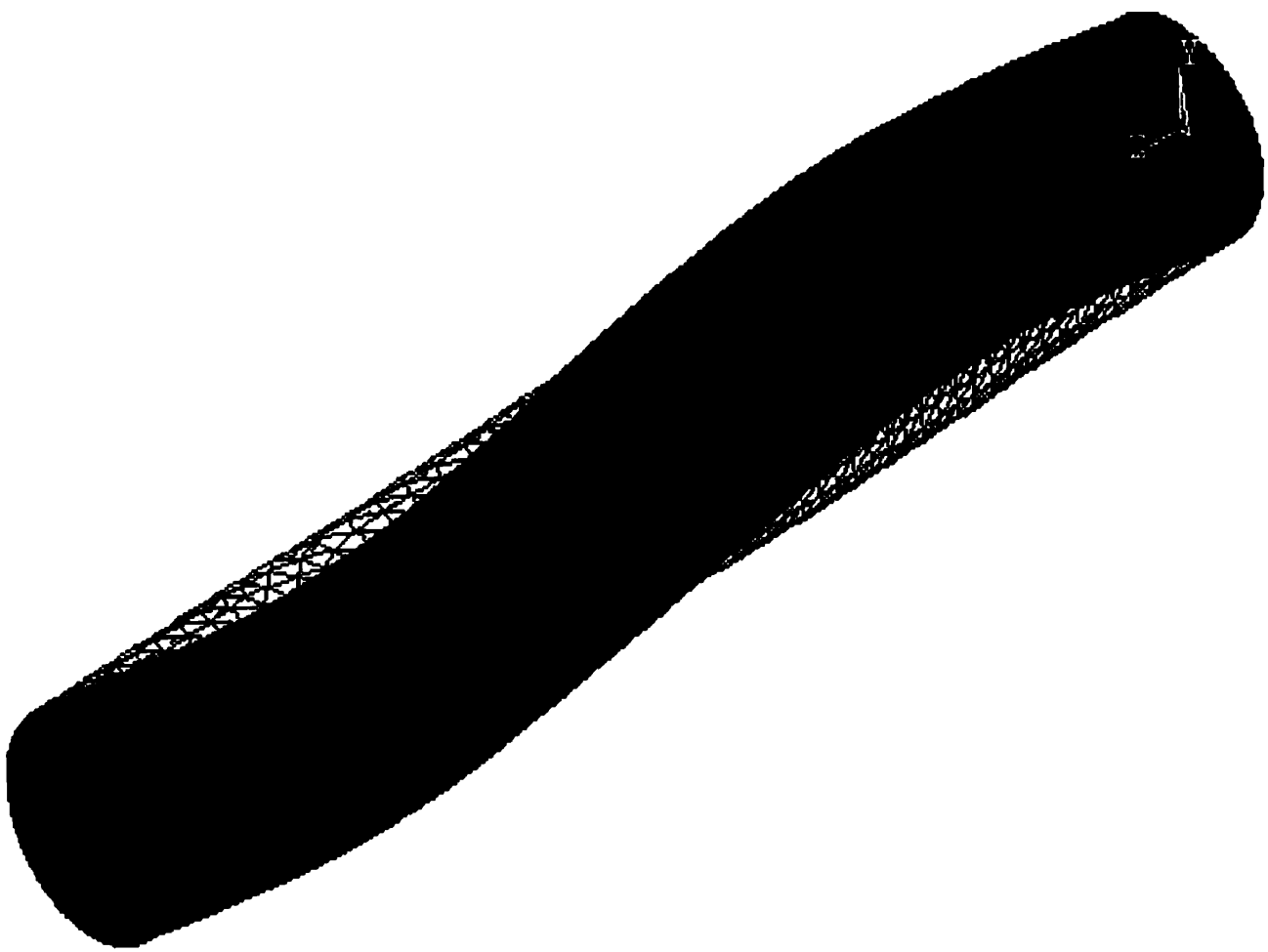

ANSYS 5.5.3
JUL 26 2001
01:39:21
DISPLACEMENT
STEP=1
SUB =5
FREQ=599.199
PowerGraphics
EFACET=4
AVRES=Mat
DMX =.35019

DSCA=1.258
XV =1
YV =1
ZV =1
DIST=4.038
XF =.001622
YF =-.522E-03
ZF =4.406
Z-BUFFER

Case1bPipeEmptyVibrations

Figure 2.22 Deformed Shape of Pipe

Case1b Pipe Empty – Mode Shapes

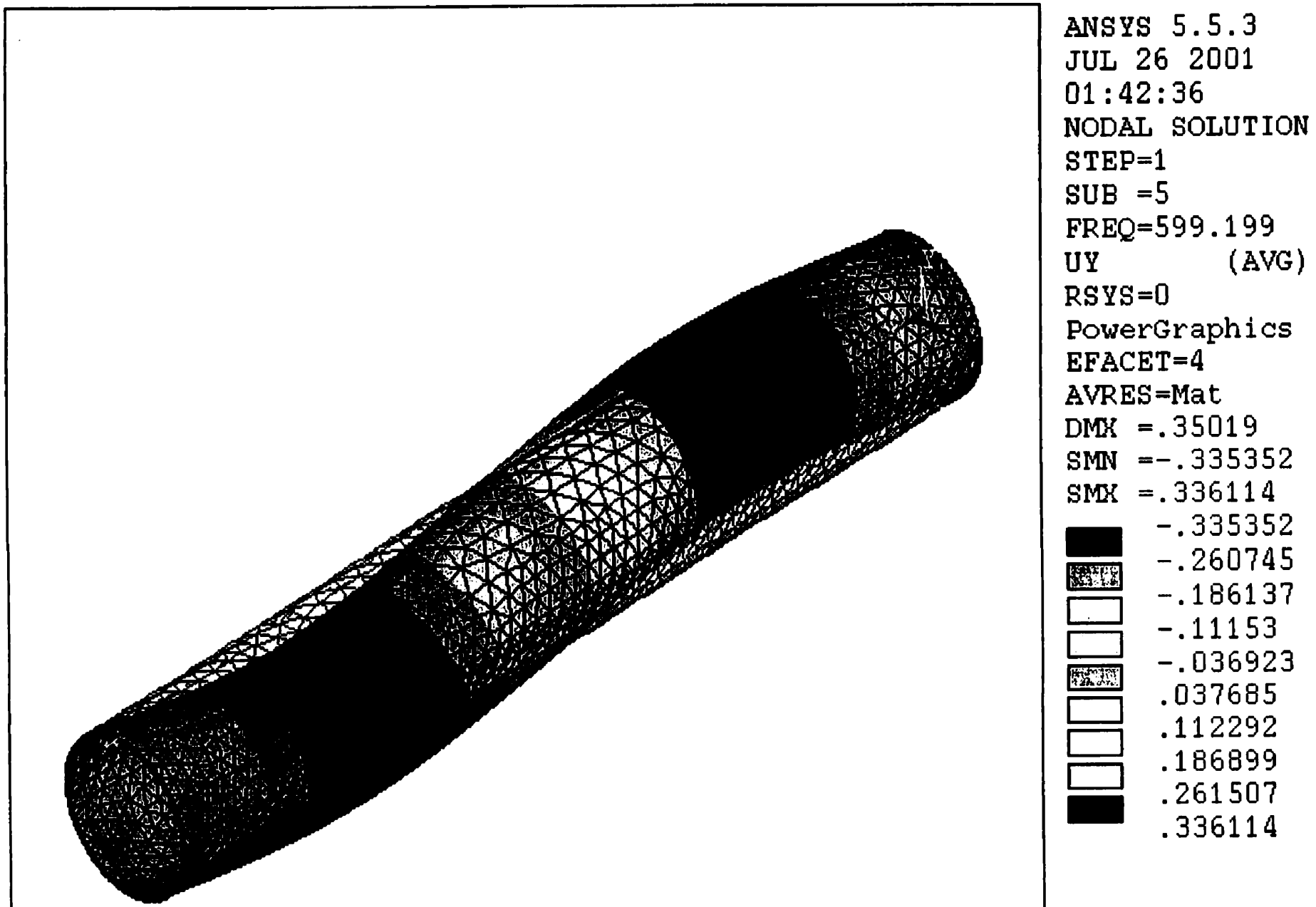

Figure 2.23 Deflections of Pipe

Case1bPipeEmptyVibrations **Case1b Pipe Empty – Mode Shapes**

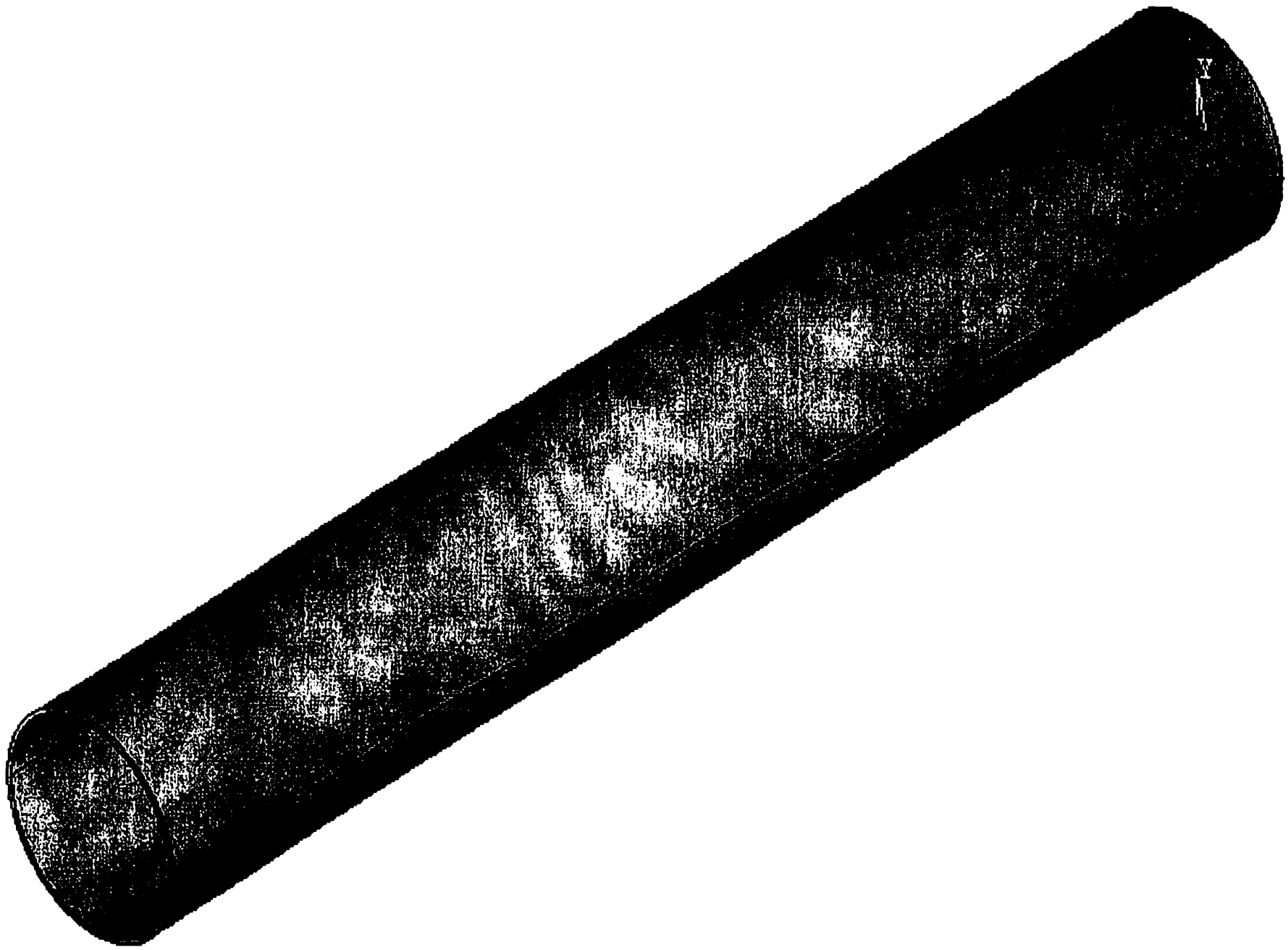

Figure 2.24 Isometric View of Pipe

Case2aPipeFluidFilledDeflStress

Case2a Pipe Fluid Filled - Deflection and Stress

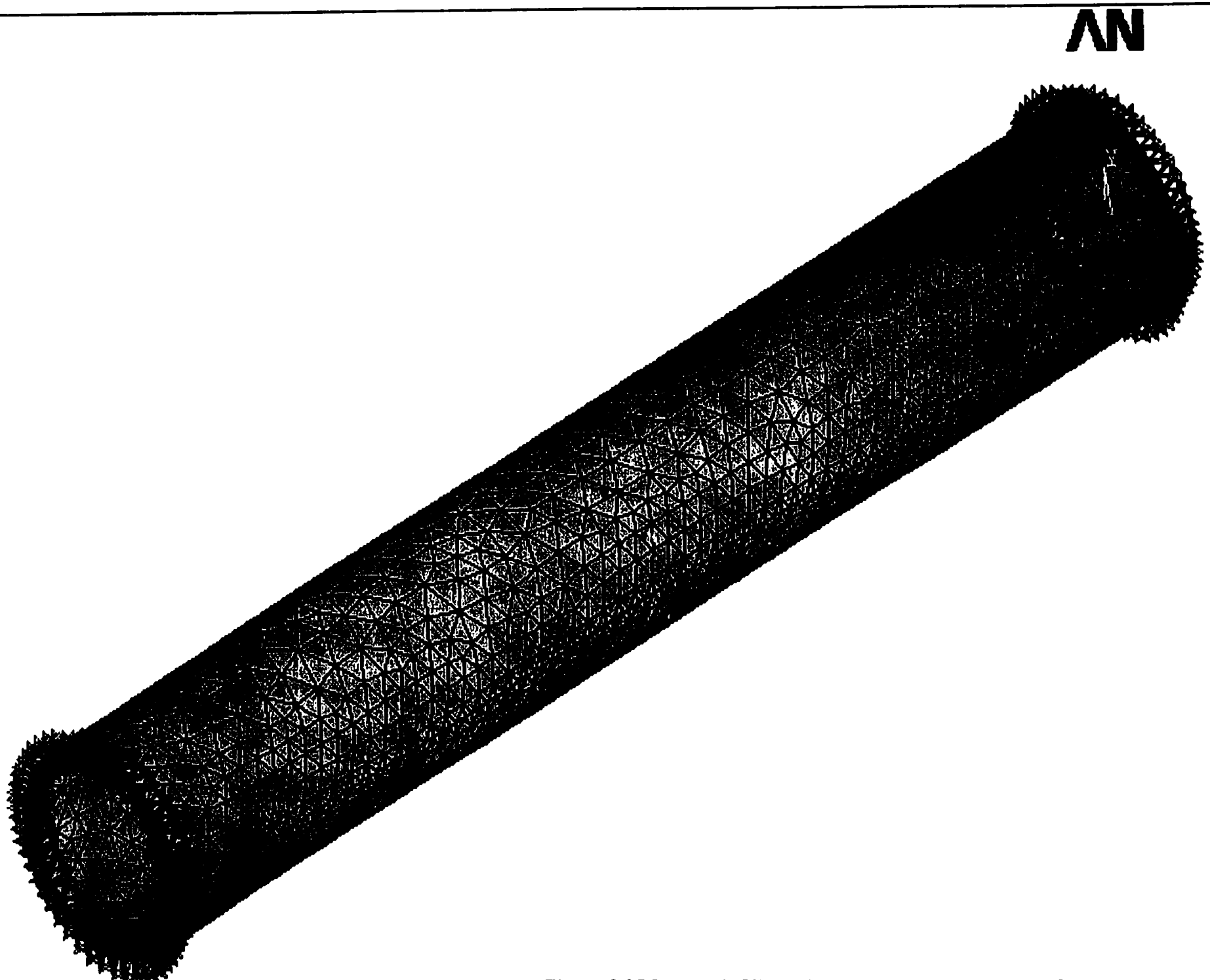

Figure 2.25 Isometric View of Pipe Meshed and Anchored

Case2a Pipe Fluid Filled - Deflection and Stress

Case2aPipeFluidFilledDeflStress

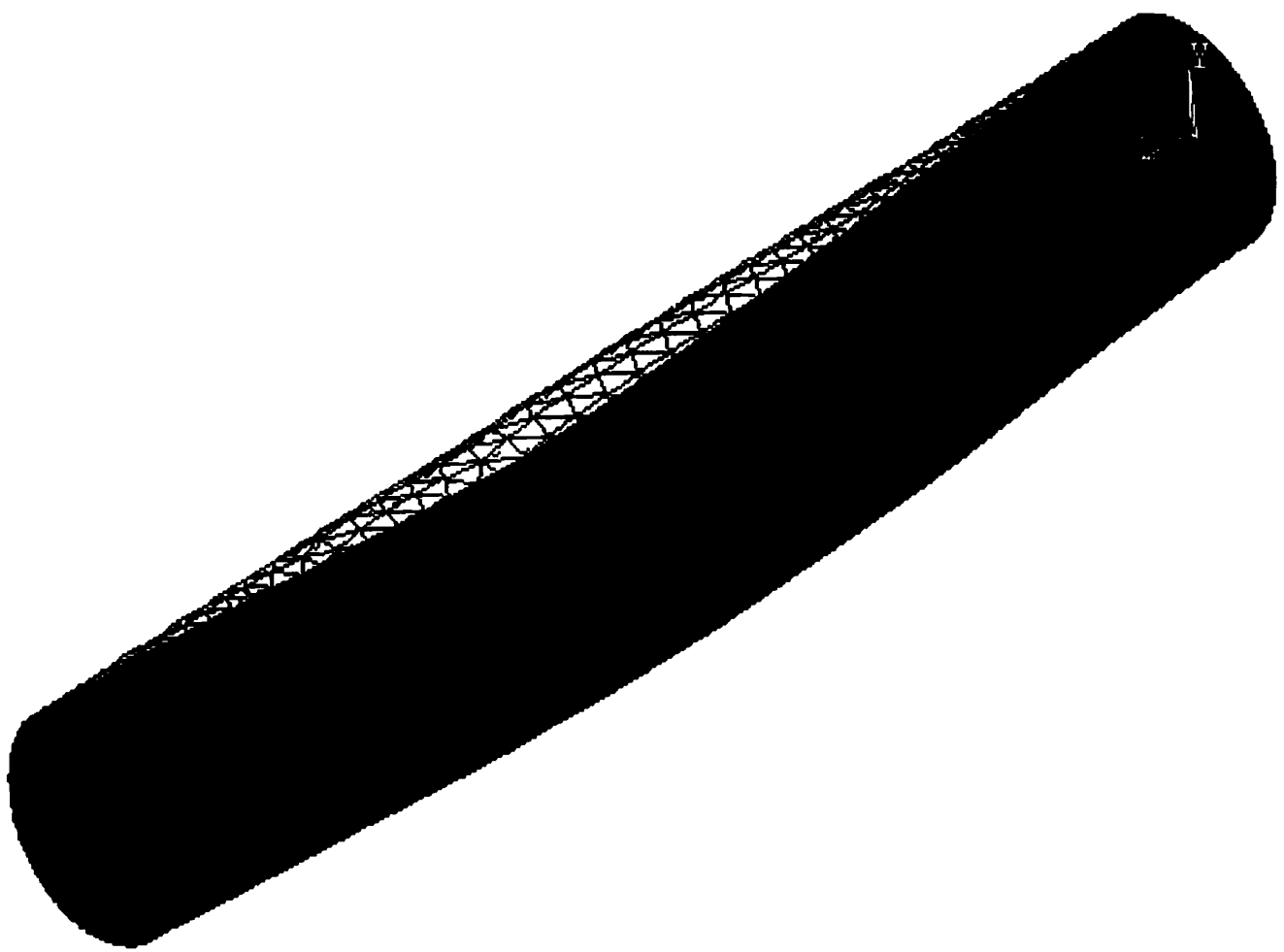

ANSYS 5.5.3
JUL 27 2001
19:43:07
DISPLACEMENT
STEP=1
SUB =1
TIME=1
PowerGraphics
EFACET=4
AVRES=Mat
DMX =.547E-04

DSCA=8060
XV =.57735
YV =.57735
ZV =.57735
DIST=3.985
XF =.001889
YF =-.050746
ZF =4.406
Z-BUFFER

Figure 2.26 Deformed Shape of Pipe

Case2aPipeFluidFilledDef1Stress **Case2a Fluid Filled - Deflection and Stress**

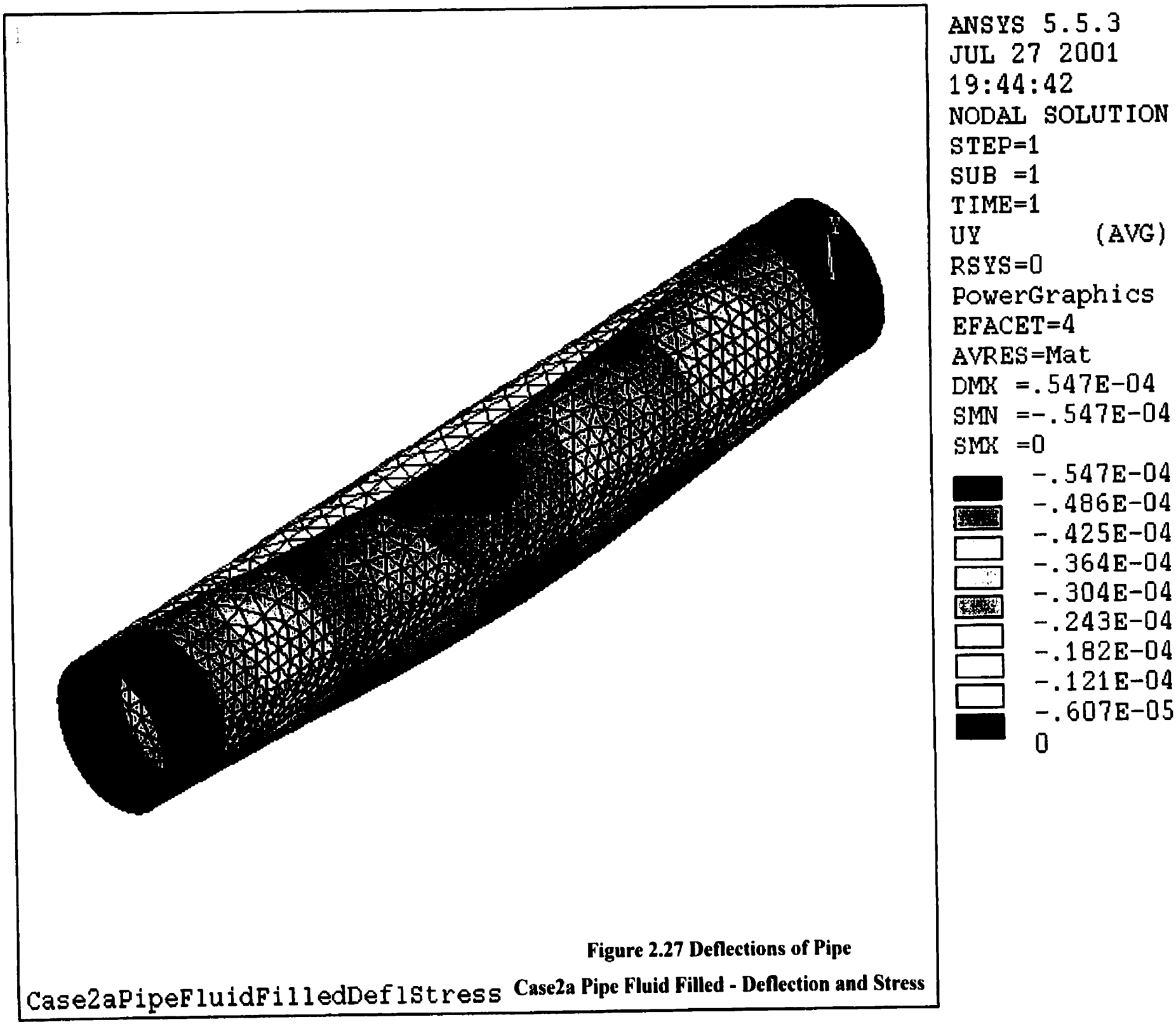

Figure 2.27 Deflections of Pipe

Case2aPipeFluidFilledDeflStress **Case2a Pipe Fluid Filled - Deflection and Stress**

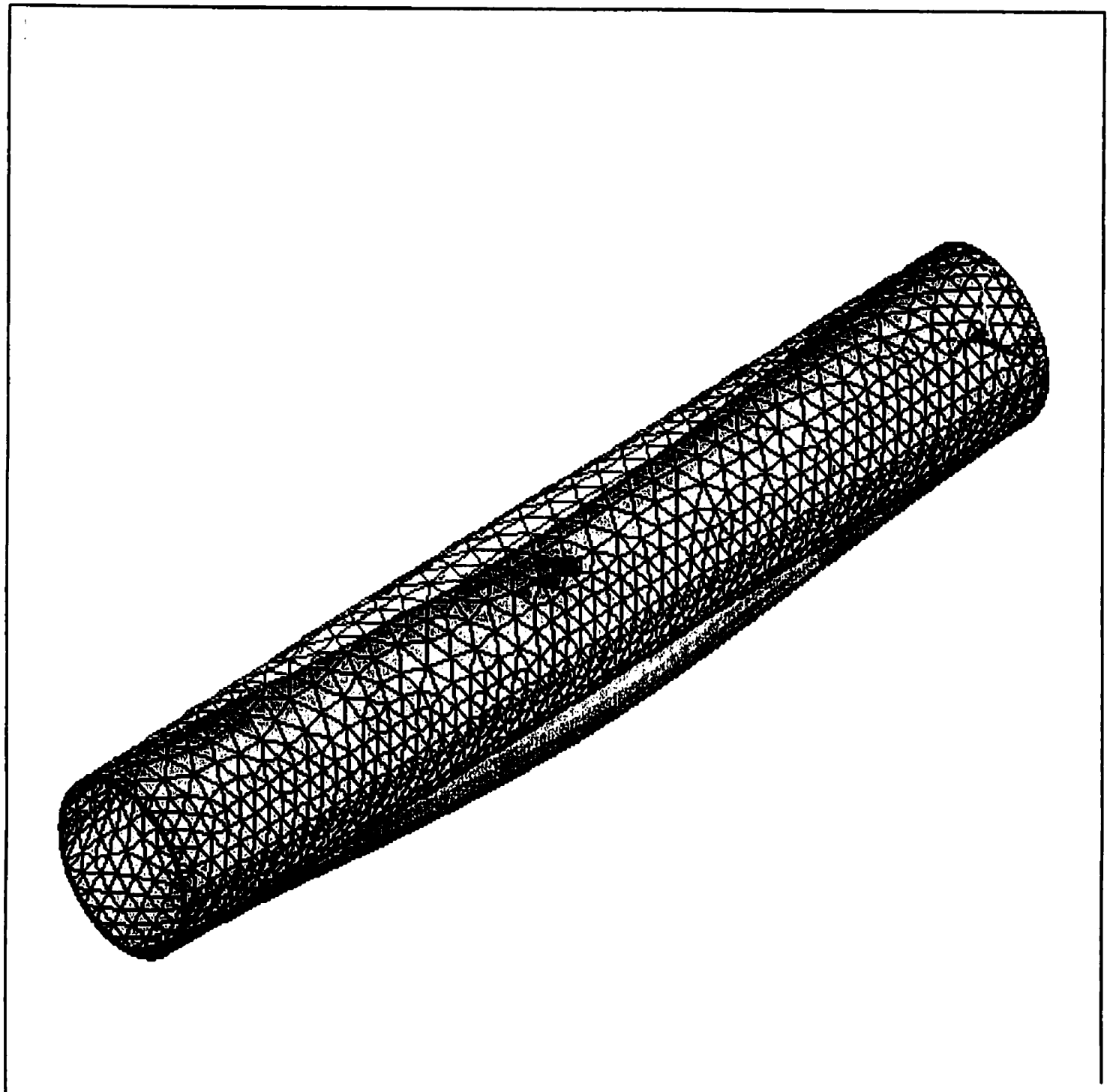

Figure 2.28 Normal Stresses in Pipe – Nodal Solution

Case2aPipeFluidFilledDeflStress **Case2a Pipe Fluid Filled - Deflection and Stress**

Figure 2.29 Shear Stresses in Pipe – Nodal Solution

Case2aPipeFluidFilledDeflStress **Case2a Pipe Fluid Filled - Deflection and Stress**

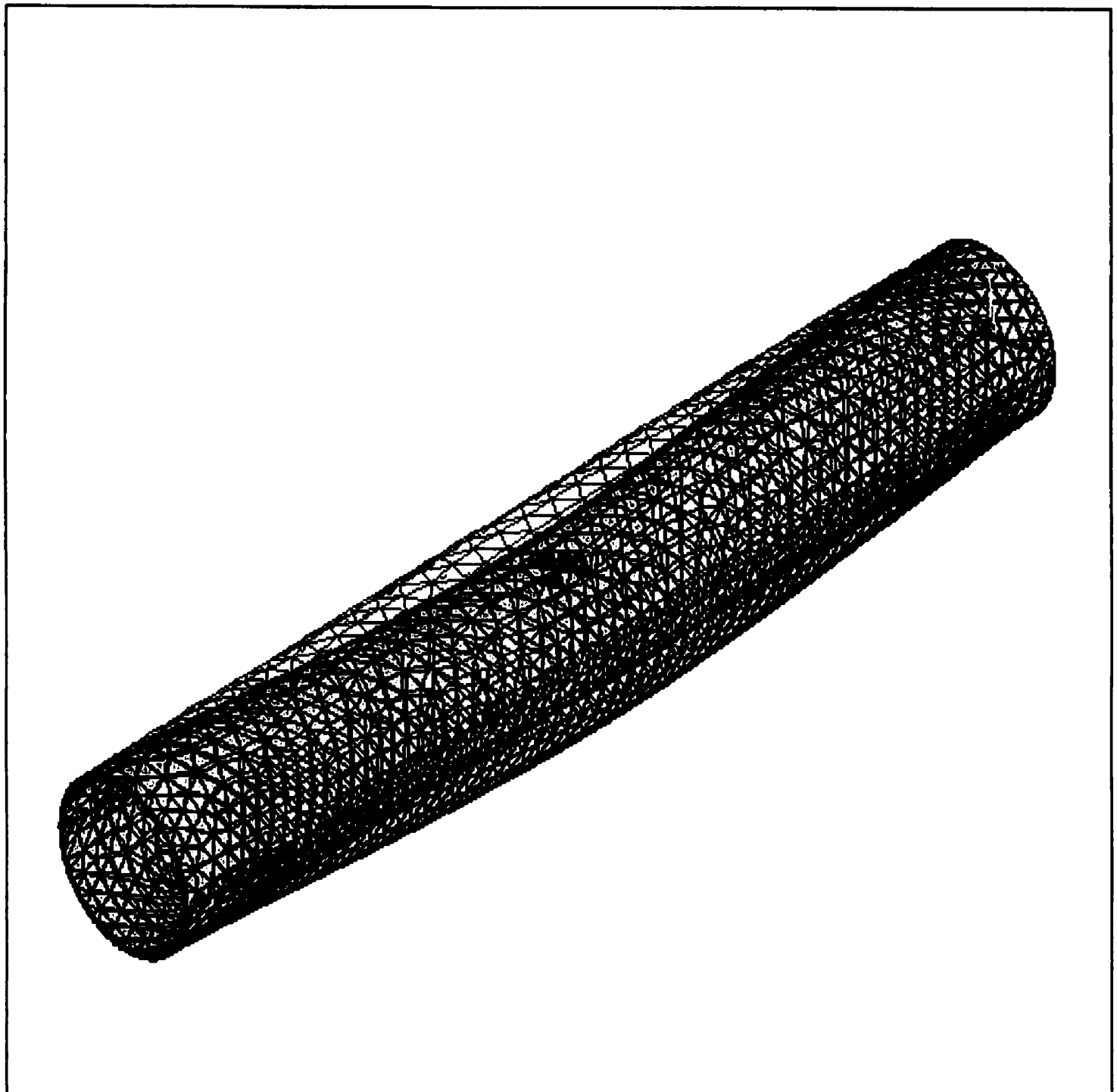

Figure 2.30 Normal Stresses in Pipe – Element Solution

Case2aPipeFluidFilledDeflStress **Case2a Pipe Fluid Filled - Deflection and Stress**

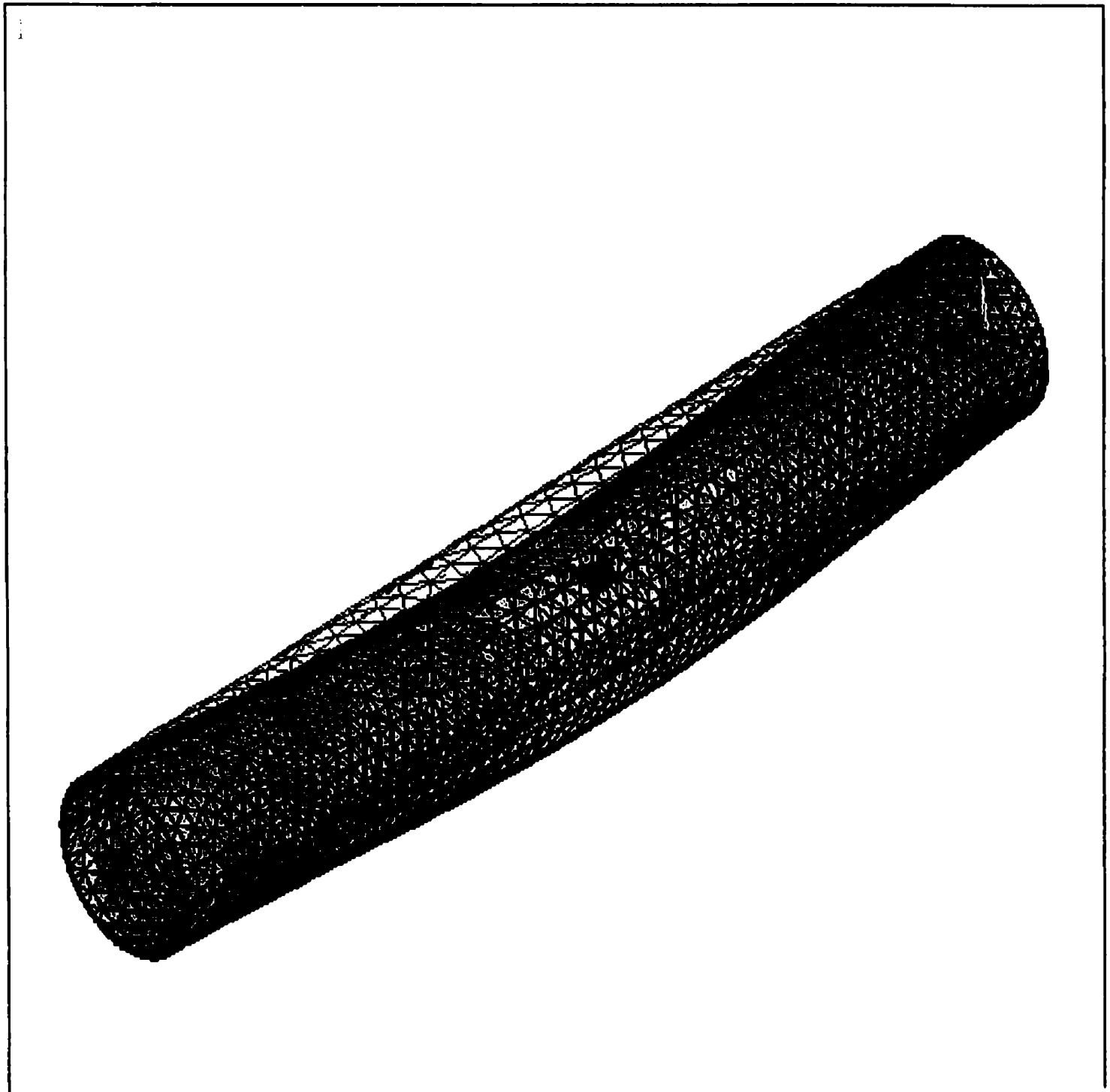

Figure 2.31 Shear Stresses in Pipe – Element Solution

Case2aPipeFluidFilledDeflStress **Case2a Pipe Fluid Filled - Deflection and Stress**

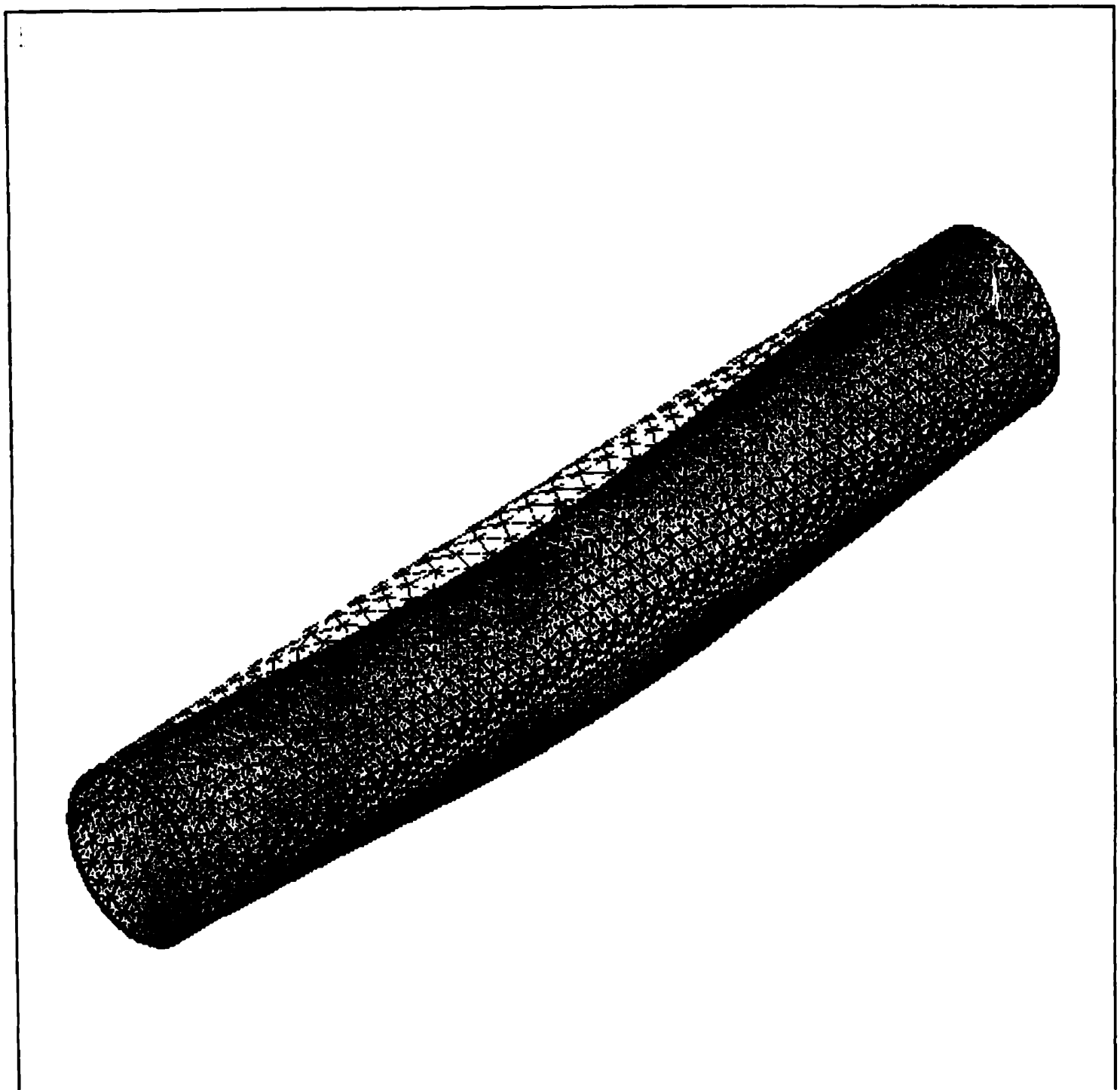

Figure 2.32 Element Forces on Pipe – Element Solution

Case2a Pipe Fluid Filled - Deflection and Stress

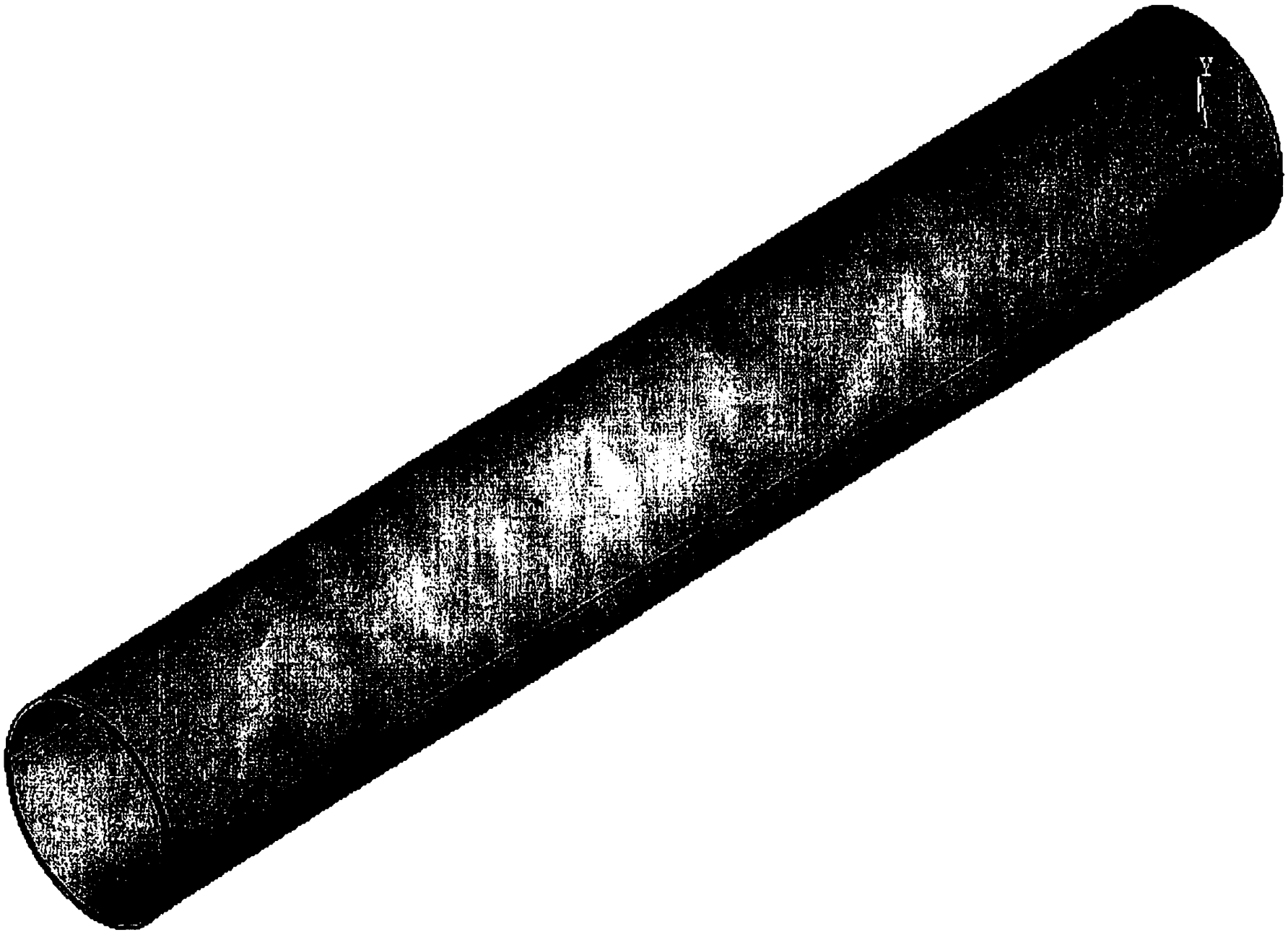

Figure 2.33 Isometric View of Pipe

Case2b Pipe Fluid Filled – Mode Shapes

Case2bPipeFluidFilledVibrations

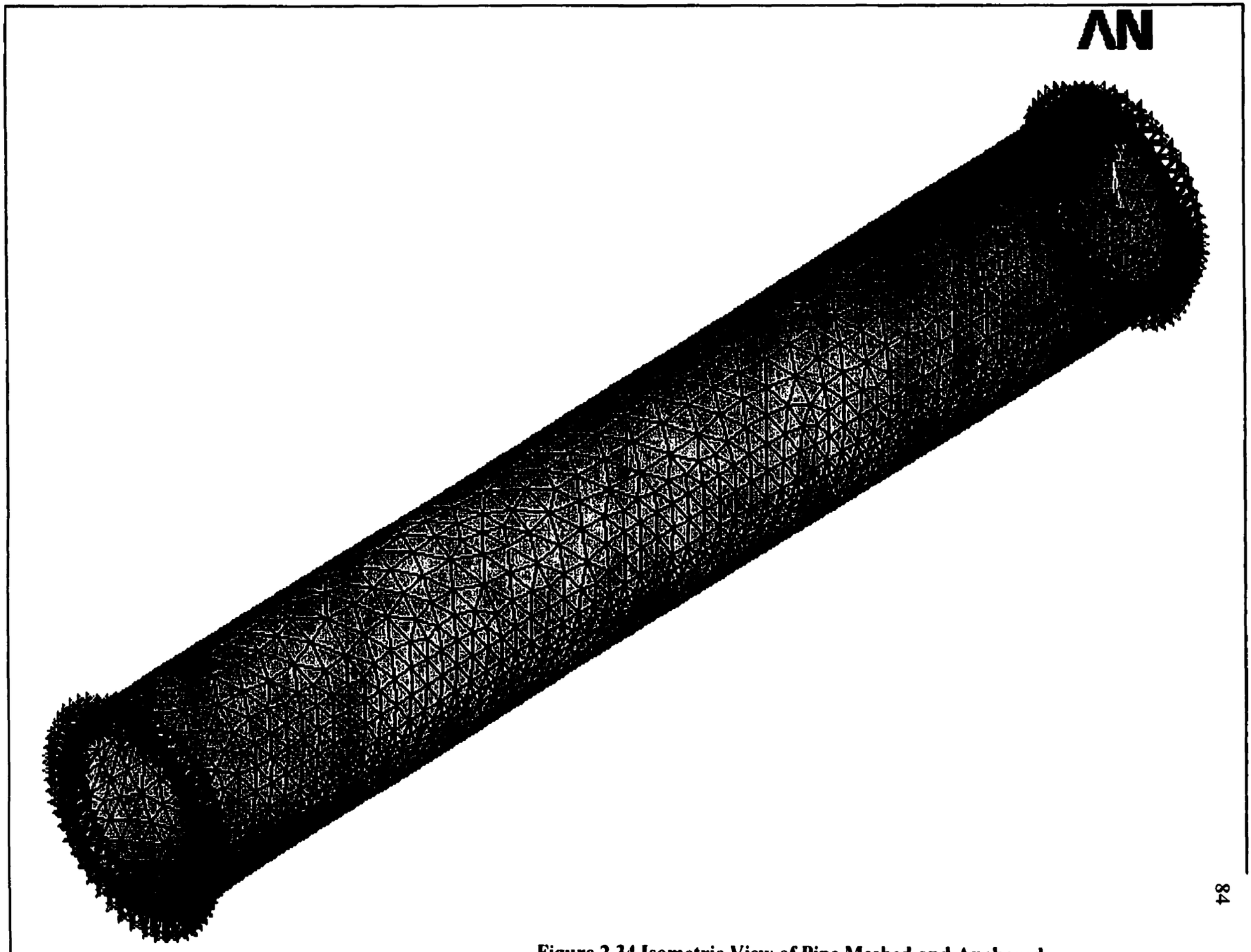

Figure 2.34 Isometric View of Pipe Meshed and Anchored

Case2bPipeFluidFilledVibrations

Case2b Pipe Fluid Filled – Mode Shapes

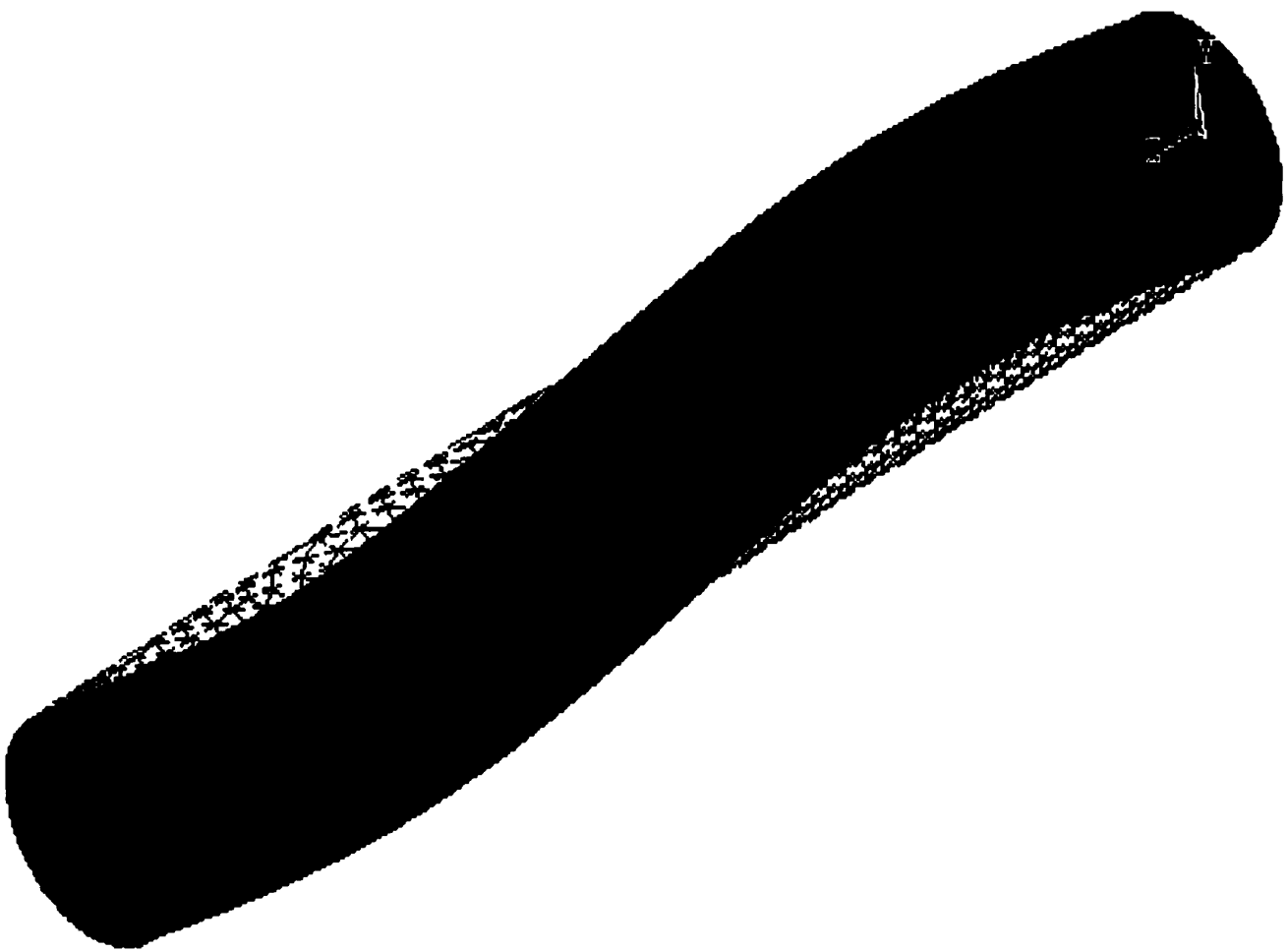

ANSYS 5.5.3
JUL 27 2001
22:42:38
DISPLACEMENT
STEP=1
SUB =5
FREQ=506.602
PowerGraphics
EFACET=1
AVRES=Mat
DMX =.296073

DSCA=1.488
XV =1
YV =1
ZV =1
DIST=4.038
XF =.001622
YF =-.296E-03
ZF =4.406
Z-BUFFER

Case2bPipeFluidFilledVibrations

Figure 2.35 Deformed Shape of Pipe

Case2b Pipe Fluid Filled – Mode Shapes

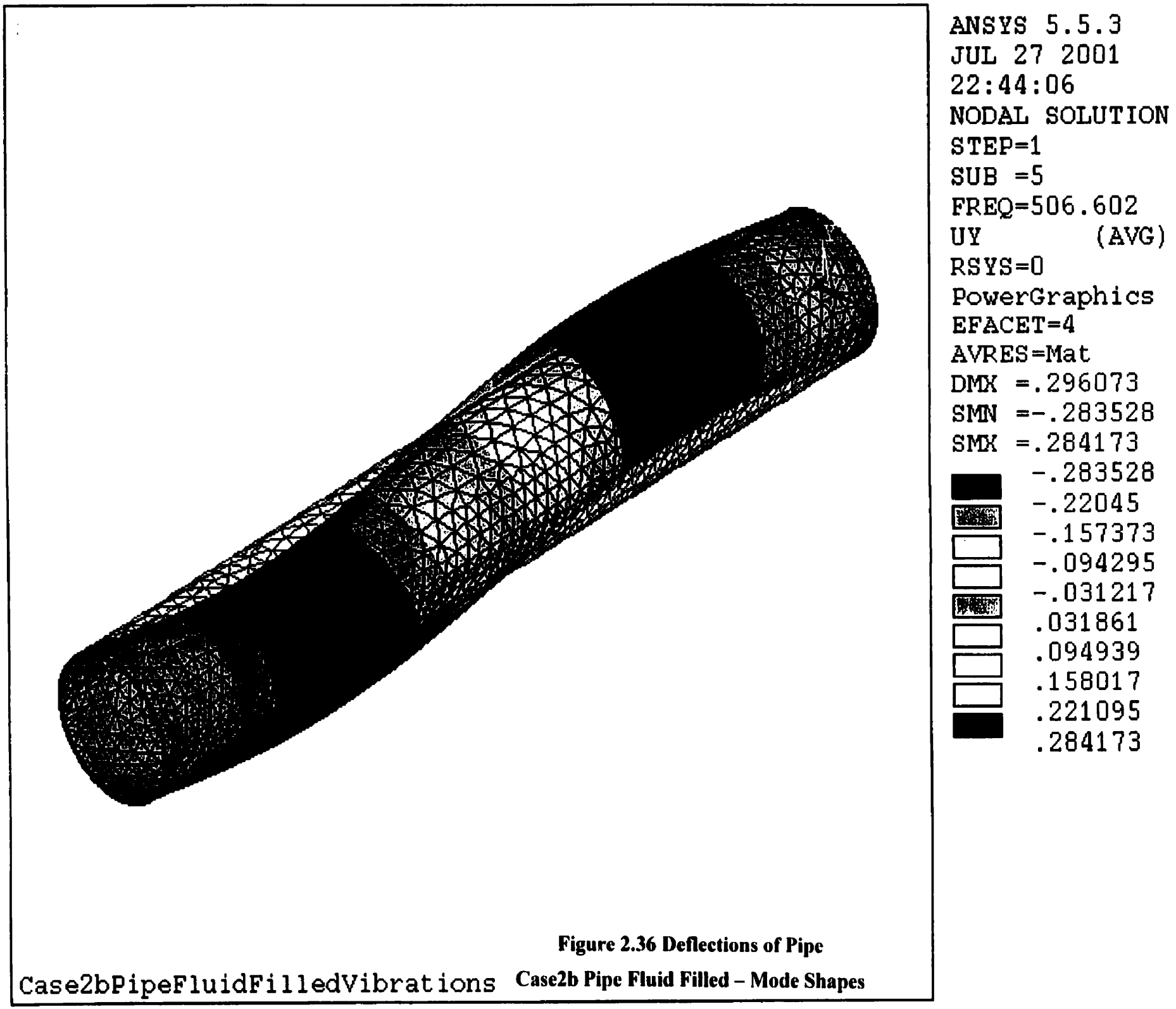

Figure 2.36 Deflections of Pipe

Case2b Pipe Fluid Filled – Mode Shapes

2.8 Analysis and Comparison

1. There is no comparison in the deflection figures between the different systems. Each deflection figure in its own system seems reasonable. They are so wide apart that comparison does not make sense. The marked difference is due to the great difference in the formulae used and the inherent assumptions.

2. As stresses have not been calculated in FEM developed in Chapter 3, thus the stresses could not be compared.

3. All 5-mode shape frequencies compare very closely in case of textbook and industrial methods. This is a very encouraging result. In case of ANSYS most probable reasons for difference in results are type of loading allowed, element type chosen and extremely coarse mesh used.

4. Although text book calculated frequencies may seem too low, in practice the natural frequency will be higher because: [28]

4.1 Actual piping system is never truly simply supported at ends. It's either fixed ends or a combination of the effects of fixed ends and simply supported end conditions.

4.2 End moments, were neglected here, will raise frequency by more than 15%.

4.3 The critical span is usually limited by stress and is rarely reached.

4.4 The piping weight assumed is often larger than the actual load.

CHAPTER 3 - FINITE ELEMENT METHOD WITH CORIOLIS FORCE

3.1 Introduction

A Finite Element Method is formulated in this chapter for the Dynamic Analysis of Fluid-Filled Pipes under the influence of Coriolis Force.

The structural analysis is done by the assemblage of elements using matrices. Forces and moments at the ends of the elements known from the structural theory, the joints between elements are matched for compatibility of displacements and the forces. Moments at the joints are established by imposing the conditions of equilibrium.

In the finite element method, the same procedure is adopted except it is a more systematic arrangement, making computer programming easier. Simpler structures with only a few elements can be analyzed using the above-mentioned structural technique or other methods and also can be analyzed using finite element method with the help of a hand held calculator. Larger structures, like the complete industrial project with in-plant piping and pressure vessels, if calculated manually would be rather a test of level of patience of the analyzer. Thus, in larger structures computers are employed to do the finite element calculations. In the finite element method, element coordinates and forces are transformed into global system of coordinates. The stiffness matrix of the whole structure is thus presented in the global coordinates system of common orientation. The development of the mass matrix with the stiffness matrix completes the basic equations of motion for the dynamic analysis. The addition of *c*-matrix adds to the complexity of the equation of motion and thus giving the necessary tool to analyze the system dynamics with the flow velocity aspect. In this matrix

lays the Coriolis Force part of the equation. A further matrix has been added to it, which has made the analysis even more interesting, the matrix constituting the contained fluid properties and flow conditions. Through this matrix the system exhibits the centrifugal force on the pipeline due to the velocity of flow and the changes in pipe curvature. Of course this adds to the complexity of the equation at hand, but these added dimensions give a finite element method in which we can simulate the fluid properties and the flow conditions and thus study the effects of Coriolis Force.

There are quite a few Finite Element Techniques developed for the analysis of pipelines with and without fluid filled. Most techniques use the route of taking lumped mass matrices.

In this thesis a technique utilizing consistent mass matrices has been used.

Consistent mass matrices give accuracy in results. Of course they take up considerable memory space of the computer. Short run of a pipe can be analyzed, as done in this thesis, manually with the aid of hand held scientific calculator. Manually it will take forever if full length of pipeline as in the sample project used in this thesis was taken. Thus the use of a computer program is employed. ANSYS software was used for the purpose, though unfortunately we have only the student version thus limited by the number of elements in the meshed model to 16000 maximum and also limited by the available memory space on the computer network system at the Department of Mechanical and Manufacturing Engineering.

The accuracy of finite element depends upon the choice of the shape functions. These shape functions should satisfy the following three conditions, which will ensure convergence to correct answers when a finer finite element mesh is used: [21]

1. The displacements of adjacent elements along a common boundary must be identical.

2. When the nodal displacements correspond to rigid-body-motion, the strains must be equal to zero.

3. The shape functions must allow the element to be in a state of constant strain.

The derivations of shape functions and the formulation of individual matrices [K]; [m]; [c] and [D] is given in Appendix A.

In addition to the free single element, the case of two elements is considered. The two elements are considered adjacent to each other forming the beam or the pipe in question. Thus the assemblage of the matrices is conducted; loads and the boundary conditions are applied.

The assemblage of the matrices enables us to present this Finite Element Method with the ability to calculate the deflections, mode shape frequencies etc, with the application of external forces. Thus this FEM can now be compared with its results to that obtained using other methods discussed in this thesis. Also this enables the use of this FEM in conjunction with the research work done by other scholars, and thus obtaining results in our area of interest while using the research methodology of other researchers. This goes to show the universality of this FEM.

3.2 Cases Considered

The following possible variations will be considered:

3.2.1 Empty Pipe and Uniform Radius all through.

3.2.2 Fluid Filled Pipe, No Flow Velocity and Uniform Radius all through.

3.2.3 Fluid Filled Pipe with a Constant Low Flow Velocity.

3.2.4 Fluid Filled Pipe with a Constant Medium Flow Velocity.

3.2.5 Fluid Filled Pipe with a Constant High Flow Velocity.

3.2.6 Fluid Filled Pipe with a Constant Extra High Flow Velocity.

3.2.7 Fluid Filled Pipe with a Constant Ultra High Flow Velocity.

3.2.8 Fluid Filled Pipe with a Constant Near Sonic Flow Velocity.

3.2.9 Fluid Filled Pipe with a Constant Sonic Flow Velocity.

3.3 The Finite Element Method with Coriolis Force

Consider a pipe with fluid flowing at velocity v. The curvature is assumed by the pipe due to deflections resulting from self-load, internal and external forces, as in Figure 3.1.

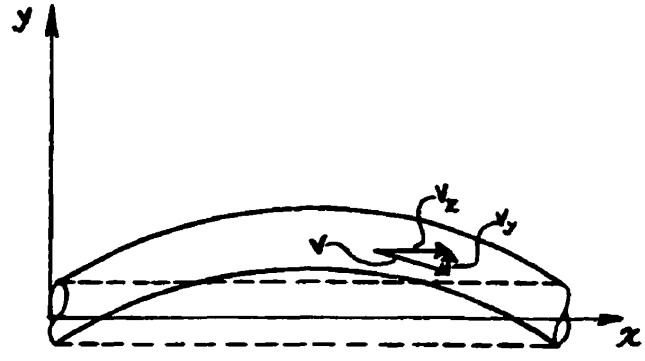

Figure 3.1: Pipe and Flowing Fluid Coordinate System
Pipe with Fluid Flowing and Curvature Change

Under appropriate simplifying assumptions, the behavior of a fluid-filled pipe is governed by the stationarity of the integral:

$$J = \int_0^t \int_0^l \left[\frac{1}{2}(m-\rho)\dot{y}^2 + \frac{1}{2}\rho\left[v^2 + (\dot{y} + vy')^2\right] - \frac{1}{2}EIy''^2 \right] dx dt \qquad (3.1)$$

Where the terms:

$\frac{1}{2}EIy''^2$ is the strain energy per unit length of the pipe.

$\frac{1}{2}\rho\left[v^2+(\dot{y}+vy')^2\right]$ is the kinetic energy of the fluid in the pipe.

$\frac{1}{2}(m-\rho)\dot{y}^2$ is the kinetic energy of the pipe.

Our interest is in developing a finite element model for the spatial part.

Consider the variation of equation (3.1) as:

$$\delta J=\int_0^t\int_0^l\left[\frac{1}{2}m\delta\dot{y}^2-\frac{1}{2}\rho\delta\dot{y}^2+\frac{1}{2}\rho\left[\delta(\dot{y}+vy')^2\right]-\frac{1}{2}EI\delta y''^2\right]dxdt$$

Simplifying above equation:

$$\delta J=\int_0^t\int_0^l\left[m\dot{y}\delta\dot{y}-EIy''\delta y''-\rho\dot{y}\delta\dot{y}+\rho\left[(\delta\dot{y}+v\delta y')(\dot{y}+vy')\right]\right]dxdt$$

$$\delta J=\int_0^t\int_0^l\left[\begin{array}{c} m\dot{y}\delta\dot{y}-EIy''\delta y''-\rho\dot{y}\delta\dot{y}+\rho\dot{y}\delta\dot{y}+\rho v\dot{y}\delta y' \\ +\rho v y'\delta\dot{y}+\rho v^2 y'\delta y' \end{array}\right]dxdt$$

$$\delta J=\int_0^t\int_0^l\left[m\dot{y}\delta\dot{y}-EIy''\delta y''+\rho v\dot{y}\delta y'+\rho v y'\delta\dot{y}+\rho v^2 y'\delta y'\right]dxdt \qquad (3.2)$$

Where:

$$\dot{y} = \frac{dy}{dt}$$

$$\ddot{y} = \frac{d^2y}{dt^2}$$

$$y' = \frac{dy}{dx}$$

$$y'' = \frac{d^2y}{dx^2}$$

$$\dot{y}' = \frac{d^2y}{dtdx}$$

We integrate by parts equation (3.2) only those terms containing time – t derivatives of the variation δy and ignoring the boundary terms to give us:

$$\delta J = \int_0^t \int_0^l \left[-m\ddot{y}\delta y - EIy''\delta y'' - \rho v\dot{y}'\delta y - \rho v\dot{y}'\delta y - \rho v^2 y''\delta y \right] dxdt + \text{boundary terms}$$

$$\delta J = \int_0^t \int_0^l \left[m\ddot{y}\delta y + EIy''\delta y'' + 2\rho v\dot{y}'\delta y + \rho v^2 y''\delta y \right] dxdt + \text{bounadry terms} \qquad (3.3)$$

$m\ddot{y} \rightarrow$ is inertia force due to vertical acceleration of pipe

$EIy''' \rightarrow$ is contribution of elastic force

$2\rho v\dot{y}' \rightarrow$ is Coriolis Force associated with Coriolis acceleration. As fluid has velocity v, relative to pipe. The pipe angular velocity is $\dot{y}'$, which varies along the x-coordinate.

$\rho v^2 y'' \rightarrow$ is inertia force due to directional change in velocity v, with curvatures of pipe.

Next, we integrate the following expansion in terms of spatial shape functions $N_i(x)$ and time dependent coefficients $\Delta_i(t)$: [30] [21]

$$y(x,t) = \sum_{i=1}^{n} \Delta_i(t) N_i(x) = \Delta^i(t) N_i(x) \tag{3.4}$$

Where we have used the summation convention on the index i.

The summation ranges from 1 to n, the number of assumed degrees of freedom.

We shall adopt the standard beam theory shape functions (with i =1 to 4), and interpret Δ_i as nodal displacements and rotations. We have taken a bar element here.

The positive sense of the coordinates, forces and moments is arbitrarily chosen here:

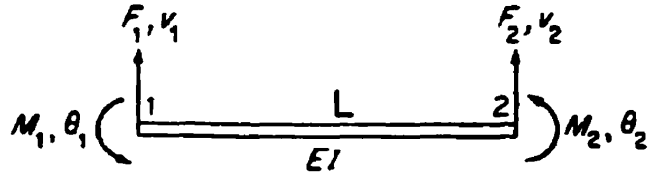

Figure 3.2: Pipe or Beam in Bending [30]
Displacements and Forces taken in positive sense

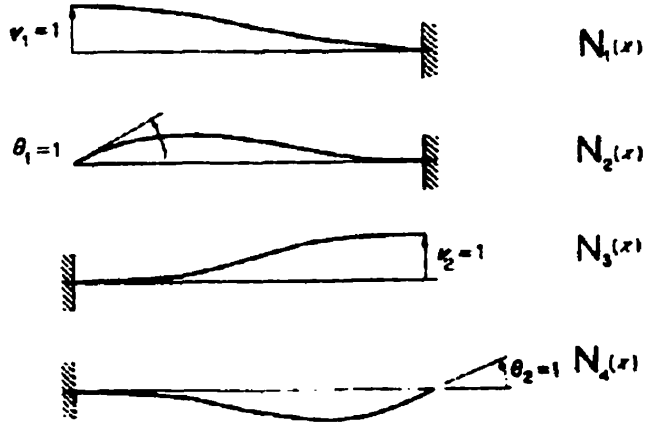

Figure 3.3: Displacements and Shapes of the Pipe or Beam [30]
Fixed Ends Condition.

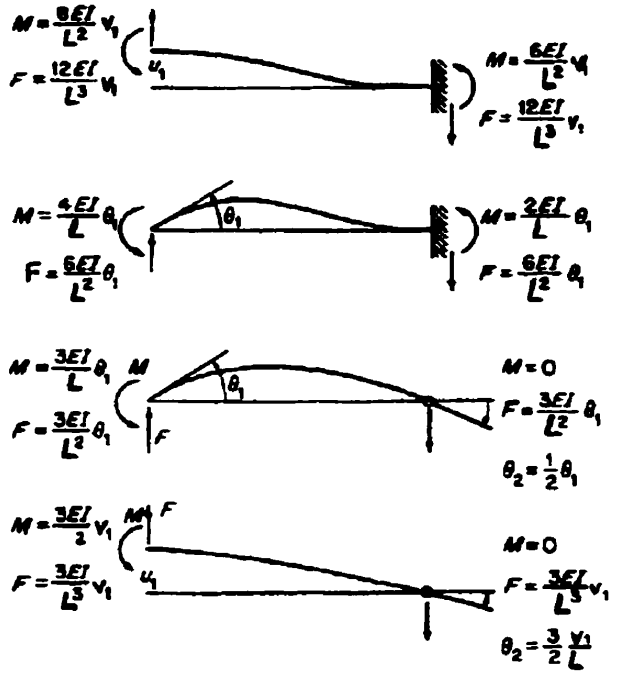

Figure 3.4: Lateral Forces and Moments of Uniform Pipe or Beam Element [30] Fixed Ends Condition.

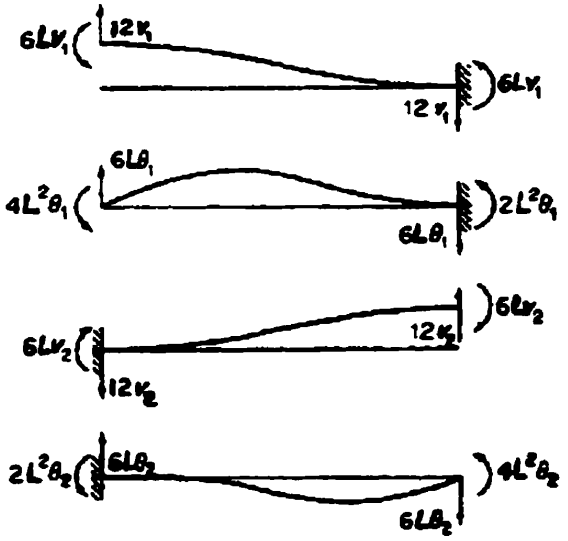

Figure 3.5: Lateral Forces and Moments of Uniform Pipe or Beam Element [30] Fixed Ends Condition. Omitting the Material Property EI/L3

The shape functions as derived in Appendix A in reference to the above diagrams, are:

$$N_1 = \frac{1}{L^3}(x-L)^2(L+2x) \tag{3.5.1}$$

$$N_2 = \frac{1}{L^2}x(x-L)^2 \tag{3.5.2}$$

$$N_3 = \frac{1}{L^3}x^2(3L-2x) \tag{3.5.3}$$

$$N_4 = \frac{1}{L^2}x^2(x-L) \tag{3.5.4}$$

The shape functions are substituted in equation (3.4) and then back in equation (3.3) to yield:

$$\delta J = \int_0^t \int_0^l [m\ddot{\Delta}^i N_i N_j \delta\Delta^j + EI N_i'' N_j'' \Delta^i \delta\Delta^j + 2\rho v(\dot{\Delta}^i N_i') N_j \delta\Delta^j + \rho v^2(\Delta^i N_i'') N_j \delta\Delta^j]dxdt \tag{3.6}$$

Which can be written as:

$$\delta J = \int_0^T [m_{ij}\ddot{\Delta}^j + (k_{ij} + D_{ij})\Delta^j + c_{ij}\dot{\Delta}^j]\delta\Delta^j dt \tag{3.7}$$

Or in matrix notation:

$$\delta J = \int_0^T [\{\delta\Delta\}^T([m]\{\ddot{\Delta}\} + ([k]+[D])\{\Delta\} + [c]\{\dot{\Delta}\})]dt \tag{3.8}$$

Where:

$$k_{ij} = \int_0^L EI N_i'' N_j'' dx \tag{3.9.1}$$

$$m_{ij} = \int_0^L (m) N_i N_j dx \tag{3.9.2}$$

$$c_{ij} = \int_0^L 2\rho v N_i' N_j dx \tag{3.9.3}$$

$$D_{ij} = \int_0^L \rho v^2 N_i'' N_j dx \tag{3.9.4}$$

If there are external forces acting on the pipe, the virtual work will be given by an expression of the form:

$$\delta W = \int_0^t \{\delta \Delta\}^T \{\mathbb{R}\} dt \tag{3.10}$$

Where $\mathbb{R}$ is to be calculated for each type of loading.

Equating identically, according to D'Alembert's Principle, equation (3.8) and equation (3.10) yields the dynamic equations for a free element as:

$$([k]+[D])\{\Delta\}+[c]\{\dot{\Delta}\}+[m]\{\ddot{\Delta}\}= \{\mathbb{R}\} \tag{3.11}$$

A pains taking, but straight forward, calculation yields the following matrices for the bar element in bending when, using the standard interpolation functions:

$$[k]= EI\begin{bmatrix} \frac{12}{L^3} & \frac{6}{L^2} & \frac{-12}{L^3} & \frac{6}{L^2} \\ \frac{6}{L^2} & \frac{4}{L} & \frac{-6}{L^2} & \frac{2}{L} \\ \frac{-12}{L^3} & \frac{-6}{L^2} & \frac{12}{L^3} & \frac{-6}{L^2} \\ \frac{6}{L^2} & \frac{2}{L} & \frac{-6}{L^2} & \frac{4}{L} \end{bmatrix} \tag{3.12}$$

$$[D]=\rho v^2\begin{bmatrix} \frac{-6}{5L} & \frac{-1}{10} & \frac{6}{5L} & \frac{-1}{10} \\ \frac{-1}{10} & \frac{-2L}{15} & \frac{1}{10} & \frac{L}{30} \\ \frac{6}{5L} & \frac{1}{10} & \frac{-6}{5L} & \frac{19}{10} \\ \frac{-1}{10} & \frac{L}{30} & \frac{19}{10} & \frac{-2L}{15} \end{bmatrix} \tag{3.13}$$

$$[c]=2\rho v\begin{bmatrix} \frac{-1}{2} & \frac{-L}{10} & \frac{-1}{2} & \frac{L}{10} \\ \frac{L}{10} & 0 & \frac{-L}{10} & \frac{L^2}{60} \\ \frac{1}{2} & \frac{L}{10} & \frac{1}{2} & \frac{-L}{10} \\ \frac{-L}{10} & \frac{-L^2}{60} & \frac{L}{10} & 0 \end{bmatrix} \tag{3.14}$$

$$[m]=(m)\begin{bmatrix} \frac{13L}{35} & \frac{11L^2}{210} & \frac{9L}{70} & \frac{-13L^2}{420} \\ \frac{11L^2}{210} & \frac{L^3}{105} & \frac{13L^2}{420} & \frac{-L^3}{140} \\ \frac{9L}{70} & \frac{13L^2}{420} & \frac{13L}{35} & \frac{-11L^2}{210} \\ \frac{-13L^2}{420} & \frac{-L^3}{140} & \frac{-11L^2}{210} & \frac{L^3}{105} \end{bmatrix} \tag{3.15}$$

This is a consistent mass matrix, as opposed to a simplistic lumping on the diagonal of the translational degrees of freedom. It is consistent mass matrix, as it is based on the same beam functions as used for the stiffness matrix.

3.4 Numerical Analysis of Finite Element Method

In this section the numerical results are obtained using the Finite Element Method formulated in the above sections and also as in Appendix A. This section serves to test the formulated Finite Element Method to an actual industrial project.

3.4.1 Procedure for the Numerical Analysis

Reference is made to equation (3.11):

$$([k]+[D])\{\Delta\}+[c]\{\dot{\Delta}\}+[m]\{\ddot{\Delta}\}=\{\mathbb{R}\}$$

Also refer to equation (A.A.34):

$$\begin{Bmatrix} F_1 \\ M_1 \\ F_2 \\ M_2 \\ F_3 \\ M_3 \end{Bmatrix} = EI \begin{bmatrix} k_{11} & k_{12} & k_{13} & k_{14} & & \\ k_{21} & k_{22} & k_{23} & k_{24} & & \\ k_{31} & k_{32} & k_{33}+k_{11} & k_{34}+k_{12} & k_{13} & k_{14} \\ k_{41} & k_{42} & k_{43}+k_{21} & k_{44}+k_{22} & k_{23} & k_{24} \\ & & k_{31} & k_{32} & k_{33} & k_{34} \\ & & k_{41} & k_{42} & k_{43} & k_{44} \end{bmatrix} \begin{Bmatrix} v_1 \\ \theta_1 \\ v_2 \\ \theta_2 \\ v_3 \\ \theta_3 \end{Bmatrix}$$

Substituting the values from equation (3.12), we get:

$$\begin{Bmatrix} F_1 \\ M_1 \\ F_2 \\ M_2 \\ F_3 \\ M_3 \end{Bmatrix} = EI \begin{bmatrix} \frac{12}{L^3} & \frac{6}{L^2} & \frac{-12}{L^3} & \frac{6}{L^2} & & \\ \frac{6}{L^2} & \frac{4}{L} & \frac{-6}{L^2} & \frac{2}{L} & & \\ \frac{-12}{L^3} & \frac{-6}{L^2} & \frac{12}{L^3}+\frac{12}{L^3} & \frac{-6}{L^2}+\frac{6}{L^2} & \frac{-12}{L^3} & \frac{6}{L^2} \\ \frac{6}{L^2} & \frac{2}{L} & \frac{-6}{L^2}+\frac{6}{L^2} & \frac{4}{L}+\frac{4}{L} & \frac{-6}{L^2} & \frac{2}{L} \\ & & \frac{-12}{L^3} & \frac{-6}{L^2} & \frac{12}{L^3} & \frac{-6}{L^2} \\ & & \frac{6}{L^2} & \frac{2}{L} & \frac{-6}{L^2} & \frac{4}{L} \end{bmatrix} \begin{Bmatrix} v_1 \\ \theta_1 \\ v_2 \\ \theta_2 \\ v_3 \\ \theta_3 \end{Bmatrix} \tag{3.16}$$

Imposing boundary conditions for both ends fixed, as $v_1 = \theta_1 = v_3 = \theta_3 = 0$, and external forces at nodes 1 and 3 taken as $F_1 = M_1 = F_3 = M_3 = 0$, *which* wipes out columns 1, 2, 5, and 6 leaving:

$$\begin{Bmatrix} 0 \\ 0 \\ F_2 \\ M_2 \\ 0 \\ 0 \end{Bmatrix} = EI \begin{bmatrix} \frac{-12}{L^3} & \frac{6}{L^2} \\ \frac{-6}{L^2} & \frac{2}{L} \\ \frac{12}{L^3}+\frac{12}{L^3} & \frac{-6}{L^2}+\frac{6}{L^2} \\ \frac{-6}{L^2}+\frac{6}{L^2} & \frac{4}{L}+\frac{4}{L} \\ \frac{-12}{L^3} & \frac{-6}{L^2} \\ \frac{6}{L^2} & \frac{2}{L} \end{bmatrix} \begin{Bmatrix} 0 \\ 0 \\ v_2 \\ \theta_2 \\ 0 \\ 0 \end{Bmatrix} \tag{3.17}$$

The deflections and rotations, at the mid span are non-zero but are zero at the two fixed ends.

We make use of the middle rows 3 and 4 in equation (3.17):

$$\begin{Bmatrix} F_2 \\ M_2 \end{Bmatrix} = EI \begin{bmatrix} \frac{24}{L^3} & 0 \\ 0 & \frac{8}{L} \end{bmatrix} \begin{Bmatrix} v_2 \\ \theta_2 \end{Bmatrix} \tag{3.18}$$

Inverting equation (3.18):

$$\begin{Bmatrix} v_2 \\ \theta_2 \end{Bmatrix} = \frac{1}{EI}\frac{L^4}{192} \begin{bmatrix} \frac{8}{L} & 0 \\ 0 & \frac{24}{L^3} \end{bmatrix} \begin{Bmatrix} F_2 \\ M_2 \end{Bmatrix} \tag{3.19}$$

Thus the deflection v_2 and rotation θ_2 at node 2 will be:

$$v_2 = \frac{L^4}{192EI}\left(\frac{8}{L}F_2\right) \tag{3.20}$$

$$\theta_2 = \frac{L^4}{192EI}\left(\frac{24}{L^3}M_2\right) \tag{3.21}$$

In equation (3.20), F_2 and in equation (3.21), M_2 can be found by: [22]

$$F_2 = W_{eff} = \frac{3}{8}W = \frac{3}{8}[w_{pipr/ft.} + w_{fluid/ft.}]L_{pipe}$$

$F_2 = 468$ lbs. (3.22)

$M_2 = 0$ (3.23)

The above force is static; we can introduce the dynamic force at bends too.

Putting equations (3.22) and (3.23) in (3.20) and (3.21) respectively, results in:

$v_2 = 1.47 \times 10^{-3}$ in. (3.24)

$\theta_2 = 0$ (3.25)

3.5 Frequency and Deflection Equations for Case Study Using Coriolis Force

Refer to equation (3.11), as here:

$$([k]+[D])\{\Delta\}+[c]\{\dot{\Delta}\}+[m]\{\ddot{\Delta}\} = \{\mathbb{R}\}$$

Re-written as:

$$[k]\{\Delta\}+[D]\{\Delta\}+[c]\{\dot{\Delta}\}+[m]\{\ddot{\Delta}\} = \{\mathbb{R}\} = \begin{Bmatrix} F \\ M \end{Bmatrix} \quad (3.26)$$

Using values from equations (3.12), (3.13), (3.14) and (3.15) in (3.26), same procedure as shown in section 3.4.1:

$$EI\begin{bmatrix}\frac{24}{L^3} & 0\\ 0 & \frac{8}{L}\end{bmatrix}\begin{Bmatrix}v_2\\ \theta_2\end{Bmatrix}+\rho v^2\begin{bmatrix}\frac{-12}{5L} & \frac{9}{5}\\ \frac{9}{5} & \frac{-4L}{15}\end{bmatrix}\begin{Bmatrix}v_2\\ \theta_2\end{Bmatrix}+2\rho v\begin{bmatrix}0 & \frac{-L}{5}\\ \frac{L}{5} & 0\end{bmatrix}\begin{Bmatrix}\dot{v}_2\\ \dot{\theta}_2\end{Bmatrix}+m\begin{bmatrix}\frac{26L}{35} & 0\\ 0 & \frac{2L^3}{105}\end{bmatrix}\begin{Bmatrix}\ddot{v}_2\\ \ddot{\theta}_2\end{Bmatrix}=\begin{Bmatrix}F_2\\ M_2\end{Bmatrix} \quad (3.27)$$

In equation (3.27) the terms represent:

$EI\begin{bmatrix}\frac{24}{L^3} & 0\\ 0 & \frac{8}{L}\end{bmatrix}$ → stiffness matrix

$\begin{Bmatrix}v_2\\ \theta_2\end{Bmatrix}$ → displacement vector

Thus the above two terms together represent the spring force of pipe.

$2\rho v\begin{bmatrix}0 & \frac{-L}{5}\\ \frac{L}{5} & 0\end{bmatrix}\begin{Bmatrix}\dot{v}_2\\ \dot{\theta}_2\end{Bmatrix}$ → Coriolis Force

$\begin{Bmatrix}\dot{v}_2\\ \dot{\theta}_2\end{Bmatrix}$ → pipe angular velocity

Refer to section 1.2, Coriolis Force $2m\ \omega_E\ v_{rel.}$ is due to coupling between earth's angular velocity and relative velocity of the moving body. Similarly Coriolis Force $2\rho v\dot{v}_2$ due to the coupling between angular velocity of pipe and velocity of fluid flow relative to pipe.

$$\rho v^2 \begin{bmatrix} \frac{-12}{5L} & \frac{9}{5} \\ \frac{9}{5} & \frac{-4L}{15} \end{bmatrix} \begin{Bmatrix} v_2 \\ \theta_2 \end{Bmatrix} \rightarrow$$ Inertia force due to directional change in fluid flow velocity v, with changes in pipe curvature.

$$m \begin{bmatrix} \frac{26L}{35} & 0 \\ 0 & \frac{2L^3}{105} \end{bmatrix} \begin{Bmatrix} \ddot{v}_2 \\ \ddot{\theta}_2 \end{Bmatrix} \rightarrow$$ Inertia force due to vertical acceleration of pipe.

$$\begin{Bmatrix} F_2 \\ M_2 \end{Bmatrix} \rightarrow$$ External force and moment applied to the pipe.

For deflection we need the stiffness equations. For frequency we need equation with stiffness and mass. The stiffness matrix is singular and does not have an inverse. This is to be expected because no limitations have been placed on the displacements. There is no relative motion between coordinates, a situation corresponding to rigid body translation. To solve for the free vibration of beam, as transients will die out over time and we are left with steady state motion, force vector is made equal to zero and the acceleration vector is replaced by, $-\omega^2$ times the displacement [30]. Also refer to equations (1.40) and (1.42).

Reference equation (3.27), resolving by substitution: [18] [30] [42] [43]

Substituting $v_2 = v_y Sin(\omega t - \phi) = v_y e^{j(\omega t - \phi)}$ (3.28)

Taking derivatives of equation (3.28)

$$\dot{v}_2 = \omega v_y Cos(\omega t - \phi) = j\omega v_y e^{j(\omega t - \phi)} \quad (3.29)$$

$$\ddot{v}_2 = -\omega^2 v_y Sin(\omega t - \phi) = -\omega^2 v_y e^{j(\omega t - \phi)} \quad (3.30)$$

Similarly, substituting $\theta_2 = \theta_y Sin(\omega t - \phi) = \theta_y e^{j(\omega t - \phi)}$ (3.31)

$$\dot{\theta}_2 = \omega \theta_y \, Cos(\omega t - \phi) = j\omega\theta_y e^{j(\omega t - \phi)} \tag{3.32}$$

$$\ddot{\theta}_2 = -\omega^2 \, \theta_y Sin(\omega t - \phi) = -\omega^2 \theta_y e^{j(\omega t - \phi)} \tag{3.33}$$

With $j = \sqrt{-1}$, indicating $j2\omega\rho v[c]$ is in quadrature.

Applying equations (3.28) through (3.33) in vectorial form to (3.27), and setting right hand side to zero to solve for homogeneous solution:

$$EI\begin{bmatrix} \frac{24}{L^3} & 0 \\ 0 & \frac{8}{L} \end{bmatrix}\begin{Bmatrix} v_y \\ \theta_y \end{Bmatrix} + \rho v^2 \begin{bmatrix} \frac{-12}{5L} & \frac{9}{5} \\ \frac{9}{5} & \frac{-4L}{15} \end{bmatrix}\begin{Bmatrix} v_y \\ \theta_y \end{Bmatrix} + j2\omega\rho v \begin{bmatrix} 0 & \frac{-L}{5} \\ \frac{L}{5} & 0 \end{bmatrix}\begin{Bmatrix} v_y \\ \theta_y \end{Bmatrix} - \omega^2 m \begin{bmatrix} \frac{26L}{35} & 0 \\ 0 & \frac{2L^3}{105} \end{bmatrix}\begin{Bmatrix} v_y \\ \theta_y \end{Bmatrix} = \begin{Bmatrix} 0 \\ 0 \end{Bmatrix} \tag{3.34}$$

Adding matrices in equation (3.34):

$$\begin{bmatrix} \frac{840EI - 84L^2\rho v^2 - 26\omega^2 mL^4}{35L^3} & \frac{9\rho v^2 - j2\omega\rho vL}{5} \\ \frac{9\rho v^2 + j2\omega\rho vL}{5} & \frac{840EI - 28L^2\rho v^2 - 2\omega^2 mL^4}{105L} \end{bmatrix}\begin{Bmatrix} v_y \\ \theta_y \end{Bmatrix} = \begin{Bmatrix} 0 \\ 0 \end{Bmatrix} \tag{3.35}$$

Taking determinant of equation (3.35) equated to zero, with $F_2 = M_2 = 0$, to solve for ω_n:

$$\begin{vmatrix} \frac{840EI - 84L^2\rho v^2 - 26\omega^2 mL^4}{35L^3} & \frac{9\rho v^2 - j2\omega\rho vL}{5} \\ \frac{9\rho v^2 + j2\omega\rho vL}{5} & \frac{840EI - 28L^2\rho v^2 - 2\omega^2 mL^4}{105L} \end{vmatrix} = 0 \tag{3.36}$$

$$\left(\frac{52}{3675}m^2L^4\right)\omega^4+\left(\frac{896}{3675}m\,L^2\rho v^2-\frac{4}{25}\rho^2 v^2L^2-6.4E\,\mathrm{Im}\right)\omega^2 +\left(192\frac{E^2I^2}{L^4}-25.6\frac{EI\rho v^2}{L^2}-2.6\,\rho^2 v^4\right)=0 \tag{3.37}$$

Equation (3.37) is quadratic type of equation, of the 4th power in ω_n.

We solve equation (3.37) for ω_n:

Let $A_{1,2}=\omega_n^2$, thus $A^2{}_{1,2}=(\omega_n^2)^2=\omega_n^4$

We know the quadratic equation is of the form:

$$A_{1,2}=\omega_n^2=\frac{-b\pm\sqrt{b^2-4ac}}{2a} \tag{3.38}$$

Where in equation (3.38), a and b are coefficients of ω_n^4 and ω_n^2 respectively, and c is the constant terms in parenthesis.

Putting the values from equation (3.37) in (3.38) and solving:

$$\omega_n^2=A_{1,2}=\frac{\left\{-\left(\frac{896}{3675}mL^2\rho v^2-\frac{4\rho^2v^2L^2}{25}-6.4E\,\mathrm{Im}\right)\pm\sqrt{\left(\frac{896}{3675}mL^2\rho v^2-\frac{4\rho^2v^2L^2}{25}-6.4E\,\mathrm{Im}\right)^2-4\left(\frac{52}{3675}m^2L^4\right)\left(192\frac{E^2I^2}{L^4}-25.6\frac{EI\rho v^2}{L^2}-2.6\rho^2v^4\right)}\right\}}{2\left(\frac{52}{3675}m^2L^4\right)} \tag{3.39}$$

Putting values in equation (3.39) we find values of the system frequencies. We are interested in noting any effects on the values of frequencies with the changes in flow velocity and Coriolis Force. This is done in section 3.6, Case Studies.

Let us now derive for the deflections of the system.

Reference equation (3.27):

$$EI\begin{bmatrix}\frac{24}{L^3} & 0\\ 0 & \frac{8}{L}\end{bmatrix}\begin{Bmatrix}v_2\\ \theta_2\end{Bmatrix}+\rho v^2\begin{bmatrix}\frac{-12}{5L} & \frac{9}{5}\\ \frac{9}{5} & \frac{-4L}{15}\end{bmatrix}\begin{Bmatrix}v_2\\ \theta_2\end{Bmatrix}+2\rho v\begin{bmatrix}0 & \frac{-L}{5}\\ \frac{L}{5} & 0\end{bmatrix}\begin{Bmatrix}\dot{v}_2\\ \dot{\theta}_2\end{Bmatrix}$$
$$+m\begin{bmatrix}\frac{26L}{35} & 0\\ 0 & \frac{2L^3}{105}\end{bmatrix}\begin{Bmatrix}\ddot{v}_2\\ \ddot{\theta}_2\end{Bmatrix}=\begin{Bmatrix}F_2\\ M_2\end{Bmatrix}$$

Assuming free vibrations will die out over time. We consider only the particular solution to the differential equation. The particular solution depends on the form of the non-homogeneous part, i.e., $\begin{Bmatrix}F_2\\ M_2\end{Bmatrix}$.

So if $\begin{Bmatrix}F_2\\ M_2\end{Bmatrix}$ has the form $\begin{Bmatrix}F\\ M\end{Bmatrix}e^{j\omega t}$

Then $\begin{Bmatrix}v_2\\ \theta_2\end{Bmatrix}$ will also take the form $\begin{Bmatrix}v_y\\ \theta_y\end{Bmatrix}e^{j\omega t}$

3.5.1 Case 1 – Dynamic External Force:

$$\begin{Bmatrix}F_2\\ M_2\end{Bmatrix}=\begin{Bmatrix}F\\ M\end{Bmatrix}e^{j\omega t} \tag{3.40}$$

$$\begin{Bmatrix}v_2\\ \theta_2\end{Bmatrix}=\begin{Bmatrix}v_y\\ \theta_y\end{Bmatrix}e^{j\omega t} \tag{3.41}$$

taking derivatives of equation (3.41), gives:

$$\begin{Bmatrix} \dot{v}_2 \\ \dot{\theta}_2 \end{Bmatrix} = j\omega \begin{Bmatrix} v_y \\ \theta_y \end{Bmatrix} e^{j\omega t} \tag{3.42}$$

$$\begin{Bmatrix} \ddot{v}_2 \\ \ddot{\theta}_2 \end{Bmatrix} = -\omega^2 \begin{Bmatrix} v_y \\ \theta_y \end{Bmatrix} e^{j\omega t} \tag{3.43}$$

Substituting equations (3.40) through (3.43) in equation (3.27), we get:

$$EI\begin{bmatrix} \frac{24}{L^3} & 0 \\ 0 & \frac{8}{L} \end{bmatrix}\begin{Bmatrix} v_y \\ \theta_y \end{Bmatrix} e^{j\omega t} + \rho v^2 \begin{bmatrix} \frac{-12}{5L} & \frac{9}{5} \\ \frac{9}{5} & \frac{-4L}{15} \end{bmatrix}\begin{Bmatrix} v_y \\ \theta_y \end{Bmatrix} e^{j\omega t} + 2\rho v \begin{bmatrix} 0 & \frac{-L}{5} \\ \frac{L}{5} & 0 \end{bmatrix}\begin{Bmatrix} \dot{v}_y \\ \dot{\theta}_y \end{Bmatrix} j\omega e^{j\omega t} + m\begin{bmatrix} \frac{26L}{35} & 0 \\ 0 & \frac{2L^3}{105} \end{bmatrix}\begin{Bmatrix} \ddot{v}_y \\ \ddot{\theta}_y \end{Bmatrix}(-\omega^2 e^{j\omega t}) = \begin{Bmatrix} F \\ M \end{Bmatrix} e^{j\omega t} \tag{3.44}$$

Factoring, adding and simplifying equation (3.44) gives:

$$\begin{bmatrix} EI\frac{24}{L^3} - \frac{12}{5L}\rho v^2 - \frac{26L}{35}\omega^2 m & \frac{9}{5}\rho v^2 - j\frac{2}{5}\omega\rho vL \\ \frac{9}{5}\rho v^2 + j\frac{2}{5}\omega\rho vL & EI\frac{8}{L} - \frac{4L}{15}\rho v^2 - \frac{2L^3}{105}\omega^2 m \end{bmatrix}\begin{Bmatrix} v_y \\ \theta_y \end{Bmatrix} = \begin{Bmatrix} F \\ M \end{Bmatrix} \tag{3.45}$$

Determinant of the matrix in equation (3.45) is:

$$\begin{vmatrix} EI\frac{24}{L^3} - \frac{12}{5L}\rho v^2 - \frac{26L}{35}\omega^2 m & \frac{9}{5}\rho v^2 - j\frac{2}{5}\omega\rho vL \\ \frac{9}{5}\rho v^2 + j\frac{2}{5}\omega\rho vL & EI\frac{8}{L} - \frac{4L}{15}\rho v^2 - \frac{2L^3}{105}\omega^2 m \end{vmatrix}$$

The above determinant takes the form:

$$(\frac{52}{3675}m^2L^4)\omega^4+(\frac{896}{3675}mL^2\rho v^2-\frac{4}{25}\rho^2 v^2L^2-6.4mEI)\omega^2$$
$$+(192\frac{E^2I^2}{L^4}-25.6\frac{EI\rho v^2}{L^2}-2.6\,\rho^2 v^4)$$

To avoid resonance, thus the excitation frequency must be different than any of the natural frequencies; the above determinant is taken not equal to zero.

Solving equation (3.45) for deflections, we invert the matrix and divide by its determinant:

$$\begin{Bmatrix} v_y \\ \theta_y \end{Bmatrix} = \frac{\begin{bmatrix} EI\frac{8}{L}-\frac{4L}{15}\rho v^2-\frac{2L^3}{105}\omega^2 m & -\frac{9}{5}\rho v^2+j\frac{2}{5}\omega\rho vL \\ -\frac{9}{5}\rho v^2-j\frac{2}{5}\omega\rho vL & EI\frac{24}{L^3}-\frac{12}{5L}\rho v^2-\frac{26L}{35}\omega^2 m \end{bmatrix}\begin{Bmatrix} F \\ M \end{Bmatrix}}{\begin{vmatrix} EI\frac{24}{L^3}-\frac{12}{5L}\rho v^2-\frac{26L}{35}\omega^2 m & \frac{9}{5}\rho v^2-j\frac{2}{5}\omega\rho vL \\ \frac{9}{5}\rho v^2+j\frac{2}{5}\omega\rho vL & EI\frac{8}{L}-\frac{4L}{15}\rho v^2-\frac{2L^3}{105}\omega^2 m \end{vmatrix}} \tag{3.46}$$

$$v_y = \frac{\left(EI\frac{8}{L}-\frac{4L}{15}\rho v^2-\frac{2L^3}{105}\omega^2 m\right)F+\left(-\frac{9}{5}\rho v^2+j\frac{2}{5}\omega\rho vL\right)M}{\begin{vmatrix} EI\frac{24}{L^3}-\frac{12}{5L}\rho v^2-\frac{26L}{35}\omega^2 m & \frac{9}{5}\rho v^2-j\frac{2}{5}\omega\rho vL \\ \frac{9}{5}\rho v^2+j\frac{2}{5}\omega\rho vL & EI\frac{8}{L}-\frac{4L}{15}\rho v^2-\frac{2L^3}{105}\omega^2 m \end{vmatrix}} \tag{3.47}$$

$$\theta_y = \frac{\left(-\frac{9}{5}\rho v^2-j\frac{2}{5}\omega\rho vL\right)F+\left(EI\frac{24}{L^3}-\frac{12}{5L}\rho v^2-\frac{26L}{35}\omega^2 m\right)M}{\begin{vmatrix} EI\frac{24}{L^3}-\frac{12}{5L}\rho v^2-\frac{26L}{35}\omega^2 m & \frac{9}{5}\rho v^2-j\frac{2}{5}\omega\rho vL \\ \frac{9}{5}\rho v^2+j\frac{2}{5}\omega\rho vL & EI\frac{8}{L}-\frac{4L}{15}\rho v^2-\frac{2L^3}{105}\omega^2 m \end{vmatrix}} \tag{3.48}$$

$$v_y = \frac{\left(EI\frac{8}{L} - \frac{4L}{15}\rho v^2 - \frac{2L^3}{105}\omega^2 m\right)F + \left(-\frac{9}{5}\rho v^2\right)M}{\begin{vmatrix} EI\frac{24}{L^3} - \frac{12}{5L}\rho v^2 - \frac{26L}{35}\omega^2 m & \frac{9}{5}\rho v^2 - j\frac{2}{5}\omega\rho vL \\ \frac{9}{5}\rho v^2 + j\frac{2}{5}\omega\rho vL & EI\frac{8}{L} - \frac{4L}{15}\rho v^2 - \frac{2L^3}{105}\omega^2 m \end{vmatrix}} + \frac{j\left(\frac{2}{5}\omega\rho vL\right)M}{\begin{vmatrix} EI\frac{24}{L^3} - \frac{12}{5L}\rho v^2 - \frac{26L}{35}\omega^2 m & \frac{9}{5}\rho v^2 - j\frac{2}{5}\omega\rho vL \\ \frac{9}{5}\rho v^2 + j\frac{2}{5}\omega\rho vL & EI\frac{8}{L} - \frac{4L}{15}\rho v^2 - \frac{2L^3}{105}\omega^2 m \end{vmatrix}} \tag{3.49}$$

$$\theta_y = \frac{\left(EI\frac{24}{L^3} - \frac{12}{5L}\rho v^2 - \frac{26L}{35}\omega^2 m\right)M + \left(-\frac{9}{5}\rho v^2\right)F}{\begin{vmatrix} EI\frac{24}{L^3} - \frac{12}{5L}\rho v^2 - \frac{26L}{35}\omega^2 m & \frac{9}{5}\rho v^2 - j\frac{2}{5}\omega\rho vL \\ \frac{9}{5}\rho v^2 + j\frac{2}{5}\omega\rho vL & EI\frac{8}{L} - \frac{4L}{15}\rho v^2 - \frac{2L^3}{105}\omega^2 m \end{vmatrix}} - \frac{j\left(\frac{2}{5}\omega\rho vL\right)F}{\begin{vmatrix} EI\frac{24}{L^3} - \frac{12}{5L}\rho v^2 - \frac{26L}{35}\omega^2 m & \frac{9}{5}\rho v^2 - j\frac{2}{5}\omega\rho vL \\ \frac{9}{5}\rho v^2 + j\frac{2}{5}\omega\rho vL & EI\frac{8}{L} - \frac{4L}{15}\rho v^2 - \frac{2L^3}{105}\omega^2 m \end{vmatrix}} \tag{3.50}$$

Using exponential notation, as complex numbers given in equations (3.49) and (3.50) can be written as:

$$v_y = \left(\left| \frac{\left(EI\frac{8}{L} - \frac{4L}{15}\rho v^2 - \frac{2L^3}{105}\omega^2 m \right)F - \left(\frac{9}{5}\rho v^2 \right)M}{\begin{vmatrix} EI\frac{24}{L^3} - \frac{12}{5L}\rho v^2 - \frac{26L}{35}\omega^2 m & \frac{9}{5}\rho v^2 - j\frac{2}{5}\omega\rho vL \\ \frac{9}{5}\rho v^2 + j\frac{2}{5}\omega\rho vL & EI\frac{8}{L} - \frac{4L}{15}\rho v^2 - \frac{2L^3}{105}\omega^2 m \end{vmatrix}} \right|^2 + \left| \frac{\left(\frac{2}{5}\omega\rho vL \right)M}{\begin{vmatrix} EI\frac{24}{L^3} - \frac{12}{5L}\rho v^2 - \frac{26L}{35}\omega^2 m & \frac{9}{5}\rho v^2 - j\frac{2}{5}\omega\rho vL \\ \frac{9}{5}\rho v^2 + j\frac{2}{5}\omega\rho vL & EI\frac{8}{L} - \frac{4L}{15}\rho v^2 - \frac{2L^3}{105}\omega^2 m \end{vmatrix}} \right|^2 \right) e^{j\phi_1} \tag{3.51}$$

$$\phi_1 = \tan^{-1}\left(\frac{\left(\frac{2}{5}\omega\rho vL \right)M}{\left(EI\frac{8}{L} - \frac{4L}{15}\rho v^2 - \frac{2L^3}{105}\omega^2 m \right)F + \left(-\frac{9}{5}\rho v^2 \right)M} \right) (\phi_1 \text{ is phase shift}) \tag{3.52}$$

$$\theta_y = \left(\left| \frac{\left(EI\frac{24}{L^3} - \frac{12}{5L}\rho v^2 - \frac{26L}{35}\omega^2 m \right)M - \left(\frac{9}{5}\rho v^2 \right)F}{\begin{vmatrix} EI\frac{24}{L^3} - \frac{12}{5L}\rho v^2 - \frac{26L}{35}\omega^2 m & \frac{9}{5}\rho v^2 - j\frac{2}{5}\omega\rho vL \\ \frac{9}{5}\rho v^2 + j\frac{2}{5}\omega\rho vL & EI\frac{8}{L} - \frac{4L}{15}\rho v^2 - \frac{2L^3}{105}\omega^2 m \end{vmatrix}} \right|^2 + \left| \frac{\left(\frac{2}{5}\omega\rho vL \right)F}{\begin{vmatrix} EI\frac{24}{L^3} - \frac{12}{5L}\rho v^2 - \frac{26L}{35}\omega^2 m & \frac{9}{5}\rho v^2 - j\frac{2}{5}\omega\rho vL \\ \frac{9}{5}\rho v^2 + j\frac{2}{5}\omega\rho vL & EI\frac{8}{L} - \frac{4L}{15}\rho v^2 - \frac{2L^3}{105}\omega^2 m \end{vmatrix}} \right|^2 \right) e^{j\phi_2} \tag{3.53}$$

$$\phi_2 = \tan^{-1}\left(\frac{\left(-\frac{2}{5}\omega\rho vL\right)F}{\left(EI\frac{24}{L^3}-\frac{12}{5L}\rho v^2-\frac{26L}{35}\omega^2 m\right)M+\left(-\frac{9}{5}\rho v^2\right)F}\right) \text{ (ϕ_2 is phase shift)} \qquad (3.54)$$

Multiplying equation (3.51) by $e^{j\omega t}$ and substituting $v_2 = v_y e^{j\omega t}$, gives:

$$v_2 = \left(\left|\frac{\left(EI\frac{8}{L}-\frac{4L}{15}\rho v^2-\frac{2L^3}{105}\omega^2 m\right)F-\left(\frac{9}{5}\rho v^2\right)M}{\begin{vmatrix} EI\frac{24}{L^3}-\frac{12}{5L}\rho v^2-\frac{26L}{35}\omega^2 m & \frac{9}{5}\rho v^2-j\frac{2}{5}\omega\rho vL \\ \frac{9}{5}\rho v^2+j\frac{2}{5}\omega\rho vL & EI\frac{8}{L}-\frac{4L}{15}\rho v^2-\frac{2L^3}{105}\omega^2 m \end{vmatrix}}\right|^2 + \left|\frac{\left(\frac{2}{5}\omega\rho vL\right)M}{\begin{vmatrix} EI\frac{24}{L^3}-\frac{12}{5L}\rho v^2-\frac{26L}{35}\omega^2 m & \frac{9}{5}\rho v^2-j\frac{2}{5}\omega\rho vL \\ \frac{9}{5}\rho v^2+j\frac{2}{5}\omega\rho vL & EI\frac{8}{L}-\frac{4L}{15}\rho v^2-\frac{2L^3}{105}\omega^2 m \end{vmatrix}}\right|^2\right)^{\frac{1}{2}} e^{j(\omega t+\phi_1)} \qquad (3.55)$$

Multiplying equation (3.53) by $e^{j\omega t}$ and substituting $\theta_2 = \theta_y e^{j\omega t}$, gives:

$$\theta_2 = \left(\left| \frac{\left(EI\frac{24}{L^3} - \frac{12}{5L}\rho v^2 - \frac{26L}{35}\omega^2 m \right) M - \left(\frac{9}{5}\rho v^2 \right) F}{\begin{vmatrix} EI\frac{24}{L^3} - \frac{12}{5L}\rho v^2 - \frac{26L}{35}\omega^2 m & \frac{9}{5}\rho v^2 - j\frac{2}{5}\omega\rho vL \\ \frac{9}{5}\rho v^2 + j\frac{2}{5}\omega\rho vL & EI\frac{8}{L} - \frac{4L}{15}\rho v^2 - \frac{2L^3}{105}\omega^2 m \end{vmatrix}} \right|^2 + \left| \frac{\left(\frac{2}{5}\omega\rho vL \right) F}{\begin{vmatrix} EI\frac{24}{L^3} - \frac{12}{5L}\rho v^2 - \frac{26L}{35}\omega^2 m & \frac{9}{5}\rho v^2 - j\frac{2}{5}\omega\rho vL \\ \frac{9}{5}\rho v^2 + j\frac{2}{5}\omega\rho vL & EI\frac{8}{L} - \frac{4L}{15}\rho v^2 - \frac{2L^3}{105}\omega^2 m \end{vmatrix}} \right|^2 \right)^{\frac{1}{2}} e^{j(\omega t + \phi_2)} \tag{3.56}$$

For maximum value of v_2 and θ_2, $e^{j(\omega t+\phi_1)}$ in equation (3.55) and $e^{j(\omega t+\phi_2)}$ in equation (3.56), respectively must equal unity. If needed one can use $e^{j(\omega t+\phi_1)}$ and $e^{j(\omega t+\phi_2)}$ to trace the plot of deflections to the forcing sine wave.

3.5.2 Case 2 – Static External Force:

If $\begin{Bmatrix} F_2 \\ M_2 \end{Bmatrix}$ takes the form $\begin{Bmatrix} F \\ M \end{Bmatrix}$ where F_2, F, M_2 and M are constants.

Then $\begin{Bmatrix} v_2 \\ \theta_2 \end{Bmatrix}$ takes the form $\begin{Bmatrix} v_y \\ \theta_y \end{Bmatrix}$ where v_2, v_y, θ_2 and θ_y are constants.

Taking derivatives of deflections and rotations as above, gives:

$$\begin{Bmatrix} \dot{v}_2 \\ \dot{\theta}_2 \end{Bmatrix} = \begin{Bmatrix} \ddot{v}_2 \\ \ddot{\theta}_2 \end{Bmatrix} = 0 \tag{3.57}$$

Putting equation (3.57) in equation (3.27), results in:

$$EI\begin{bmatrix}\frac{24}{L^3} & 0\\ 0 & \frac{8}{L}\end{bmatrix}\begin{Bmatrix}v_2\\ \theta_2\end{Bmatrix}+\rho v^2\begin{bmatrix}\frac{-12}{5L} & \frac{9}{5}\\ \frac{9}{5} & \frac{-4L}{15}\end{bmatrix}\begin{Bmatrix}v_2\\ \theta_2\end{Bmatrix}=\begin{Bmatrix}F_2\\ M_2\end{Bmatrix} \tag{3.58}$$

Simplifying equation (3.58):

$$\begin{bmatrix}\frac{24EI}{L^3}-\frac{12\rho v^2}{5L} & \frac{9}{5}\rho v^2\\ \frac{9}{5}\rho v^2 & \frac{8EI}{L}-\frac{4\rho v^2 L}{15}\end{bmatrix}\begin{Bmatrix}v_2\\ \theta_2\end{Bmatrix}=\begin{Bmatrix}F_2\\ M_2\end{Bmatrix} \tag{3.59}$$

Taking the determinant of equation (3.59) and to avoid resonance, the excitation frequency must be different than any of the natural frequencies; the above determinant is taken not equal to zero:

$$\begin{vmatrix}\frac{24EI}{L^3}-\frac{12\rho v^2}{5L} & \frac{9}{5}\rho v^2\\ \frac{9}{5}\rho v^2 & \frac{8EI}{L}-\frac{4\rho v^2 L}{15}\end{vmatrix}\neq 0$$

Solving for deflections, we invert the matrix in equation in equation (3.59) and divide by its determinant:

$$\begin{Bmatrix}v_2\\ \theta_2\end{Bmatrix}=\frac{\begin{bmatrix}\frac{8EI}{L}-\frac{4\rho v^2 L}{15} & -\frac{9}{5}\rho v^2\\ -\frac{9}{5}\rho v^2 & \frac{24EI}{L^3}-\frac{12\rho v^2}{5L}\end{bmatrix}}{\begin{vmatrix}\frac{24EI}{L^3}-\frac{12\rho v^2}{5L} & \frac{9}{5}\rho v^2\\ \frac{9}{5}\rho v^2 & \frac{8EI}{L}-\frac{4\rho v^2 L}{15}\end{vmatrix}}\begin{Bmatrix}F_2\\ M_2\end{Bmatrix} \tag{3.60}$$

Solving equation (3.60) for v_2 and θ_2, we get:

$$v_2 = \frac{\left(\frac{8EI}{L} - \frac{4\rho v^2 L}{15}\right)F_2 - \left(\frac{9}{5}\rho v^2\right)M_2}{\begin{vmatrix} \frac{24EI}{L^3} - \frac{12\rho v^2}{5L} & \frac{9}{5}\rho v^2 \\ \frac{9}{5}\rho v^2 & \frac{8EI}{L} - \frac{4\rho v^2 L}{15} \end{vmatrix}} \tag{3.61}$$

$$\theta_2 = \frac{\left(\frac{24EI}{L^3} - \frac{12\rho v^2}{5L}\right)M_2 - \left(\frac{9}{5}\rho v^2\right)F_2}{\begin{vmatrix} \frac{24EI}{L^3} - \frac{12\rho v^2}{5L} & \frac{9}{5}\rho v^2 \\ \frac{9}{5}\rho v^2 & \frac{8EI}{L} - \frac{4\rho v^2 L}{15} \end{vmatrix}} \tag{3.62}$$

3.6 Case Studies – Numerical Analysis

In the previous sections we have studied and derived equations with a view to include Coriolis Force in the equations of motion of this system.

Now we shall see how that translates numerically using the project data, through nine case studies.

Though any of the parameters in equations (3.39), (3.55), (3.56), (3.61) and (3.62) can be varied and their effects studied, here we are going to keep our focus on the effects of Coriolis Force, with the flow velocity variations, on the system deflections and frequencies.

In Chapter 2, we used the data from an industrial project to compare the different calculating methods. This data provides us with static external force values, thus we shall make use of equation (3.61) to find the deflections and equation (3.39) for frequencies of the system. We will use the following values for the industrial project taken, though any values for the case scenario may be used:

Taking $M_2 = 0$ and $\theta_2 = 0$

Putting following values in equations (3.39) and (3.61), we find the system deflections:

$E = 27.4 \times 10^6$ psig

$I = 562$ in^4

$\rho = 0.677$ lb-sec^2/in

$L = 105.75$ in

$m = 1.213$ or 0.536 lb-sec^2/in (varies depending on case, empty pipe or with fluid)

v = 0; 1492.89; 2985.77; 6000; 7876.15; 9752.3; 11628.45 and 13504.6 in/sec (different values of velocity have been considered keeping in mind the conditions of the project considered. These velocities reflect the effects of the variation of Coriolis Force on the system.)

F_2 = static loads like: self load of pipe with or without fluid, external load, internal fluid constant velocity-static load case, external static steady wind load etc. [22] [23]

$F_2 = F_2 \, Sin \, \alpha \, t$, dynamic loads like: seismic, wind, internal dynamic force due to fluid velocity etc. [19] [21] [22] [23] [28] [34] [35] [39] [44]

For our ease we re-write equations (3.39) and (3.61) here:

$$\omega_n^2 = A_{1,2} = \frac{\left\{ -\left(\frac{896}{3675} mL^2 \rho v^2 - \frac{4\rho^2 v^2 L^2}{25} - 6.4 E \, \mathrm{Im} \right) \pm \sqrt{\left(\frac{896}{3675} mL^2 \rho v^2 - \frac{4\rho^2 v^2 L^2}{25} - 6.4 E \, \mathrm{Im} \right)^2 - 4\left(\frac{52}{3675} m^2 L^4 \right)\left(192 \frac{E^2 I^2}{L^4} - 25.6 \frac{EI\rho v^2}{L^2} - 2.6\rho^2 v^4 \right)} \right\}}{2\left(\frac{52}{3675} m^2 L^4 \right)}$$

$$v_2 = \frac{\left(\frac{8EI}{L} - \frac{4\rho v^2 L}{15}\right)F_2 - \left(\frac{9}{5}\rho v^2\right)M_2}{\begin{vmatrix} \frac{24EI}{L^3} - \frac{12\rho v^2}{5L} & \frac{9}{5}\rho v^2 \\ \frac{9}{5}\rho v^2 & \frac{8EI}{L} - \frac{4\rho v^2 L}{15} \end{vmatrix}}$$

Putting values in equations (3.39) and (3.61) for the conditions defined in each of the nine cases, we evaluate the system frequencies and deflections.

3.6.1 Case – I Empty Pipe

Conditions: No fluid inside pipe and no internal or external forces acting on pipe. Only pipe self-load acting.

$v = \rho = 0.$

$$\left.\begin{aligned} \omega_1 &= 310.15 \text{ cps} \\ \omega_2 &= 86.15 \text{ cps} \end{aligned}\right\} \quad (3.48)$$

$v_y = 6.62 \times 10^{-4}$ in. (3.49)

3.6.2 Case – II Fluid Filled Pipe, No Flow Velocity

Conditions: Pipe and fluid self-load acting, no other external or internal forces on pipe.

$v = 0.$

$$\left.\begin{aligned} \omega_1 &= 206.48 \text{ cps} \\ \omega_2 &= 57.67 \text{ cps} \end{aligned}\right\} \quad (3.50)$$

$v_y = 1.498 \times 10^{-3}$ in. (3.51)

3.6.3 Case – III Fluid Filled Pipe, Medium Flow Velocity

Conditions: Pipe and fluid self load acting, flow velocity at half the design pressure.

v = 1492.89 in/sec.

ω_1 = 204.70 cps
ω_2 = 52.87 cps } (3.52)

$v_y = 1.72 \times 10^{-3}$ in. (3.53)

3.6.4 Case – IV Fluid Filled Pipe, High Flow Velocity

Conditions: Pipe and fluid self load acting, flow velocity at design pressure.

v = 2985.77 in/sec.

ω_1 = 201.29 cps
ω_2 = 23.16 cps } (3.54)

$v_y = 8.23 \times 10^{-3}$ in. (3.55)

3.6.5 Case – V Fluid Filled Pipe, Very High Flow Velocity

Conditions: Pipe and fluid self load acting, flow velocity at higher than design pressure.

v = 6000 in/sec.

ω_1 = 209.93 cps
ω_2 = 133.32 cps } (3.56)

$v_y = -1.1 \times 10^{-4}$ in. (3.57)

3.6.6 Case – VI Fluid Filled Pipe, Extra High Flow Velocity

Conditions: Pipe and fluid self load acting, flow velocity at higher than design pressure.

v = 7876.15 in/sec.

ω_1 = 110.03 cps
ω_2 = imaginary roots (3.56)

v_y = -996.34 in. (3.57)

3.6.7 Case – VII Fluid Filled Pipe, Ultra-High Flow Velocity

Conditions: Pipe and fluid self load acting, flow velocity at higher than design pressure.

v = 9752.3 in/sec.

ω_1 = 203.75 cps
ω_2 = imaginary roots (3.56)

v_y = 2.4 x 10^{-5} in. (3.57)

3.6.8 Case – VIII Fluid Filled Pipe, Near Sonic Flow Velocity

Conditions: Pipe and fluid self load acting, flow velocity at higher than design pressure.

v = 11628.45 in/sec.

ω_1 = 0.18 cps
ω_2 = imaginary roots (3.56)

v_y = 280.25 in. (3.57)

3.6.9 Case – IX Fluid Filled Pipe, Sonic Flow Velocity

Conditions: Pipe and fluid self-load acting, sonic flow velocity.

v = 13504.6 in/sec.

$$\left.\begin{array}{l}\omega_1 = 324.71 \text{ cps} \\ \omega_2 = \text{imaginary roots}\end{array}\right\} \tag{3.56}$$

$$v_y = 2.49 \times 10^{-5} \text{ in.} \tag{3.57}$$

The results of the above nine case studies are plotted in Figure 3.6, frequency verses flow velocity, and in Figure 3.7, deflection verses flow velocity.

Figure 3.8 being the superimposed view of Figures 3.6 and 3.7.

Figures 3.6, 3.7 and 3.8, have been plotted to give a good overall view of the pipe behaviour with the increasing flow velocities. These plots show harmony between system frequencies and deflections to the corresponding flow velocities. Also showing effects of Coriolis Force in terms of pipe erratic behaviour at relatively higher flow velocities.

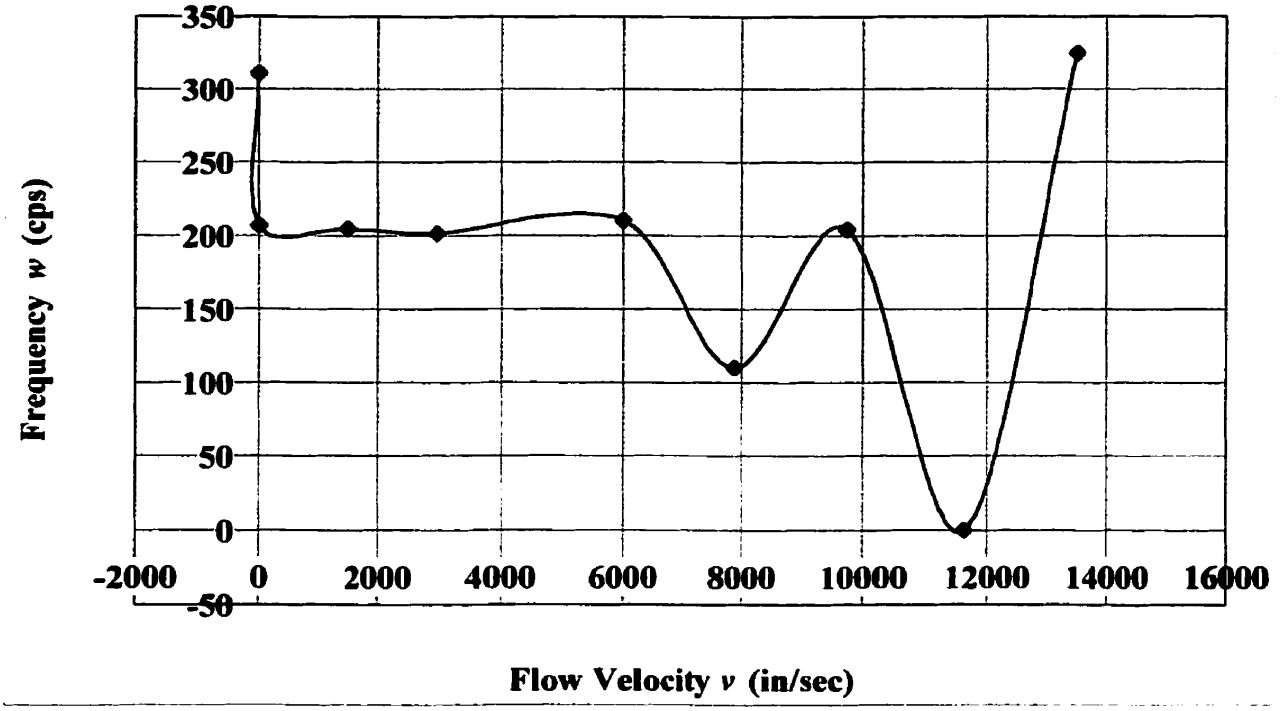

Figure 3.6: System Frequencies Curve in relation to Coriolis Force

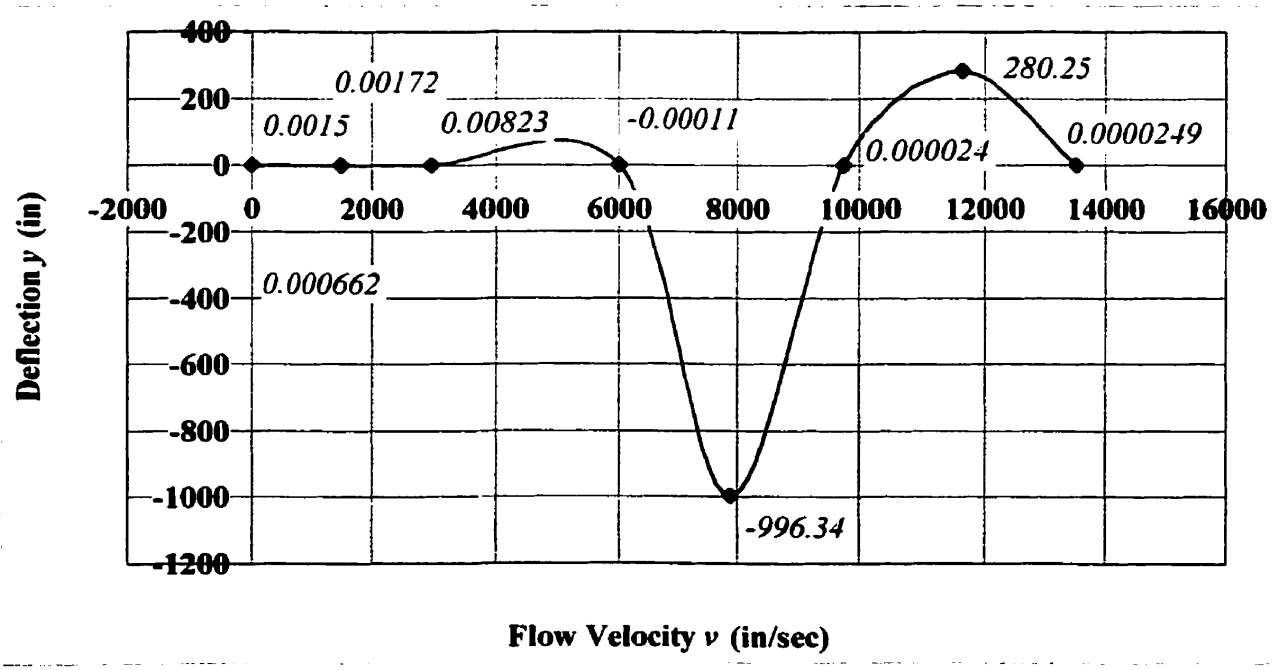

Figure 3.7: System Deflections Curve in relation to Coriolis Force

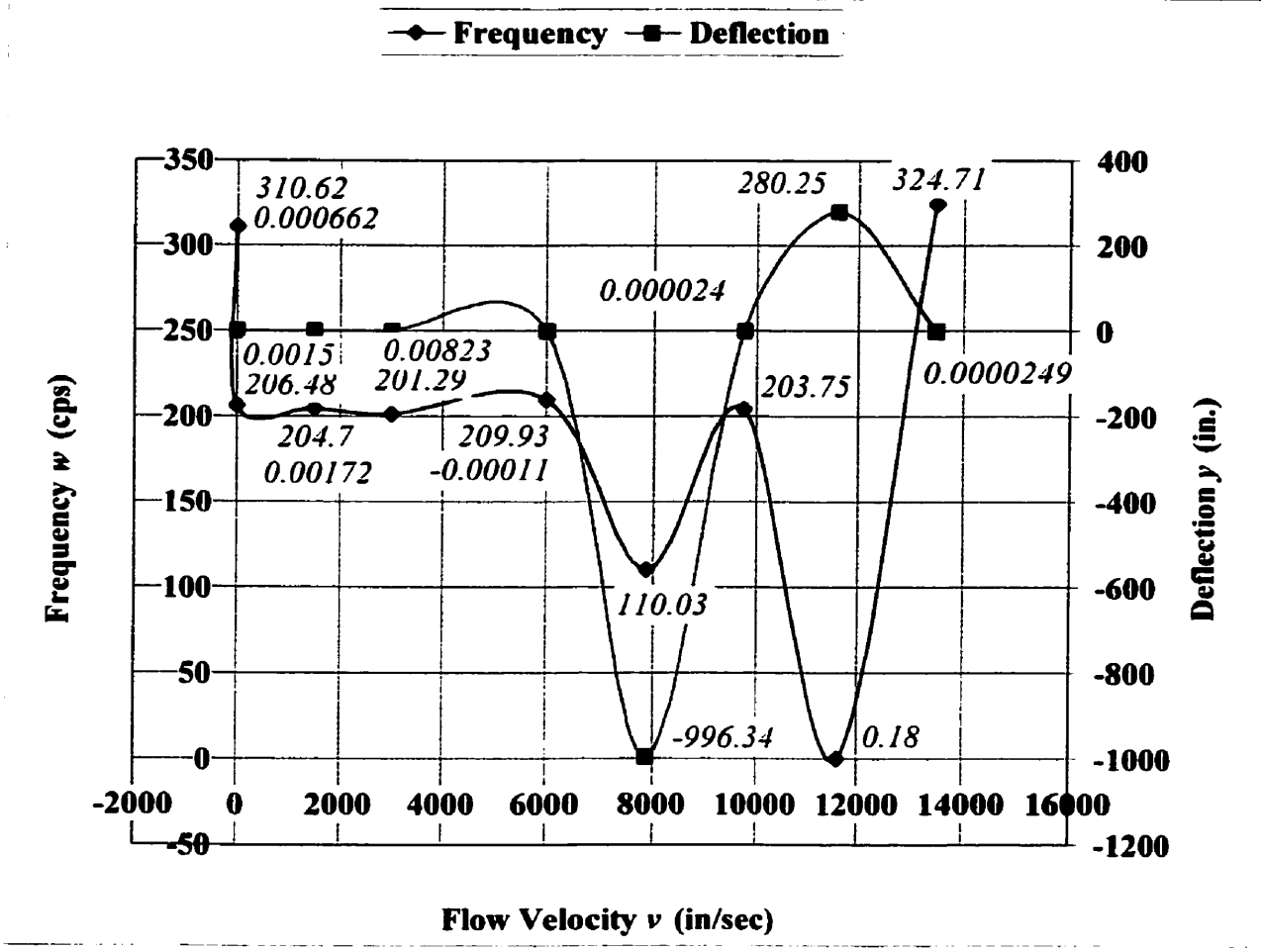

Figure 3.8: System Deflections and Frequencies in relation to Coriolis Force Frequency and Deflection Curves vs. Flow Velocity

3.7 Conclusions

Referring to section 3.4.1, the derivation does not show presence of the effects of Coriolis Force and easily we derive equations (3.20) and (3.21) for the deflection v_2 and slope θ_2. On the other hand section 3.5 shows quite a bit of involved work to derive equations (3.39), (3.55), (3.56), (3.61) and (3.62) for the frequency, deflection and slope. Equations (3.20) and (3.21) do not give us the ability to introduce the fluid flow velocity and determine if there in fact are any effects of Coriolis Force. But if we continue our pursuit, as in the nine case

studies in section 3.6 using equations (3.39) and (3.61), we find marked differences in the calculated values of deflection and frequency as we vary the velocity of flow. The difference comes from the effects of the Coriolis Force.

With reference to Figure 3.6, we find that with velocity of flow being zero the frequency reduced with the addition of the fluid weight. This is expected if we look at equation (3.39). Now as we increase the fluid velocity there is very little change in the frequency till it reaches about over 1500 in/sec. That is where we see that with the increase in velocity of another approximately 1500 in/sec. there is a drop of 5 cps in frequency value. While further increase in flow velocity beyond 6000 in/sec., to reach sonic flow velocity, the system clearly becomes erratic and out of control. This result clearly shows the effects of Coriolis Force due to fluid flow velocity on the vibration of pipes. It confirms the pipe behavior reported in other research papers [10] [13][15] [27] [69].

Now refer to Figure 3.7. We see an increase in deflection with the introduction of fluid weight. This was expected looking at equation (3.61). Increase of fluid velocity to over 1500 in/sec. starts to show the difference in deflection values. As we go over 6000 in/sec. to reach sonic flow velocity, a pronounced increase and decrease in deflections of the pipe is seen. This behavior is called pipe flutter or erratic behavior. Some of the numerically high deflection values, not possible practically, go to show the system theoretically is out of control but practically the pipe would have failed with this behavior. These results, just as explained for Figure 3.6, bring out the possible effects of Coriolis Force due to the fluid flow velocity.

Now let us examine Figure 3.8. It is the Figures 3.6 and 3.7 superimposed. We see as the pipe deflection increases and decreases with the increase in fluid flow velocity, the frequency

of the pipe conversely decreases and increases correspondingly. This is the expected characteristic of the pipe behavior. Thus this study of Figure 3.8 shows that the effects of Coriolis Force on the pipe are in harmony with the pipe characteristics. These characteristics of pipe behavior, to varied extent, were reported by some other researchers, [8] [10] [13] [15] [38] [58] [69], using some other different analytical and experimental techniques.

CHAPTER 4 - DYNAMIC RESPONSE OF PIPING MULTI-SUPPORT SYSTEM WITH GAP

4.1 Introduction

Finite Element Method developed in Chapter – 3 of this Thesis is quite versatile in its utility, as mentioned earlier. Application of this Finite Element Method to the Research Work of other scholars is shown here.

In this Chapter it has been shown as to how the Finite Element Method developed in Chapter 3 can be used in conjunction with the research work by other scholars. It is interesting to note the fact that this Finite Element Method can be used in linear analysis as well as non-linear analysis, as shown in this chapter too.

Three specific research papers by other scholars titled: Influence of Gap Size on the Dynamic behavior of Piping Systems, by J. P. Vayda [3]; A Test and Analysis of the Multiple Support Piping Systems, by T. Chiba, R. Koyanagi, N. Ogawa and C. Minowa [4]; and Dynamic Response Studies of Piping-Support Systems [5], have been studied here.

It is desired by the author of this Thesis to show the relationship between this Thesis and the research by other scholars. It is hoped that the similarity in the equations of motion presented here will be exploited to its full extent. It is obvious that the possible superimposition of the equations of motion in [4] and this Thesis will result in that extra power and advantage to the analysis in this field.

4.2 Research Paper: Influence of Gap Size on the Dynamic Behaviour of Piping Systems [3]

4.2.1 Abstract

The effects of dynamic events induced by support motion on piping systems with snubbers having variable gap sizes have been studied. Examination of piecewise a non-linear 1-DOF mass-spring-snubber system representing a 3-dimensional piping system was utilized [3].

The snubber dead band is a well-known phenomenon in the analysis of piping systems. However, the effect of the gap size is ignored in most piping codes. The procedure assumes, for simplicity, a snubber force-deflection relationship passing through the origin, as shown in Figure 4.1. In the derivations the origin offset, shown in Figure 4.2, is examined for an optimal gap size for a wide range of dynamic loading events. Even in the absence of damping, a system subjected to forced vibration at resonance attains infinite amplitude only after infinite time. Thus it takes many cycles to build up significant amplitudes.

But with the presence of small non-zero gap sizes, the system stiffness and therefore eigenvalues change continually as various snubbers open and close. As a result, the number of cycles or increase of amplitude is severely limited before a new configuration arises [3].

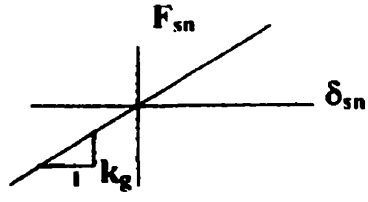

Figure 4.1: Snubber Force-Deflection [3] without origin offset

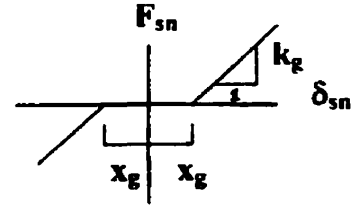

Figure 4.2: Snubber Force-Deflection [3] with origin offset

4.2.2 3-Dof Mass-Spring-Snubber Non-Linear Analysis

In order to correlate with the ideas and nomenclature of the 1-DOF systems, the 3-D piping system was reduced by means of static condensation to an analogous 1-DOF mass-spring-snubber system at Gap I, II and III, shown in Figure 4.3. The results of 3-D piping analysis are presented in the paper. The general behavior of 3-D system corresponds closely to 1-D system. This similarity can be observed by comparing the 3-D system results to that of 1-D given in the [3].

Figure 4.3 shows 3-D piping system analyzed by means of a Finite Element system program (ANSYS). Each computer run included the 4 subsystems to generate a table, given in the [3].

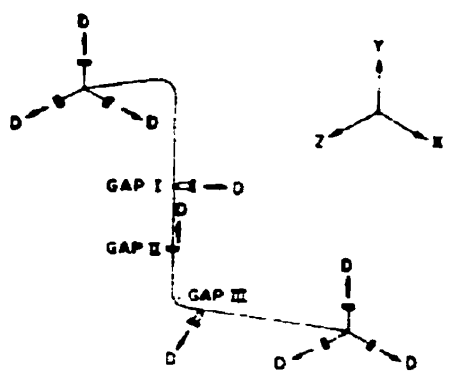

Figure 4.3: Basic 3D Piping System with 3 Gaps [3]

4.2.3 Equation of Motion [3]

Using Newton's Second Law of motion, we can derive the general equation of motion for the 3 cases as here, while keeping Figure 4.4 and 4.5 in view:

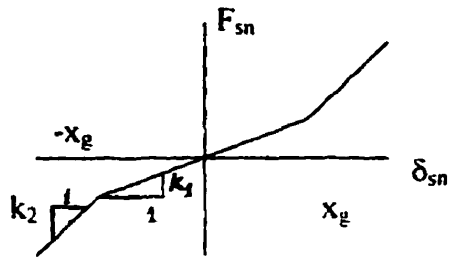

Figure 4.4: System Force-Deflection [3]

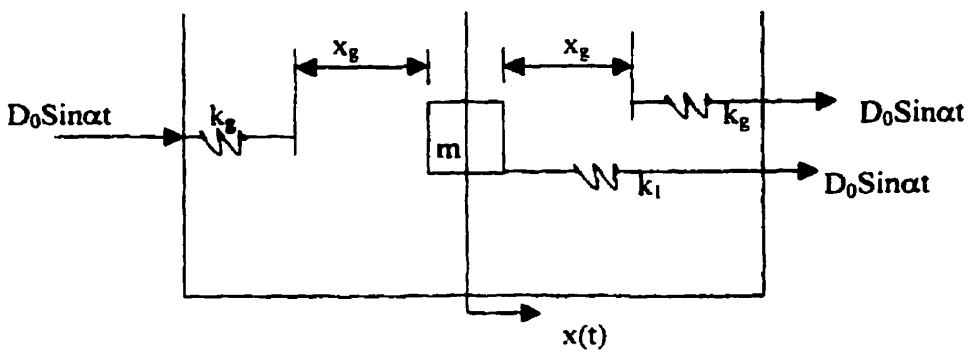

Figure 4.5: 1 – DOF System with 1 gap [3]

CASE – I

When the mass is in middle not touching either of the snubbers, called open system:

$S = 0, for -x_g < x < x_g$

CASE – II

When the mass is to the right side touching the snubber, called the closed system:

$S = 1, for\ x_g \leq x$

CASE – III

Similarly we derive for mass m touching left snubber:

$S = -1$, *for* $-x_g \geq x$

From the three cases, we can deduce a general equation:

$$\ddot{x} + \omega_i^2 \, x = q_i Sin\alpha \, t + Sk_g \frac{x_g}{m} \tag{4.1}$$

Where:

k_g = snubber stiffness

x_g = gap size

q_i = loading amplitude

$$q_i = \frac{k_i D_0}{m} \quad \textit{(by definition)}$$

$$\omega_i^2 = \frac{k_i}{m}$$

With i = 1, 2

S = parameter depending on position of m

From equation (4.1), we can derive the solution: [3]

$$x = \frac{q_i}{\omega_i^2 - \alpha^2}\left[Sin\,\alpha \, t - \frac{\alpha}{\omega_i} Sin\omega_i t \right] \tag{4.2}$$

Generally the second term in equation (4.2) is ignored as part of free vibrations which dies out with time, due to one kind of damping or another.

However, in piping applications, the assumed damping values are very low, usually not more than 2%. It is thus imperative to consider equation (4.2) in its entirety.

A more general solution, to equation of motion as in equation (4.1), is given by: [3]

$$x(t) = x_0 Cos\,\omega_i\,(t-t_0) + \frac{\dot{x}_0}{\omega_i} Sin\,\omega_i\,(t-t_0) + \frac{1}{\omega_i}\int_{\tau=t_0}^{\tau=t} Sin\,\omega_i\,(t-\tau)[q_i Sin\,\alpha\,\tau + \frac{SK_g x_g}{m}]d\tau \tag{4.3}$$

Integrating equation (4.3) for the last part, we get:

$$x_i(t) = \frac{q_i}{\omega_i^2-\alpha^2}[Sin\,\alpha\,t - Sin\,\alpha\,t_0 Cos\,\omega_i(t-t_0) - \frac{\alpha}{\omega_i} Cos\,\alpha\,t_0 Sin\omega_i(t-t_0)] + \frac{SK_g x_g}{K_2}[1-Cos\omega_2(t-t_0)] \tag{4.4}$$

The derivatives of equation (4.4) are:

$$\dot{x}_i(t) = \frac{d\{x_i(t)\}}{dt} = \frac{q_i}{\omega_i^2-\alpha^2}[\alpha\,Cos\alpha\,t - \alpha\,t_0 Cos\alpha\,t_0 t - \alpha\,Cos\alpha\,t_0 Cos\omega_i t] + \frac{SK_g x_g \omega_2}{K_2} Sin\omega_2\,t \qquad \textit{(velocity)} \tag{4.5}$$

$$\ddot{x}_i(t) = \frac{d^2\{x_i(t)\}}{dt^2} = \frac{q_i}{\omega_i^2-\alpha^2}[-\alpha^2\,Sin\alpha\,t + \alpha^2\,t_0^2 Sin\alpha\,t_0 t + \alpha\,\omega_i Cos\alpha\,t_0 Sin\omega_i t] + \frac{SK_g x_g \omega_2^2}{K_2} Cos\omega_2\,t \qquad \textit{(acceleration)} \tag{4.6}$$

Equation (4.4) and its two derivatives given in equations (4.5) and (4.6), are then programmed. The 1-DOF spring-mass-snubber system is subjected to harmonic sinusoidal support motions, experimentally, and data obtained for comparison with that obtained from the program, as given in [3].

4.2.4 Taking Advantage of F.E.M with Coriolis Force and [3]

Using equations (4.4), (4.5), (4.6) and the F.E.M with Coriolis Force, we utilize the ω_i, [K] and [m] matrices, the results will include the effects of support gap as well that of Coriolis Force.

4.3 Research Papers: A Test and Analysis of the Multiple Support Piping Systems [4] and Dynamic Response Studies of Piping-Support Systems [5]

4.3.1 Abstract

In the design of the piping system of a nuclear power plant, the dynamic analysis plays a major role to assure the safety of the piping systems. Actual piping systems are generally supported by independent structures such as vessels and steel structures. Current practice addresses design margins for the pipe supports and the piping independently. Actual nuclear piping systems designed by the current seismic design criteria have many supports such as frame restraints, rod restraints, mechanical snubbers, etc. These supports exhibit some non-linear characteristics for dynamic loadings because they contain clearance gaps that accommodate thermal movements. Therefore, under the dynamic loadings, the response of an actual system is usually larger than that of the corresponding linear system. So, it is very important to clarify the behavior of the piping systems during seismic events. By predicting more accurate response of a piping system, it is possible to reduce the number of supports and to improve the reliability of the piping system.

An integrated approach to the piping design, which considers the interaction between support and piping, will be necessary to improve the reliability and the overall performance of the piping system.

These papers [4] and [5] are based on experimental study using a realistic large scale model with support gaps and then the computational method is assessed.

Similar scenario is experienced with in-plant piping other than nuclear plants too. Thus this study is considered in this Thesis. It may be noted that the equations of motion formulated in [4] and that formulated in Chapter 3 of this Thesis are very similar. The exception being that in [4] the fluid is assumed to be present but its velocity is zero. In this study we assume fluid mass to be in motion, resulting in Coriolis effects. The author of [4] through email informed that they developed a piping analysis program ISAP based on Finite Element Method. This Thesis formulates a new equation of motion utilizing a Finite Element Method by taking into account effects of Coriolis Force. ANSYS program for various case studies is also made use of, but without Coriolis Force effects, as ANSYS does not give that facility with this version.

4.3.2 Fundamental Equations for Multiple Support Excitation Problems

The equations of the motion of the piping system subjected to the multiple support excitations as presented in Figures 4.6 and 4.7 can be written as:

$$\left[\begin{array}{c|c} M_a & 0 \\ \hline 0 & M_b \end{array}\right]\left\{\begin{array}{c} \ddot{x}_a \\ \ddot{x}_b \end{array}\right\}+\left[\begin{array}{c|c} C_a & C_{ab} \\ \hline C_{ba} & C_b \end{array}\right]\left\{\begin{array}{c} \dot{x}_a \\ \dot{x}_b \end{array}\right\}+\left[\begin{array}{c|c} K_a & K_{ab} \\ \hline K_{ba} & K_b \end{array}\right]\left\{\begin{array}{c} x_a \\ x_b \end{array}\right\}=\left\{\begin{array}{c} 0 \\ F_b \end{array}\right\}$$

There are two different methods that can be employed here to arrive at the same well-known matrix equation of motion. One method is what [4] utilizes and the other is from the theory of relative displacement of support motion or base excitation. [30] [42] [64]

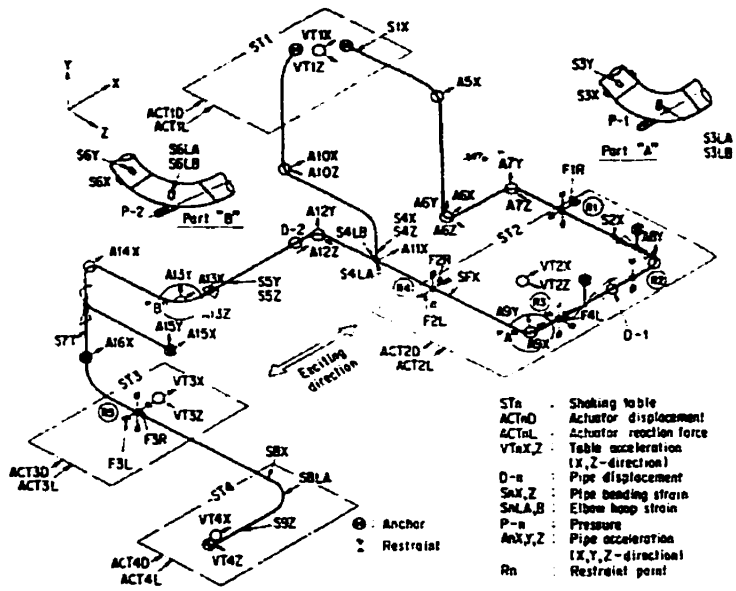

Figure 4.6: Piping Isometric [4]
Connected to Pump at ST4 and Pressure Vessel at ST1

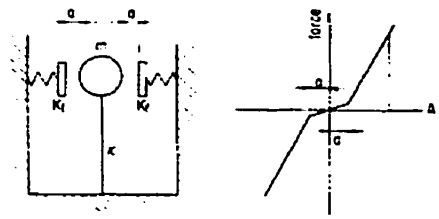

Figure 4.7: Simplified Analysis Model
(a) Spring-Mass Model (b) Force-Displacement Relation

Refer to Figures 4.6 and 4.7.

In many cases the motion of a system is excited by the sudden displacement, velocity or acceleration of the support points of the system.

Let y be the harmonic displacement of the support point and measure the displacement x, of the mass m, from an inertial reference. The relative displacement can be expressed, referring to Figure 4.8:

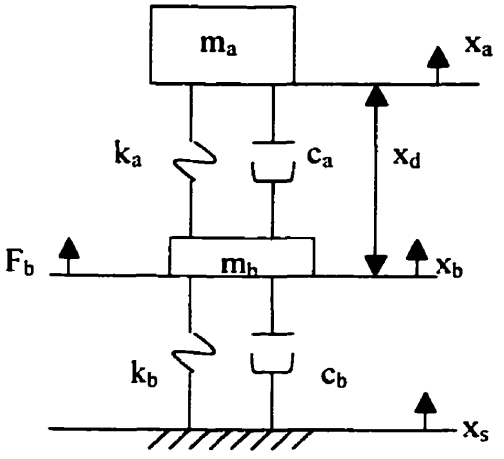

Figure 4.8: Support Point Excited Relative Motion

The system response can be represented by two components: one is an inertial component induced and the other is a pseudo-static component induced by the differential motion x_b of the support points, as:

$$x_a = x_d + x_s \tag{4.7}$$

The pseudo-static component can be expressed as

$$x_s = Tx_b \tag{4.8}$$

Where $T = -k_a^{-1}k_{ab}$

Equation of motion can be written as, as seen from Figure: 4.8:

$$m_a\ddot{x}_a + c_a(\dot{x}_a - \dot{x}_s) + k_a(x_a - x_s) = 0 \tag{4.9}$$

m_b does not contribute after first excitation, thus this is not taken in equation of motion.

From equation (4.9) we can drive the following well-known matrix formation: [30]

$$m_a\ddot{x}_d + c_a\dot{x}_d + k_a x_d = -m_a T\ddot{x}_b \tag{4.10}$$

Equation (4.10) is the well-known matrix formation. [30] [42] [64]

The same equation (4.10) can be achieved using a slightly different approach as used in [4] but with the addition of the use of Static Condensation Method, as given below:

The equations of motion of the piping system subjected to the multiple support excitations can be written as:

$$\left[\begin{array}{c|c} m_a & 0 \\ \hline 0 & m_b \end{array}\right]\left\{\begin{array}{c} \ddot{x}_a \\ \ddot{x}_b \end{array}\right\} + \left[\begin{array}{c|c} c_a & c_{ab} \\ \hline c_{ba} & c_b \end{array}\right]\left\{\begin{array}{c} \dot{x}_a \\ \dot{x}_b \end{array}\right\} + \left[\begin{array}{c|c} k_a & k_{ab} \\ \hline k_{ba} & k_b \end{array}\right]\left\{\begin{array}{c} x_a \\ x_b \end{array}\right\} = \left\{\begin{array}{c} 0 \\ F_b \end{array}\right\} \tag{4.11}$$

Where:

a = dynamic degree of freedom, which means the dependent degrees of freedom.

b = boundary degrees of freedom, which are the independent degrees of freedom.

$\{x_b\}$= differential motion of the support points.

$\{x_a\}$= system response

$\{x_d\}$= inertial component of system response.

$\{x_s\}$= pseudo-static component, induced by the differential motion $\{x_b\}$ of support.

$[m_a]$= mass matrix of the dynamic system, i.e., pipes and ancillaries.

$[m_b]$= mass matrix of the support system, i.e., pipe supports and platforms.

$[c_a]$= damping factor matrix for the piping system.

$[c_b]$= damping factor matrix for the support system.

$[k_a]$= spring constant of the piping system, or stiffness matrix of the piping system.

$[k_b]$= spring constant of the support system, or stiffness matrix of the support system.

$\{F_b\}$= external force applied to the supports.

The displacement vector can be written as:

$$\begin{Bmatrix} x_a \\ x_b \end{Bmatrix} = \left[\begin{array}{c|c} I & T \\ \hline 0 & I \end{array}\right] \begin{Bmatrix} x_d \\ x_b \end{Bmatrix} = [A] \begin{Bmatrix} x_d \\ x_b \end{Bmatrix} \tag{4.12}$$

Let $$[A] = \left[\begin{array}{c|c} I & T \\ \hline 0 & I \end{array}\right] \tag{4.13}$$

Substituting equation (4.12) in (4.11) and pre multiplying by $[A]$ we get:

$$[A]\left[\begin{array}{c|c} m_a & 0 \\ \hline 0 & m_b \end{array}\right][A]\begin{Bmatrix} \ddot{x}_d \\ \ddot{x}_b \end{Bmatrix} + [A]\left[\begin{array}{c|c} c_a & c_{ab} \\ \hline c_{ba} & c_b \end{array}\right][A]\begin{Bmatrix} \dot{x}_d \\ \dot{x}_b \end{Bmatrix} + [A]\left[\begin{array}{c|c} k_a & k_{ab} \\ \hline k_{ba} & k_b \end{array}\right][A]\begin{Bmatrix} x_d \\ x_b \end{Bmatrix} = \begin{Bmatrix} o \\ F_b \end{Bmatrix} \tag{4.14}$$

Because of the pseudo-static component induced by the differential motion $\{x_b\}$ of the support points, we see that $[m_b]=0$, as $[m_b]$ has no more function in the excitation force. $[m_b]$ is used only for the initial deflection and then it is static. The authors of [4] have ignored c_b , c_{ab} *and* c_{ba}, as if support-damping contributions are zero.

Equated to zero for complementary/homogenous solution and the above given and assumed conditions, thus equation (4.14) would become:

$$\left[\begin{array}{c|c} I & T \\ \hline 0 & I \end{array}\right]\left[\begin{array}{c|c} m_a & 0 \\ \hline 0 & m_b \end{array}\right]\left[\begin{array}{c|c} I & T \\ \hline 0 & I \end{array}\right]\left\{\begin{array}{c} \ddot{x}_d \\ \ddot{x}_b \end{array}\right\}+\left[\begin{array}{c|c} I & T \\ \hline 0 & I \end{array}\right]\left[\begin{array}{c|c} c_a & 0 \\ \hline 0 & 0 \end{array}\right]\left[\begin{array}{c|c} I & T \\ \hline 0 & I \end{array}\right]\left\{\begin{array}{c} \dot{x}_d \\ \dot{x}_b \end{array}\right\}$$
$$+\left[\begin{array}{c|c} I & T \\ \hline 0 & I \end{array}\right]\left[\begin{array}{c|c} k_a & 0 \\ \hline 0 & 0 \end{array}\right]\left[\begin{array}{c|c} I & T \\ \hline 0 & I \end{array}\right]\left\{\begin{array}{c} x_d \\ x_b \end{array}\right\}=\left\{\begin{array}{c} 0 \\ 0 \end{array}\right\} \qquad (4.15)$$

We have taken in equations (4.14) or (4.15) the right hand side equated to zero as we need to study the steady state motion and the transients are being assumed to die out over time, in the harmonic motion after the seismic impulse wave has passed.

Rearranging and resolving equation (4.15) gives:

$$[m_a]\{\ddot{x}_d\}+[c_a]\{\dot{x}_d\}+[k_a]\{x_d\}=-[m_a][T]\{\ddot{x}_b\} \qquad (4.16)$$

Equation (4.16) is the matrix form of well-known equation of motion, driven through static condensation method.

Refer to equations (4.11), (4.16) and (3.11). We can see a correlation between the equations. The combination of these equations or the implantation of results from one equation into the other will give that extra advantage of studying the effects of support gap in the presence of Coriolis Force.

An attempt was made to use the equation of motion and other equations along with the data as in [4], into the Thesis but was found not possible, as the required data from [4] is not available.

4.4 Conclusion

1. The equations of [3] and [4] were derived by the authors for a different purpose. But the Finite Element Method given in Chapter 3 and Appendix A have been shown to be directly applicable to the work in [3] and [4]. It is obvious by comparison that equations in the Thesis and those in [3] and [4] are related.

2. [3] takes into account the fact that transients do not die out in the case of pipes. But it does not include the fluid flow conditions.

3. [4] includes fluid mass, but as an integral part of the pipe mass, and fluid flow conditions are not included.

4. The Thesis includes the fluid flow condition and thus the effects of Coriolis Force are studied. The thesis does not take lumping of the mass as the criterion, as taken in [3] and [4], it takes consistent mass matrix and thus the results would be more realistic.

CHAPTER 5 - CONCLUSIONS AND FUTURE SCOPE OF WORK

5.1 Conclusions

1. The Finite Element Method with Coriolis Force provides an important tool in Pipeline vibration analysis and an improvement in problem resolution.

2. The Finite Element Method, as applied in this study, is usable in-parts or as a whole in conjunction with the other research methods.

3. Formulae used in Industrial calculations give reasonably accurate results in most engineering problems. These formulae do take into account forces like end moments more realistically than those used by the formulae in the textbooks. Refer to section 2.5, 2.6 and 2.8 Para 4.

4. That these industrial formulae have been used for large projects built successfully worth billions of dollars for more than 70 years, speaks for their authenticity.

5. In textbooks the natural frequency for a simple beam corresponding to 1-inch sag is 3.12 c.p.s. One reason for limiting the deflection is to make the pipe stiff enough with high enough natural frequency to avoid large amplitude under any small disturbing forces, refer to sections 2.5.3.2, 2.5.4.2 and 2.5.5.2. This may seem too low; in practice the natural frequency will be higher.

6. The reason for natural frequency to be higher in practice are: [28]

6.1 End moments which, are neglected in the textbook formulae, will raise the frequency in practice.

6.2 The critical pipe span is usually limited by stress and rarely reached, refer to sections 2.5.4.1, 2.5.5.1 and 2.5.6.1.

6.3 The piping weight assumed is often more than the actual load.

7. The natural frequency of 3.6 c.p.s as obtained by text book formulae, refer to sections 2.5.4.1, 2.5.5.1 and 2.5.6.1 also [28], using maximum allowable deflection as one inch is lower than the first mode shape frequency using again textbook formulae with no limits on maximum allowable deflection. This is due to the difference in criteria used in the two formulae. Thus if the pipe was built to the formula giving frequency of 3.6 c.p.s, it will fail. This again shows in certain scenarios the textbook formulae are not usable in practice. But these formulae are extremely important as they form basis of the industrial formulae.

8. If for a design higher mode shapes are expected, due to seismic loads or high wind loads, the industrial practice would reduce the pipe span length, and/or increase value of E and/or I. Thus, making the pipe more rigid and correspondingly increasing the natural frequency of the pipe in the span supported. All these mean higher project cost.

9. The case studies in this thesis, refer to sections 2.5, 2.6, 2.7 and 3.2, using actually designed and successfully built operating model, clearly show the limitations of the various calculating methods and the embedded assumptions.

10. In the textbook and industrial procedures we have some established relationships to estimate and use formulae, which might be closer to actual conditions. This is very difficult to achieve in the computer programs commercially available. An example would be formulae for simply supported beams and pipes and those for fixed ends. To simulate results closer to actual conditions, when pipe is supported simply but is also joined on both ends to the contiguous pipes or other equipment like pressure vessels, we estimate the end conditions as in-between simple support and fixed ends. A scenario not readily available in computer analysis. In computerized analysis, one could release some of the end constraints but then could not be sure of the effects on the results.

11. Table 5.1 summarises the results of deflections and frequencies using the various calculating methods presented in the thesis. This chart also presents the results due to the effects of Coriolis Force on the pipeline. It clearly shows that this capability of calculating the Coriolis Force effects on the pipeline as available through the use of this Finite Element Method derived in Chapter 3 and Appendix A, is not available with the other various calculating methods shown in Chapter 2. It also clearly shows the effects of Coriolis Forces on Pipeline deflections and mode shape frequencies as the velocity of flow changes.

	Textbook Method	Industrial Method	ANSYS Method	FEM with Coriolis Force Method
Deflections of (in inch) Empty Pipe:	1.1×10^{-4}	0.828×10^{-4}	0.148×10^{-4}	6.62×10^{-4}
Deflections of (in inch) Fluid Filled Pipe v = 0:	2.5×10^{-4}	1.87×10^{-4}	0.547×10^{-4}	1.498×10^{-3}
Deflections with Coriolis Force (in inch) Flow velocity medium: Flow velocity high: Flow velocity very high: Flow velocity extra high: Flow velocity ultra high: Flow velocity near sonic: Flow velocity sonic:	Not Possible	Not Possible	Not Possible	 1.72×10^{-3} 8.23×10^{-3} -1.1×10^{-4} -996.34 2.4×10^{-5} 280.25 2.49×10^{-5}
Frequency of (cps) Empty Pipe: 	334.21 937.31 1838.17 3038.30 4530.10	339.81 937.33 1836.47 3036.29 4535.82	265.53 266.07 580.15 598.16 599.20	310.62
Frequency of (cps) Fluid Filled Pipe v = 0: 	222.14 623.0 1221.76 2019.45 3010.99	225.85 623.01 1223.64 2018.11 3014.8	224.5 224.96 490.5 505.72 506.6	206.48
Frequency with Coriolis Force (cps) Flow velocity medium: Flow velocity high: Flow velocity very high: Flow velocity extra high: Flow velocity ultra high: Flow velocity near sonic: Flow velocity sonic:	Not Possible	Not Possible	Not Possible	 204.70 201.29 209.93 110.03 203.75 0.18 324.71

Table 5.1: Summary of Deflections and Mode Shape Frequencies Various Calculating Methods

12. It is evident from Table 5.1 that excepting for textbook and industrial methods, which are within 75% accuracy of each other, there is no comparison in deflections between the various calculating methods given. It probably is due to the inherent fact that

equations in each method are based on various assumptions and factor of safety. In spite of that, the values of deflections within a calculating method are quite reasonable and acceptable. Thus due diligence is required with the method chosen for each project scenario.

13. Analysis of mode shape frequencies in Table 5.1 shows encouraging results. Comparing the 2nd mode shape frequency as obtained using this FEM to any other method in Table 5.1 gives us an accuracy of 83% to 85%. Except, comparing this FEM with empty pipe case using ANSYS, where we get 94% accuracy in mode shape frequencies.

14. Mode shape frequencies as obtained using the FEM with Coriolis Force at different velocities could not be compared with the other methods given in Table 5.1, as those methods do not provide for such an option.

15. The results of FEM with Coriolis Force as obtained in Chapter 3 and summarised in Table 5.1 have another significance too. This pipe behaviour of very small deflections and small changes in frequency at low flow velocities, and then large deflections and large frequency changes to the extent of becoming erratic, with the noticeably high flow velocities, has been reported to varied extent by other scholars, [8] [10] [13] [15] [38] [58] [69], too. Though they all used other different analytical and experimental techniques. Thus this similarity goes to prove that the FEM with Coriolis Force as derived and used in Chapter 3 is true.

16. Given the fact that we have room for improvement in the results as obtained using Finite Element Method with Coriolis Force derived in Chapter 3, it is very encouraging that we have achieved some positive results and that the approach is correct. The

deviation of results, from that obtained using other methods given in Chapter 2 has number of reasons. Firstly the methods presented in Chapter 2 are based on some assumptions and approximations. Secondly, though the equations for a single element as derived for the FEM with Coriolis Force in Chapter 3 are accurate, but as only two elements were used in the assemblage, thus the results were not as accurate as would have been with the use of many more elements in the matrices assemblage.

17. Within the model presented large deviations were obtained, as expected. One must point out that accuracy of the value obtained is not the focus of the thesis, but the overall deviation.
18. This thesis highlights the importance of considering the effects of Coriolis force in the calculations. That goal is clearly and objectively achieved through the results presented in Chapter 3 and Table 5.1.
19. Accuracy of the system can further be improved through various techniques, which includes increased number of elements and changing type of elements used. But that is beyond the scope of this Thesis, which can be taken up as a future research endeavour.
20. The Coriolis Force, *c*-matrix in equation (A.A.23) and (A.A.32) is non-symmetric. This is an important matrix, as due to the fluid flow velocity here in represents the Coriolis Force part of the equation. This c-matrix looks very much like a damping matrix but it is not a damping matrix.
21. The *D*-matrix in equations (A.A.23) and (A.A.32) is symmetric. It is interesting to note that though velocity is constant but here we get the inertia force due to changes in direction of velocity vector, corresponding the changes in pipe curvature.

5.2 Future Scope Of Work

1. Explore other Finite Elements, appropriate to pipes, improving accuracy of results, capacity and versatility of application of the current method.
2. Apply this Finite Element Method to other fluid flow applications and compare.
3. Consider large amplitude vibrations in derivation of equations and introduce the non-linear terms.
4. Use materials with mass density variations, such as non-homogeneity, thus the non-linearity.
5. Effects of damping by pipe itself, as its transients do not die out over time as found by other researchers like Vayda [3], Chiba [4] [5] etc.
6. Use the scenario of continually changing fluid velocity and pressures.
7. Consider bi-flow fluid conditions: gas and oil together; flow slurries in flare outs; water and oil. Bi-Flow means two viscosities mixed and flowing in the same pipe.
8. Consider effects of transverse shear and rotary inertia.
9. Write computer code using FEM with Coriolis Force and include non-linearity.
10. Future work can be undertaken to generate curves and charts using a range of values for: weights of system, pipeline lengths, fluid mass, modulus of elasticity and area moment of inertia, velocity of flow and find real and complex eigen values of the system.
11. The horizontal L shape system shown in Chapter 2 should be analyzed using the FEM method with Coriolis Force.
12. Apply a wide range of different internal and external forces to a pipeline, along with the Coriolis Force effects, and study its response.

13. It would be interesting and useful to be able to combine the attributes of this thesis with those of [3], [4] and [5]. To include the damping effects of supports, support-pipe interaction and the transients into the equations of this study.
14. Friction forces due to pipeline interaction with supports and/or internal friction and damping due to fluid flow could be introduced as linear or non-linear quantity, in the equations of this Thesis.
15. Effects of Coriolis Force due to velocity of fluid flow on the piping system should be investigated in the presence of the pumps, compressors and turbines connected to piping system. Adding to this studies the effects due to support interaction as in [3], [4] and [5] as well as due to friction force would give a very interesting and important turn to the analysis.

BIBLIOGRAPHY

1- Timoshenko, S., Young, D. H. and Weaver, W., (1974), Vibration Problems in Engineering, John Wiley and Sons Inc., Toronto.

2- Swanson Analysis Systems, Inc., (1993), ANSYS Users Manuals, Swanson Analysis Systems, Inc. Houston.

3- Vayda, J.P., (1981), Influence of Gap Size on the Dynamic Behavior of Piping Systems, Journal of Nuclear Engineering and Design, Vol. 67, pp. 145-164.

4- Chiba, T., Koyanagi, R., Ogawa, N. and Minowa, C., (1989), A Test and Analysis of the Multiple Support Piping Systems, Journal of Pressure Vessel Technology, Vol. 111, pp. 291- 299.

5- Chiba, T. and Koyanagi, R., (1990), Dynamic Response Studies of Piping-Support Systems, Journal of Pressure Vessel Technology, Vol. 112, pp. 39 – 45.

6- Chiba, T. and Kobayashi, H., (1990), Response Characteristics of Piping System Supported by Visco-Elastic and Elasto-Plastic Dampers, Journal of Pressure Vessel Technology, Vol. 112, pp. 34 – 38.

7- Vashi, K.M., (1975), Seismic Spectral Analysis of Structural Systems Subject to Nonuniform Excitation at Supports, 2nd ASCE Specialty Conference on Structural Design of Nuclear Plant Facilities, Structural Design of Nuclear Plant Facilities, Vol. I-A, pp. 188 – 216.

8- Ashley, H. and Havilland,G., (1950), Bending Vibrations of a Pipeline Containing a Flowing Fluid, Journal of Applied Mechanics, Vol.17, pp. 229 – 232.

9- Lockau, J., Haas, E. and Steinwender, F., (1984), The Influence of High-Frequency Excitation on Piping and Support Design, Journal of Pressure Vessel Technology, Vol. 106, pp. 175 – 187.

10- Housner, G. W., (1952), Bending Vibrations of a Pipeline Containing a Flowing Fluid, Journal of Applied Mechanics, Vol.19, pp. 205 – 208.

11- Moore, S. E. and Rodabaugh, E. C., (1982), Background for Changes in the 1981 Edition of the ASME Nuclear Power Plant Components Code for Controlling Primary Loads in Piping Systems, Journal of Pressure Vessel Technology, Vol. 104, pp. 351 – 361.

12- Luo, H. and Hanagud, S., (1998), On the Dynamics of Vibration Absorbers with Motion- Limiting Stops, Journal of Applied Mechanics, Vol. 65, pp. 223 – 233.

13- Naguleswaran, S and Williams,C.J. (1968), Lateral Vibration of a Pipe Conveying Fluid, The Journal of Mechanical Engineering Science, Vol. 10, pp. 228 - 238.

14- Wiercigroch, M. and Sin, V. W. T., (1998), Experimental Study of a Symmetrical Piecewise Base-Excited Oscillator, Journal of Applied Mechanics, Vol. 65, pp. 657 – 663.

15- Thurman, A. L. and Mote Jr., C. D., (1969), Non-Linear Oscillation of a Cylinder Containing Flowing Fluid, Journal of Engineering for Industry, Transactions of the American Society of Mechanical Engineers, Vol. 91, pp. 1147 – 1155.

16- Chiba, T. and Koyanagi, R., (1988), An Experimental Study of the Response of Multiple Support Piping Systems, Res Mechanica, Vol. 25, pp. 145 – 157.

17- Burgreen, D., (1977), Principles of Piping Analysis, C. P. Press, New York.

18- Hatter, D.J., (1973), Matrix Computer Methods of Vibration Analysis, Butterworth and Co (Canada) Ltd., Toronto.

19- Paz, M., (1985), Structural Dynamics, Macmillan of Canada, Toronto.

20- Boresi. A. P., Schmidt. R. J. and Sidebottom. O. M, (1993), Advanced Mechanics of Materials, John Wiley and Sons, Inc., Toronto.

21- Ghali, A. and Neville, A. M., (1989), Structural Analysis, Chapman and Hall Ltd. New York.

22- Fluor Daniel Corp., (1986), Pipe Stress Analyst Design Guide, Fluor Engineers and Constructors, Inc., California.

23- M. W. Kellogg Co., (1956), Design of Piping Systems, John Wiley and Sons, Inc., New York.

24- Nolte, C. B., (1979), Optimum Pipe Size Selection, Gulf Publishing Co., Houston.

25- Pipeline Industry, (1978), Pipeline Rules of Thumb Handbook, Gulf Publishing Co., Houston.

26- Wolfram. S., (1996), The Mathematica Book, Wolfram Media Inc., New York.

27- Kaladi, V. M., (1984), Vibration of Piping Systems, M. Sc. E. Thesis, University of Calgary.

28- Kannappan, S., (1986), Introduction to Pipe Stress Analysis, John Wiley and Sons Inc. Toronto.

29- Beer, F. P. and Johnston, E. R., (1992), Mechanics of Materials, McGraw-Hill Inc., Toronto.

30- Thomson, W. T., (1981), Theory of Vibration with Applications, Prentice-Hall Inc., Toronto.

31- Warnock, F. V. and Benham, P. P., (1965). Mechanics of Solids and Strength of Materials, Isaac Pitman and Sons (Canada) Ltd., Toronto.

32- Timoshenko, S. P. and Gere, J. M., (1972), Mechanics of Materials, Van Nostrand Reinhold Ltd., New York.

33- Wang, P. C., (1966), Numerical and Matrix Methods in Structural Mechanics, John Wiley and Sons Inc., New York.

34- American Society of Testing and Materials (ASTM)- (2001), ASTM A53/A53M-01, ASTM New York.

35- American Society of Mechanical Engineers (ASME), (2001), ASME B31.3, ASME New York.

36- American Petroleum Institute (API), (1993), API 5L, API Washington.

37- Perry, R. H. and Chilton, C. H., (1973), Chemical Engineer's Handbook, McGraw-Hill, Paris.

38- Chen, S. S., (1971), Dynamic Stability of a Tube Conveying Fluid, Journal of the Engineering Mechanics Division, Proceedings of the American Society of Civil Engineers, Vol. 97, pp. 1469 – 1485.

39- Fluor Daniel Corp., (1986), Piping Design Guide, Fluor Engineers and Constructors Inc., California.

40- American National Standards Institute (ANSI), (1985), Standards ANSI B36.10 M, Welded and Seamless Pipe Steel, ASME New York.

41- American society of Mechanical Engineers (ASME) - Boiler and Pressure Vessel Code (BPV), (1998), Section II and III – Div-1, ASME New York.

42- Hartog, J. P. D., (1956), Mechanical Vibrations, McGraw-Hill Book Co Inc., Toronto.

43- Wylie, E. B., and Streeter, V. L., (1978), Fluid Transients, McGraw-Hill International Book Co., Toronto.

44- Bednar, H. H., (1986), Pressure Vessel Design Handbook, Macmillan of Canada, Ontario.

45- Crocker, S., and King, R. C., (1973), Piping Handbook, McGraw-Hill Inc., New York.

46- Harris, C. M., and Crede, C. E., (1961), Shock and Vibration Handbook, McGraw-Hill Book Co., New York.

47- Roark, R. J., and Young, W. C., (1976), Formulas for Stress and Strain, McGraw-Hill Inc., London.

48- Jacobsen, L. S., and Ayre, R. S., (1958), Engineering Vibrations with Applications to Structures and Machinery, The Maple Press Co., Toronto.

49- Steidel, R. F., (1989), An Introduction to Mechanical Vibrations, John Wiley And Sons Inc., Toronto.

50- Chen, Y., (1966), Vibrations: Theoretical Methods, Addison-Wesley (Canada) Ltd., Ontario.

51- White, R. G., and Walker, J. G., (1982), Noise and Vibration, John Wiley and Sons, Toronto

52- Francis, S. T., Morse, I. E., and Hinkle, R. T., (1963), Mechanical Vibrations, Allyn and Bacon Inc., Boston.

53- Bishop, R. E. D., (1979), Vibration, Cambridge University Press, New York.

54- Collacott, R. A., (1947), Mechanical Vibrations, Pitman and Sons Ltd., London.

55- Roseau, M., (1987), Vibrations in Mechanical Systems – Analytical Methods and Applications, Springer-Verlag, Berlin.

56- McCallion, H., (1973), Vibration of Linear Mechanical Systems, Longman Group Ltd., London.

57- Baker, J. K., (1975), Vibration Isolation, Oxford University Press, Hampshire.

58- Paz, M. and Michelow,J., (1977), Stiffness Analysis of Network Pipes Conveying Fluid, 3rd International Conference on Pressure Vessel Technology, pp. 143 – 148.

59- Crede, C. E., (1965), Shock and Vibration Concepts in Engineering Design, Prentice-Hall Inc., Toronto.

60- Timoshenko, S. P., and Goodier, J. N., (1970), Theory of Elasticity, McGraw-Hill Book Co., Toronto.

61- Timoshenko, S., (1956), Strength of Materials, D. Van Nostrand Co. Inc., Toronto.

62- Blake, A., (1990), Practical Stress Analysis in Engineering Design, Marcel Dekker Inc., New York.

63- Seto, W. W., (1964), Theory and Problems of Mechanical Vibrations, McGraw-Hill Book Co., Toronto.

64- Arya, S., O'Neill and Pincus, G., (1979), Design of Structures and Foundations for Vibrating Machines, Gulf Publishing Co., Houston.

65- The Institution of Mechanical Engineers and The British Nuclear Energy Society, (1985), Pipework Design and Operation, Waveney Print Services Ltd., Suffolk.

66- Stijgeren, E. V., (1981), Computer Aided Design of Pipe and Pipe Supports, The Pressure Vessels and Piping Division – ASME, New York.

67- Swanson Analysis Systems, Inc., (1996), ANSYS Expanded Workbook, Swanson Analysis Systems, Inc. Houston.

68- Paidoussis, M. P. and Issid, N. T. (1974), Dynamic Stability of Pipes Conveying Fluid, Journal of Sound and Vibration, Vol. 33, pp: 267-294.

69- Keskinen, R., (1979), Vibrations of Three-Dimensional Piping Subject to Pump Pulsation, International conference on Structural Mechanics and Reactor Technology, Transactions Part F 4.3.

70- Chen, S. H. and Chen. S. S., (1996), Chaotic Vibration in Fluid-Stiffness-Controlled Instability of a Tube Row in Crossflow, Journal of Applied Mechanics, Vol. 63, pp: 487-492.

71- Newmark, N. W., (1959), A Method of Computation for Structural Dynamics, Journal of Engineering Mechanics, ASCE, Vol. 85, pp: 67-94.

72- Bedford, A. and Wallace, F., (1995), Dynamics, Addison-Wesley Publishing Co. Inc., Don Mills-Ontario.

APPENDIX A - FINITE ELEMENT DEVELOPMENT DETAILS

A.A.1 Introduction

In this appendix the basics of the development of the Finite Element Method with the Coriolis Force as given and used in Chapter 3 are given. This Finite Element formulation is has been developed for the dynamic analysis of fluid filled pipelines, under the influence of Coriolis Force.

The accuracy of a finite element depends upon the choice of the shape functions. Shape functions should satisfy conditions that will ensure convergence to correct results when a finer finite element mesh is utilized.

The shape functions should satisfy following three conditions, for monotonous convergence to the correct results. [21]

The displacements of adjacent elements along a common boundary must be identical.

When the nodal displacements correspond to rigid-body motion, the strains must be equal to zero.

The shape functions must allow the element to be in a state of constant strain.

The element taken for this development is bar in bending with transverse deflections in the *y*-direction at any section taken along with the nodal displacements.

The deflections are u and v translations in *x* and *y*-directions respectively.

The number of terms in the matrix must equal number of nodal degrees of freedom.

This element being taken as rigidly connected at its ends to the adjoining structure, in other words the both ends of pipe are fixed to the supports, this element will now act like a beam with moments and lateral forces at the fixed ends also called joints. The relative axial displacement u_2 and u_1 in the x-direction is taken to be zero, being much smaller than the lateral displacements v_1 and v_2 in y-direction at the two fixed ends.

Each joint has lateral displacement v_i and rotation θ_i. Thus resulting in four local coordinates v_1, θ_i for joint one and v_2, θ_2 for joint two. Thus the four displacement coordinates are taken as the four shapes called N_1, N_2, N_3, N_4. The forces and moments given in Figure 3.3 shall be used here, as required at the two end conditions of this beam element.

A.A.2 Derivation of the Shape Functions

We write the cubic equation for the beam end with the coordinates $x = 0$ @ $L = 0$; with the boundary conditions $v_i = \theta_i = 0$.

$$N_i = (x - L)^2 (a x + b) \tag{A.A.1}$$

Differentiating equation (A.A.1) gives:

$$N_i' = 2 (x - L) (a x + b) + (x - L)^2 a \tag{A.A.2}$$

At $i = 1$; $x = 0$; $v_1 = 1$; $N_1 = 1$ and $N_1' = 0$

Thus from equation (A.A.1), we get:

$$b = \frac{1}{L^2} \tag{A.A.3}$$

From equation (A.A.2), we get:

$$0 = -2Lb + L^2 a \qquad \text{(A.A.4)}$$

Hence, $$a = \frac{2}{L^3} \qquad \text{(A.A.5)}$$

Now putting equation (A.A.3) and (A.A.5) in equation (A.A.1):

$$N_1 = (x-L)^2(2x+L)\frac{1}{L^3} \qquad \text{(A.A.6)}$$

At $i = 2; x = 0; \theta_1 = 1;\ N_2 = 0$ and $N_2' = 1$

Thus from equation (A.A.1), we get:

$$b = 0 \qquad \text{(A.A.7)}$$

From equation (A.A.2), we get:

$$1 = -2Lb + aL^2 \qquad \text{(A.A.8)}$$

Putting equation (A.A.7) in (A.A.8):

$$a = \frac{1}{L^2} \qquad \text{(A.A.9)}$$

Putting equations (A.A.7) and (A.A.9) in (A.A.1):

$$N_2 = \frac{x}{L^2}(x-L)^2 \qquad \text{(A.A.10)}$$

We write the cubic equation for the beam end with the coordinates $x = L$; with the boundary conditions $v_i = \theta_i = 0$.

$$N_i = x^2 (a\,x + b) \qquad \text{(A.A.11)}$$

Differentiating equation (A.A.11) gives:

$$N_i' = 2x(ax+b) + ax^2 \qquad \text{(A.A.12)}$$

At $i = 3;\ x = L;\ v_3 = 1;\ N_3 = 1$ and $N_3' = 0$

Thus from equation (A.A.11), we get:

$$b = \frac{1}{L^2} - aL \qquad \text{(A.A.13)}$$

From equation (A.A.12), we get:

$$0 = 2L(aL + b) + aL^2 \qquad \text{(A.A.14)}$$

Putting equation (A.A.13) in (A.A.14):

$$a = \frac{-2}{L^3} \qquad \text{(A.A.15)}$$

Putting equation (A.A.15) in (A.A.13):

$$b = \frac{1}{L^2} + \frac{2}{L^2} \qquad \text{(A.A.16)}$$

Putting equation (A.A.15) and (A.A.16) in (A.A.11):

$$N_3 = \frac{x^2}{L^3}(3L - 2x) \qquad \text{(A.A.17)}$$

Putting in equations (A.A.11) and (A.A.12), $x = L;\ \theta_2 = 1;\ N_4 = 0$ *and* $N_4' = 1$, and resolving for values of a and b:

$$b = -aL \qquad \text{(A.A.18)}$$

$$a = \frac{1}{L^2} \qquad \text{(A.A.19)}$$

Putting equation (A.A.19) in (A.A.18) gives:

$$b = -\frac{1}{L} \tag{A.A.20}$$

Putting equations (A.A.19) and (A.A.20) in (A.A.11):

$$N_4 = \frac{x^2}{L^2}(x - L) \tag{A.A.21}$$

A.A.3 Formulation of Matrices

The individual matrices [k]; [m]; [c] and [D] are formulated for the free element using equations (3.9.1); (3.9.2); (3.9.3) and (3.9.4) respectively. It is a painstaking procedure, though straightforward.

The following equations (A.A.22), (A.A.23) and (A.A.24) as taken from Chapter 3 section 3.3 Equations (3.6), (3.7) and (3.8), have been re-written here for ease of their use:

$$\delta J = \int_0^t \int_0^L [m\ddot{\Delta}^i N_i N_j \delta\Delta^j + EI N_i'' N_j'' \Delta^i \delta\Delta^j + 2\rho v(\dot{\Delta}^i N_i') N_j \delta\Delta^j + \rho v^2 (\Delta^i N_i'') N_j \delta\Delta^j] dx dt \tag{A.A.22}$$

Which can be written as:

$$\delta J = \int_0^T [m_{ij}\ddot{\Delta}^i + (k_{ij} + D_{ij})\Delta^i + c_{ij}\dot{\Delta}^i]\delta\Delta^j dt \tag{A.A.23}$$

Or in matrix notation:

$$\delta J = \int_0^T [\{\delta\Delta\}^T([m]\{\ddot{\Delta}\} + ([k] + [D])\{\Delta\} + [c]\{\dot{\Delta}\})] dt \tag{A.A.24}$$

Where in, from equations (A.A.22) and (A.A.24) the following equations (A.A.26), (A.A.27), (A.A.28) and (A.A.29) apply to be true:

$$k_{ij} = \int_0^L EIN_i'' N_j'' dx \qquad \text{(A.A.26)}$$

$$m_{ij} = \int_0^L (m) N_i N_j dx \qquad \text{(A.A.27)}$$

$$c_{ij} = \int_0^L 2\rho v N_i' N_j dx \qquad \text{(A.A.28)}$$

$$D_{ij} = \int_0^L \rho v^2 N_i'' N_j dx \qquad \text{(A.A.29)}$$

Taking twice their derivative of the shape functions, and using in equations (A.A.26), (A.A.27), (A.A.28) and (A.A.29) for the formulation of matrices:

Putting values of N_i, N_i', N_i'' *with* $i = 1 \rightarrow 4$ *; and* N_j, N_j', N_j'' *with* $j = 1 \rightarrow 4$ in equations (A.A.26), (A.A.27), (A.A.28) and (A.A.29) and solving gives the following pipe stiffness matrix, mass matrix, damping matrix and fluid flow induced centrifugal force matrix:

$$[k_{ij}] = EI \begin{bmatrix} \frac{12}{L^3} & \frac{6}{L^2} & \frac{-12}{L^3} & \frac{6}{L^2} \\ \frac{6}{L^2} & \frac{4}{L} & \frac{-6}{L^2} & \frac{2}{L} \\ \frac{-12}{L^3} & \frac{-6}{L^2} & \frac{12}{L^3} & \frac{-6}{L^2} \\ \frac{6}{L^2} & \frac{2}{L} & \frac{-6}{L^2} & \frac{4}{L} \end{bmatrix} \qquad \text{(A.A.30)}$$

The above stiffness matrix in equation (A.A.30) is a symmetric matrix.

$$[m_{ij}] = (m)\begin{bmatrix} \frac{13L}{35} & \frac{11L^2}{210} & \frac{9L}{70} & \frac{-13L^2}{420} \\ \frac{11L^2}{210} & \frac{L^3}{105} & \frac{13L^2}{420} & \frac{-L^3}{140} \\ \frac{9L}{70} & \frac{13L^2}{420} & \frac{13L}{35} & \frac{-11L^2}{210} \\ \frac{-13L^2}{420} & \frac{-L^3}{140} & \frac{-11L^2}{210} & \frac{L^3}{105} \end{bmatrix} \quad \text{(A.A.31)}$$

The above mass matrix in equation (A.A.31) is symmetric as is based on same beam functions as the stiffness matrix, and it is a consistent matrix as opposed to lumped mass on the diagonal.

$$[c_{ij}] = 2\rho v\begin{bmatrix} \frac{-1}{2} & \frac{-L}{10} & \frac{-1}{2} & \frac{L}{10} \\ \frac{L}{10} & 0 & \frac{-L}{10} & \frac{L^2}{60} \\ \frac{1}{2} & \frac{L}{10} & \frac{1}{2} & \frac{-L}{10} \\ \frac{-L}{10} & \frac{-L^2}{60} & \frac{L}{10} & 0 \end{bmatrix} \quad \text{(A.A.32)}$$

The above internal damping matrix in equation (A.A.32) is non-symmetric. This is an important matrix, as due to the fluid flow velocity here in lays the Coriolis Force part of the equation.

$$[D_{ij}] = \rho v^2\begin{bmatrix} \frac{-6}{5L} & \frac{-1}{10} & \frac{6}{5L} & \frac{-1}{10} \\ \frac{-1}{10} & \frac{-2L}{15} & \frac{1}{10} & \frac{L}{30} \\ \frac{6}{5L} & \frac{1}{10} & \frac{-6}{5L} & \frac{19}{10} \\ \frac{-1}{10} & \frac{L}{30} & \frac{19}{10} & \frac{-2L}{15} \end{bmatrix} \quad \text{(A.A.33)}$$

Equation (A.A.33) is another non-symmetric matrix. This matrix shows the application of centrifugal force on the pipe due to the fluid flow velocity and changes in pipe curvature.

A.A.4 Assemblage of Matrices

In addition to the free single element, the case of two elements is considered. The two elements are considered to adjacent to each other forming the beam or the pipe in question. Thus the assemblage of the matrices is conducted and the application of the boundary conditions and the loads are applied.

The assemblage of the matrices enables us to present this Finite Element Method with the ability to calculate the deflections etc with the application of external forces. Thus this FEM can now be compared with its results to that obtained using other methods discussed in this thesis. Also this enables the use of this FEM in conjunction with the research work done by other authors, and thus obtaining results in our area of interest while using the research methodology of other researchers. This goes to show the universality of this FEM.

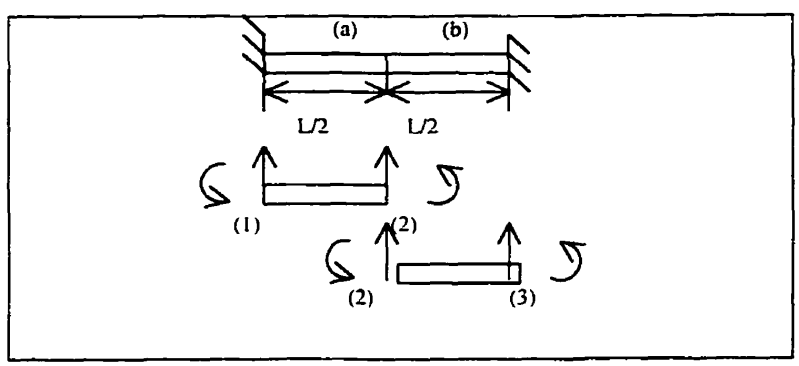

Figure A.A.1: Element/Matrix Assemblage
Fixed Ends Pipe

A.A.4.1 Detailed Assemblage of Matrices

Refer to Chapter 3 section 3.4. Taking the two elements a and b for assemblage we proceed as follows:

$$\begin{Bmatrix} F_1 \\ M_1 \\ F_2 \\ M_2 \\ F_3 \\ M_3 \end{Bmatrix} = \begin{bmatrix} k_{11} & k_{12} & k_{13} & k_{14} & & \\ k_{21} & k_{22} & k_{23} & k_{24} & & \\ k_{31} & k_{32} & k_{33}+k_{11} & k_{34}+k_{12} & k_{13} & k_{14} \\ k_{41} & k_{42} & k_{43}+k_{21} & k_{44}+k_{22} & k_{23} & k_{24} \\ & & k_{31} & k_{32} & k_{33} & k_{34} \\ & & k_{41} & k_{42} & k_{43} & k_{44} \end{bmatrix} \begin{Bmatrix} v_1 \\ \theta_1 \\ v_2 \\ \theta_2 \\ v_3 \\ \theta_3 \end{Bmatrix} \qquad \text{(A.A.34)}$$

As $v_1 = \theta_1 = v_3 = \theta_3 = 0$, we strike out columns 1, 2, 5 and 6. Also F_1, M_1, F_3 and M_3, being at fixed ends 1 and 3, rows 1, 2, 5 and 6 are taken out:

Reference equation (A.A.30), Thus we are left with $[k_{ij}]$ assembled matrix as:

$$\begin{Bmatrix} F_2 \\ M_2 \end{Bmatrix} = \begin{bmatrix} k_{33}+k_{11} & k_{34}+k_{12} \\ k_{43}+k_{21} & k_{44}+k_{22} \end{bmatrix} \begin{Bmatrix} v_2 \\ \theta_2 \end{Bmatrix}$$

$$\begin{Bmatrix} F_2 \\ M_2 \end{Bmatrix} = EI \begin{bmatrix} \frac{24}{L^3} & 0 \\ 0 & \frac{8}{L} \end{bmatrix} \begin{Bmatrix} v_2 \\ \theta_2 \end{Bmatrix} \qquad \text{(A.A.35)}$$

Similarly, $[m_{ij}]$ assembled matrix will be:

$$\begin{Bmatrix} F_2 \\ M_2 \end{Bmatrix} = \begin{bmatrix} m_{33}+m_{11} & m_{34}+m_{12} \\ m_{43}+m_{21} & m_{44}+m_{22} \end{bmatrix} \begin{Bmatrix} \ddot{v}_2 \\ \ddot{\theta}_2 \end{Bmatrix}$$

Reference equation (A.A.31), we are left with:

$$\begin{Bmatrix} F_2 \\ M_2 \end{Bmatrix} = (m) \begin{bmatrix} \frac{26L}{35} & 0 \\ 0 & \frac{2L^3}{105} \end{bmatrix} \begin{Bmatrix} \ddot{v}_2 \\ \ddot{\theta}_2 \end{Bmatrix} \qquad \text{(A.A.36)}$$

Similarly, $[C_{ij}]$ assembled matrix will be: (Reference equation (A.A.32))

$$\begin{Bmatrix} F_2 \\ M_2 \end{Bmatrix} = \begin{bmatrix} c_{33}+c_{11} & c_{34}+c_{12} \\ c_{43}+c_{21} & c_{44}+c_{22} \end{bmatrix} \begin{Bmatrix} \dot{v}_2 \\ \dot{\theta}_2 \end{Bmatrix}$$

$$\begin{Bmatrix} F_2 \\ M_2 \end{Bmatrix} = 2\rho v \begin{bmatrix} 0 & \frac{-L}{5} \\ \frac{L}{5} & 0 \end{bmatrix} \begin{Bmatrix} \dot{v}_2 \\ \dot{\theta}_2 \end{Bmatrix} \tag{A.A.37}$$

Similarly, and $[D_{ij}]$ assembled matrix will be: (Reference equation (A.A.33))

$$\begin{Bmatrix} F_2 \\ M_2 \end{Bmatrix} = \begin{bmatrix} D_{33} + D_{11} & D_{34} + D_{12} \\ D_{43} + D_{21} & D_{44} + D_{22} \end{bmatrix} \begin{Bmatrix} v_2 \\ \theta_2 \end{Bmatrix}$$

$$\begin{Bmatrix} F_2 \\ M_2 \end{Bmatrix} = \rho v^2 \begin{bmatrix} \frac{-12}{5L} & \frac{9}{5} \\ \frac{9}{5} & \frac{-4L}{15} \end{bmatrix} \begin{Bmatrix} v_2 \\ \theta_2 \end{Bmatrix} \tag{A.A.38}$$

These equations (A.A.35), (A.A.36), (A.A.37), (A.A.38) can now be put together for use in equations of motion as deemed necessary.

APPENDIX B - COST COMPARISON

B.1 Engineering Cost verses Producing Returns [25]

1. The throughput of a pipeline is given by:

   500 x $(D_{nom.})^2$ = b.p.d (500 is a factor taken from industrial experience)

   Thus; 500 x $(16)^2$ = 128,000 b.p.d or 128 M.B.O.D

2. Volume of pipeline per linear foot is given by:

   Approximate volume = $(I.D)^2$ / 1000 = b.p.d/ft.

   $(15.25)^2$ / 1000 = 0.2325625 b.p.d/ft.

   While the accurate volume will be = Approx. volume – 3% of approx. volume

   0.2325625 - 0.006976875 = 0.225585625 b.p.d/ft.

3. Cost of constructed pipeline is given by:

   Cost of a 16 inch dia. Pipe = U.S $ 2849 / inch dia. /mile

   Cost of 160 K.M pipeline would be = $2849 \times 16 \times 100 \times 0.625$ = U.S $ 4558400

4. Cost of crude oil in market was approx. = U.S $ 15 /barrel

   Thus revenue earned per day by the producer =128,000 x 15 =U.S $ 1,920,000

   Cost of pipeline construction will be recovered in = $\frac{4,558,400}{1,920,000}$ = 2.4days

B.2 Conclusion: Thus the rule of thumb, in the industry that approx. 2 days of oil flow in 100 miles or 160 K.M of pipeline pays for the cost of pipeline, is evidently true.